

Dipalladium(I) Terphenyl Diphosphine Complexes as Models for Two-Site Adsorption and Activation of Organic Molecules

Sibo Lin, David E. Herbert, Alexandra Velian, Michael W. Day, Theodor Agapie*

Division of Chemistry and Chemical Engineering, California Institute of Technology, Pasadena, California, 91125

Supporting Information

I. Experimental Details	
General considerations	S4
Synthesis of 3	S4
Isolation of toluene-free, acetonitrile-exchanged 3	S4
Synthesis of 4	S5
Synthesis of 5	S5
Synthesis of 6	S6
Synthesis of 7-17	S6
Characterization of 7	S7
Synthesis of 2,5-dideuterothiophene	S7
Synthesis of <i>d</i> ₂ -7	S7
Characterization of 8	S7
Characterization of 9	S8
Characterization of 10	S8
Characterization of 11	S8
Characterization of 12	S9
Characterization of 13	S9
Characterization of 14	S10
Characterization of 15	S10
Characterization of 16	S11
Characterization of 17	S11
Synthesis of 18	S11
Synthesis of 19	S12
Synthesis of 20	S12
Synthesis of 21	S13
II. Nuclear Magnetic Resonance Spectra	
Figure S1. ¹ H NMR spectra of 3	S14
Figure S2. ¹ H NMR spectra of acetonitrile-exchanged 3	S14
Figure S3. ¹ H NMR spectra of 4	S14
Figure S4. ¹ H NMR spectra of 5	S14
Figure S5. ¹ H NMR spectra of 6	S14
Figure S6. ¹ H NMR spectra of 7	S15
Figure S7. ¹ H NMR spectra of 8	S15
Figure S8. ¹ H NMR spectra of 9	S15
Figure S9. ¹ H NMR spectra of 10	S15
Figure S10. ¹ H NMR spectra of 11	S15
Figure S11. ¹ H NMR spectra of 12	S15
Figure S12. ¹ H NMR spectra of 13	S16
Figure S13. ¹ H NMR spectra of 14	S16
Figure S14. ¹ H NMR spectra of 15	S16
Figure S15. ¹ H NMR spectra of 16	S16

Figure S16. ^1H NMR spectra of 17	S16
Figure S17. ^1H NMR spectra of 18	S16
Figure S18. ^1H NMR spectra of 19	S17
Figure S19. ^1H NMR spectra of 20	S17
Figure S20. ^1H NMR spectra of 21	S17
Figure S21. Variable temperature ^1H NMR spectra of 9	S18
Figure S22. Variable temperature ^1H NMR spectra of 11	S18
Figure S23. Variable temperature ^1H NMR spectra of 13	S19
Figure S24. Stacked $^{31}\text{P}\{^1\text{H}\}$ and $^{19}\text{F}\{^1\text{H}\}$ NMR spectra of 3-21	S20
Figure S25. Stacked 1D $^{13}\text{C}\{^1\text{H}\}$ NMR spectra of 3, 5-7, 13, 15, 18-20	S21
Figure S26. HSQC spectrum (CD_2Cl_2 , 400 MHz) for toluene adduct 3	S22
Figure S27. HMBC spectrum (CD_2Cl_2 , 400 MHz) for toluene adduct 3	S22
Figure S28. HSQC spectrum (CD_3NO_2 , 400 MHz) for anisole adduct 4	S23
Figure S29. HMBC spectrum (CD_3NO_2 , 400 MHz) for anisole adduct 4	S23
Figure S30. HSQC spectrum (CD_3CN , 400 MHz) for butadiene adduct 5	S24
Figure S31. HMBC spectrum (CD_3CN , 400 MHz) for butadiene adduct 5	S24
Figure S32. HSQC spectrum (CD_3CN , 400 MHz) for 1,3-cyclohexadiene adduct 6	S25
Figure S33. HMBC spectrum (CD_3CN , 400 MHz) for 1,3-cyclohexadiene adduct 6	S25
Figure S34. HSQC spectrum (CD_3NO_2 , 400 MHz) for thiophene adduct 7	S26
Figure S35. HMBC spectrum (CD_3NO_2 , 400 MHz) for thiophene adduct 7	S26
Figure S36. HSQC spectrum (CD_3NO_2 , 400 MHz) for 2-methylthiophene adduct 8	S27
Figure S37. HMBC spectrum (CD_3NO_2 , 400 MHz) for 2-methylthiophene adduct 8	S27
Figure S38. HSQC spectrum (CD_3NO_2 , 400 MHz) for 3-methylthiophene adduct 9	S28
Figure S39. HMBC spectrum (CD_3NO_2 , 400 MHz) for 3-methylthiophene adduct 9	S28
Figure S40. HSQC spectrum (CD_3NO_2 , 400 MHz) for 2,5-Me ₂ -thiophene adduct 10	S29
Figure S41. HMBC spectrum (CD_3NO_2 , 400 MHz) for 2,5-Me ₂ -thiophene adduct 10	S29
Figure S42. HSQC spectrum (CD_3NO_2 , 400 MHz) for pyrrole adduct 11	S30
Figure S43. HMBC spectrum (CD_3NO_2 , 400 MHz) for pyrrole adduct 11	S30
Figure S44. HSQC spectrum (CD_3NO_2 , 400 MHz) for N-Me-pyrrole adduct 12	S31
Figure S45. HMBC spectrum (CD_3NO_2 , 400 MHz) for N-Me-pyrrole adduct 12	S31
Figure S46. HSQC spectrum (CD_3NO_2 , 400 MHz) for furan adduct 13	S32
Figure S47. HMBC spectrum (CD_3NO_2 , 400 MHz) for furan adduct 13	S32
Figure S48. HSQC spectrum (CD_3NO_2 , 400 MHz) for 2-methylfuran adduct 14	S33
Figure S49. HMBC spectrum (CD_3NO_2 , 400 MHz) for 2-methylfuran adduct 14	S33
Figure S50. HSQC spectrum (CD_3NO_2 , 400 MHz) for benzothiophene adduct 15	S34
Figure S51. HMBC spectrum (CD_3NO_2 , 400 MHz) for benzothiophene adduct 15	S34
Figure S52. HSQC spectrum (CD_3NO_2 , 400 MHz) for indole adduct 16	S35
Figure S53. HMBC spectrum (CD_3NO_2 , 400 MHz) for indole adduct 16	S35
Figure S54. HSQC spectrum (CD_3NO_2 , 400 MHz) for 4,6-Me ₂ -DBT adduct 17	S36
Figure S55. HMBC spectrum (CD_3NO_2 , 400 MHz) for 4,6-Me ₂ -DBT adduct 17	S36
Figure S56. HSQC spectrum (CD_3CN , 400 MHz) for THT adduct 18	S37
Figure S57. HMBC spectrum (CD_3CN , 400 MHz) for THT adduct 18	S37
Figure S58. COSY spectrum (CD_3CN , 300 MHz) for propanoate complex 19	S38

III. Computational Details

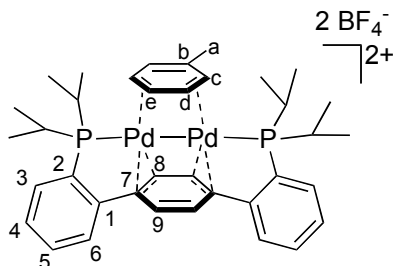
General Considerations	S39
Figure S59. Qualitative MO bonding analysis	S40
Figure S60. Examples of MOs depicting Pd-diene bonding	S41
Figure S61. Mulliken Charges of Free Heterocycles	S42
Cartesian coordinates of $[\text{Pd}_2\text{L}(\text{C}_6\text{H}_6)]^{2+}$	S43
Cartesian coordinates of $[\text{Pd}_2\text{L}(\text{C}_4\text{H}_6)]^{2+}$	S44
Cartesian coordinates of $[\text{Pd}_2\text{L}(\text{C}_6\text{H}_8)]^{2+}$	S45

Cartesian coordinates of $[Pd_2L(C_4H_4O)]^{2+}$	S46
Cartesian coordinates of $[Pd_2L(C_4H_4S)]^{2+}$	S47
Cartesian coordinates of $[Pd_2L(C_3H_5)]^+$	S48
IV. Crystallographic Data	
Refinement details	S49
Table S1. Crystal and refinement data for 3-9, 14-17, 20, 21	S50
Figure S62. Structural drawing of 3	S51
Figure S63. Structural drawing of 4	S51
Figure S64. Structural drawing of 5	S52
Figure S65. Structural drawing of 6	S52
Figure S66. Structural drawing of 7	S53
Figure S67. Structural drawing of 8	S54
Figure S68. Structural drawing of 9	S54
Figure S69. Structural drawing of 14	S55
Figure S70. Structural drawing of 15	S55
Figure S71. Structural drawing of 16	S56
Figure S72. Structural drawing of 17	S56
Figure S73. Structural drawing of 20	S57
Figure S74. Structural drawing of 21	S57
References	S58

I. Experimental Details

General considerations. All manipulations were carried out in an inert atmosphere glovebox or using standard Schlenk line techniques. Diphosphine **1** and dipalladium complex **2** were synthesized as previously reported.^{1,2} 1,4-Butadiene was used as purchased from Aldrich. Other organic reagents were dried by stirring over sodium metal or calcium hydride, degassed by 3 cycles of freeze-pump-thaw, and isolated via vacuum-transfer. Et₂O, toluene, THF, MeCN, and DCM were dried by the method of Grubbs.³ Deuterated solvents were purchased from Cambridge Isotope Laboratories and vacuum transferred from calcium hydride. All reagents, once degassed and dried, were stored in an inert atmosphere glovebox. ¹H and ¹³C NMR chemical shifts are reported relative to residual solvent peaks: CD₃NO₂ (¹H: 4.33; ¹³C: 61.39 ppm) and others as reported in the literature.⁴ ¹⁹F and ³¹P NMR chemical shifts are reported with respect to the instrument solvent lock. All NMR spectra were recorded at room temperature unless indicated otherwise. Gas chromatography-mass spectrometry (GC-MS) analysis was performed upon filtering the sample through a plug of silica gel. Fast atom bombardment-mass spectrometry (FAB-MS) analysis was performed with a JEOL JMS-600H high resolution mass spectrometer. Elemental analysis was conducted by Complete Analysis Laboratories (Parsippany, NJ).

Synthesis of **3**



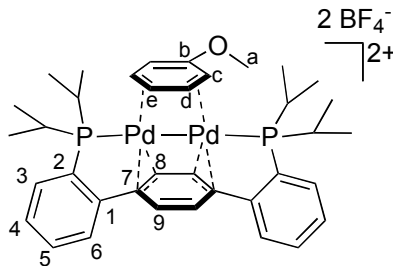
A solution of **2** (628.9 mg, 0.99 mmol) in MeCN (10 mL) was transferred over solid **1** (424.0 mg, 0.99 mmol) with stirring. After 2 h, volatiles were removed under vacuum. The solids were triturated with THF and filtered through Celite with minimal DCM (~8 mL). Toluene (6 mL) was layered on the DCM eluent. Red crystals formed and were rinsed with minimal DCM to yield pure **3** (668.1 mg, 80%). Substituting Pd₂(dba)₃ for Pd₂(dba)₃•CHCl₃ in the synthesis of **2** led to less pure **3**, as determined by crude ³¹P NMR spectroscopy. ¹H NMR (400 MHz, CD₂Cl₂) δ: 7.85 - 7.70 (m, Ar-H_{4,6}, 6H), 7.46 (app d, *J* = 7.4 Hz, Ar-H₃, 2H), 7.27 (br d, H_c, 2H), 7.21 (br t, H_d, 2H), 6.21 (s, Ar-H₈ + Ar-H₉, 4H), 6.19 (m, H_e, 1H), 3.13 (m, CH(CH₃)₂, 4H), 1.97 (s, CH₃, 3H), 1.34 (m, CH(CH₃)₂, 24H). ¹⁹F{¹H} NMR (376 MHz, CD₂Cl₂) δ: -151.9 (s). ³¹P{¹H} NMR (162 MHz, CD₂Cl₂) δ: 64.4 (s). ¹³C{¹H} NMR (101 MHz, CD₂Cl₂) δ: 146.0 (t, *J* = 11.5 Hz, Ar-C₁), 142.5 (s, tol-C_b), 133.7 (s, Ar-C₄), 132.9 (s, Ar-C₅), 132.1 (t, *J* = 8.0 Hz, Ar-C₃), 130.5 (s, Ar-C₆), 128.5 (d, *J* = 40.4 Hz, Ar-C₂), 115.0 (s, Ar-C₇), 112.9 – 109.9 (br, Ar-C₈ and Ar-C₉), 104.7 (s, tol-C_c), 100.9 (s, tol-C_e), 91.3 (s, tol-C_d), 27.8 (t, *J* = 10.1 Hz, CH(CH₃)₂), 21.4 (s, tol-CH₃), 18.4 (s, CH(CH₃)₂), 17.7 (s, CH(CH₃)₂). Anal. Calcd. for C₃₇H₄₈B₂F₈P₂Pd₂ (%): C, 47.22; H, 5.14. Found: C, 47.13; H, 5.27.

Isolation of toluene-free, acetonitrile-exchanged **3**

Method A: A sample of **3** was dissolved in minimal MeCN, precipitated with Et₂O (5:1 vs MeCN), and collected by filtration. This procedure was repeated 3 times, yielding toluene-free (as determined by ¹H NMR) **3**. *Method B:* A solution of **2** (136.8 mg, 0.216 mmol) in 10 mL and added over **1** (100.0 mg, 0.216 mmol). The mixture was stirred for 45 min, then filtered. Et₂O (50 mL) was added to precipitate out an orange powder, which was collected by filtration (150.2 mg, 55% yield assuming two acetonitrile ligands). ¹H NMR (300 MHz, CD₃CN) δ: 7.81-7.63 (m,

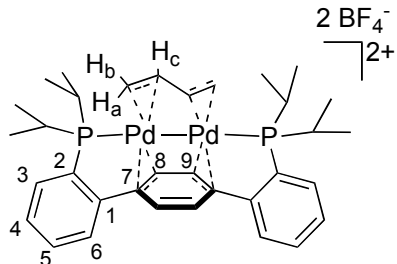
6H, aryl-*H*), 7.56 (app d, 2H, aryl-*H*), 5.99 (s, 4H, central aryl-*H*), 2.82 (m, 4H, $CH(CH_3)_2$), 1.32–1.15 (m, 24H, $CH(CH_3)_2$). $^{31}P\{^1H\}$ NMR (121 MHz, CD_3CN) δ : 62.0 (s). To observe the bound acetonitrile ligands, a 1H NMR spectrum was also recorded in CD_2Cl_2 . 1H NMR (300 MHz, CD_2Cl_2) δ : 7.83 – 7.59 (m, 6H, aryl-*H*), 7.50 (app d, 2H, aryl-*H*), 5.96 (s, 4H, central aryl-*H*), 2.91 – 2.68 (m, 4H, $CH(CH_3)_2$), 2.56 (s, 6H, $NCCH_3$), 1.47 – 1.16 (m, 24H, $CH(CH_3)_2$).

Synthesis of anisole-capped species 4



A solution of **3** (42 mg, mmol) in MeCN was concentrated under vacuum to a red-orange oil. This oil was reconstituted with DCM and layered under anisole. Red crystals were observed on the vial walls. The mother liquor was decanted and washed with Et_2O , and the crystals were collected by filtration. Recrystallization from vapor diffusion of Et_2O into a $MeNO_2$ solution yielded clean **4** (27 mg, 63%). 1H NMR (600 MHz, CD_3NO_2) δ : 7.97 (m, 2H, Ar-*H*₆), 7.86 (app t, 2H, Ar-*H*₅), 7.81 (app t, 2H, Ar-*H*₄), 7.60 (app d, 2H, Ar-*H*₃), 7.31 (app t, 2H, Ar-*H*_d), 6.95 (app d, 2H, *H*_a), 6.21 (br s, 4H, Ar-*H*₈ + Ar-*H*₉), 5.96 (app t, 1H, *H*_e), 3.51 (s, 3H, *H*_a), 3.32 (m, 4H, $CH(CH_3)_2$), 1.34 (m, 24H, $CH(CH_3)_2$). $^{31}P\{^1H\}$ NMR (162 MHz, CD_3NO_2) δ : 65.8 (br s) $^{19}F\{^1H\}$ NMR (376 MHz, CD_3NO_2) δ : -152.7 (s). $^{13}C\{^1H\}$ NMR (CD_3NO_2 , shifts determined from HSQC and HMBC 2D spectra): 162.6 (*C*_b), 145.8 (Ar-*C*₁), 133.2 (Ar-*C*₆), 133.3 (Ar-*C*₅), 131.7 (Ar-*C*₃), 130.1 (Ar-*C*₄), 130.0 (Ar-*C*₂), 114.8 (Ar-*C*₇), (Ar-*C*_{8/9}), 94.7 (*C*_d), 87.4 (*C*_e), 86.7 (*C*_c), 55.9 (*C*_a), 27.2 ($CH(CH_3)_2$), 17.1 ($CH(CH_3)_2$). Ar-*C*_{8/9} not observed by 1H - ^{13}C 2D NMR due to broadness of Ar-*H*_{8/9} signal.

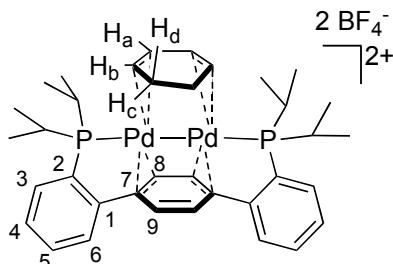
Synthesis of butadiene-capped species 5



A mixture of **3** (8.2 mg, 8.7 mmol) in CD_3CN (0.5 mL) was transferred into a J. Young NMR tube. The mixture was degassed by three freeze-pump-thaw cycles. With the aid of a manometer and calibrated gas bulb, the tube was pressurized with 3.9 atm of butadiene. The reaction turned yellow in seconds upon shaking. Reaction was confirmed by NMR, and the product was crystallized by layering the crude mixture under Et_2O to yield yellow crystals. 1H NMR (400 MHz, CD_3CN) δ : 8.03 (m, 2H, Ar-*H*), 7.88 (m, 4H, Ar-*H*), 7.75 (app d, 2H, Ar-*H*), 6.10 (d, *J* = 7.2 Hz, 2H, central aryl-*H*), 5.85 (d, *J* = 7.2 Hz, 2H, central aryl-*H*), 5.33 (m, 2H, butadiene-*H*_b), 3.36 (m, 2H, $CH(CH_3)_2$), 3.19 (m, 2H, $CH(CH_3)_2$), 3.12 (app d, *J* = 13.8 Hz, 2H, butadiene-*H*_a), 2.71 (m, butadiene-*H*_c), 1.50–0.86 (m, 24H, $CH(CH_3)_2$). $^{19}F\{^1H\}$ NMR (282 MHz, CD_3CN) δ : -151.6 (s). $^{31}P\{^1H\}$ NMR (121 MHz, CD_3CN) δ : 78.8 (s). $^{13}C\{^1H\}$ NMR (101 MHz, toluene) δ : 146.7 (app t, Ar-*C*₁), 136.7 (app t, Ar-*C*₂), 134.6 (br, Ar-*C*₆ + Ar-*C*₅), 133.9 (app t, Ar-*C*₃), 131.5 (s, Ar-*C*₄), 116.7 (app t, Ar-*C*₇), 111.3 (s, Ar-*C*_{8/9}), 109.1 (s, Ar-*C*_{9/8}), 89.4 (s, $CHCH_2$), 62.2 (s,

CHCH_2), 29.8 (app dd, $\text{CH}(\text{CH}_3)_2$), 19.4 (s, $\text{CH}(\text{CH}_3)_2$), 18.8 (s, $\text{CH}(\text{CH}_3)_2$). Anal. Calcd. for $\text{C}_{34}\text{H}_{46}\text{B}_2\text{F}_8\text{P}_2\text{Pd}_2$ (%): C, 45.22; H, 5.13. Found: C, 45.18; H, 5.02.

Synthesis of 1,3-cyclohexadiene-capped species 6



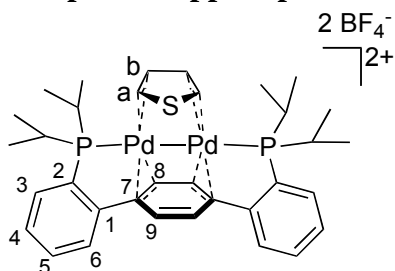
To a mixture of **3** (84.2 mg, 0.09 mmol) in MeCN (4 mL) was added 1,3-cyclohexadiene (10.4 mL, 0.11 mmol). The reaction quickly changed from red to light yellow in color. After stirring for 15 minutes, the reaction was concentrated under vacuum and washed with benzene to remove excess cyclohexadiene. The resultant solid was redissolved in MeCN and crystallized by vapor diffusion of Et₂O to yield yellow-orange crystals (73.8 mg, 89%). ¹H NMR (300 MHz, CD₃CN) δ: 8.00-7.76 (m, 8H, H₃₋₆), 7.20 (br, 2H, H_b), 6.37 (s, 2H, Ar-H₉), 5.46 (s, 2H, Ar-H₈), 4.80 (m, 2H, H_a), 3.25 (m, 2H, CH(CH₃)₂), 3.12 (m, 2H, CH(CH₃)₂), 1.97 (m, 2H, H_d), 1.47 (m, 12H, CH(CH₃)₂), 0.98 (m, 12H, CH(CH₃)₂), 0.29 (app dd, 2H, H_c). ³¹P{¹H} NMR (121 MHz, CD₃CN) δ: 66.4 (s). ¹⁹F{¹H} NMR (282 MHz, CD₃CN) δ: -151.6 (s). ¹³C{¹H} NMR (101 MHz, CD₃CN) δ: 146.7 (app t, Ar-C₁), 137.0 - 135.9 (app t, Ar-C₂), 134.5 (s, Ar-C₆), 134.4 (s, Ar-C₅), 133.8 (app t, Ar-C₃), 131.4 (s, Ar-C₄), 122.3 (s, Ar-C₉), 117.6 (app t, Ar-C₇), 97.4 (s, Ar-C₈), 83.0 (s, CH=CH-CH=CH), 81.6 (s, CH=CH-CH=CH), 28.9 (s, CH(CH₃)₂), 28.2 (app d, CH(CH₃)₂), 23.9 (s, CH=CH-CH₂), 19.7 (s, CH(CH₃)₂), 19.1 (s, CH(CH₃)₂), 18.0 (app t, J = 2.4 Hz, CH(CH₃)₂), 17.9 (s, CH(CH₃)₂). Anal. Calcd. for $\text{C}_{36}\text{H}_{48}\text{B}_2\text{F}_8\text{P}_2\text{Pd}_2$ (%): C, 46.53; H, 5.21. Found: C, 46.46; H, 5.19.

Synthesis of species 7-17

The procedure to synthesize **7** is described. This procedure was general for the synthesis of species **7-17**. To a solution of acetonitrile-exchanged **3** (112.0 mg, 0.12 mmol) in DCM (5 mL) was added slowly added excess thiophene (1 mL). The reaction changed from red to orange in color with fine precipitate in seconds. After stirring for 1 h, the suspension was filtered over Celite and washed with DCM to remove excess thiophene. The orange solids were washed through Celite with CH₃NO₂. Orange crystals (109.1 mg, 98%) were grown from vapor diffusion of Et₂O into a CH₃NO₂ solution of this compound.

For **10**, **14-17**, the product did not precipitate out of DCM. Instead, the product was crashed out of DCM by addition of Et₂O, collected by filtration, and purified by repeated cycles of dissolution in DCM, addition of excess heterocycle ligand, and precipitation with Et₂O. Crystals were similarly grown by vapor diffusion of Et₂O into CH₃NO₂.

Thiophene-capped species 7



¹H NMR (400 MHz, CD₃NO₂) δ: 8.80 (m, H_a, 2H), 7.98 (m, Ar-H₆, 2H), 7.88 (m, Ar-H₅, 2H), 7.82 (m, Ar-H₄, 2H), 7.65 (app d, Ar-H₃, 2H), 6.49 (app t, H_b, 2H), 6.25 (s, Ar-H₈₊₉, 2H), 3.30 (m, CH(CH₃)₂, 4H), 1.36 (m, CH(CH₃)₂, 24H). ¹⁹F NMR (376 MHz, CD₃NO₂) δ: -152.3 (s). ³¹P NMR (162 MHz, CD₃NO₂) δ: 65.1 (s). ¹³C NMR (101 MHz, CD₃NO₂) δ: 146.1 (app t, Ar-C₁), 134.3 (app t, Ar-C₂), 133.7 (s, Ar-C₆), 133.5 (s, Ar-C₅), 132.3 (app t, Ar-C₃), 130.2 (app t, Ar-C₄), 116.4 (app t, Ar-C₇), 111.6 (br s, Ar-C₈₊₉), 99.0 (app t, C_b), 89.2 (s, C_a), 27.2 (app td, CH(CH₃)₂), 17.7 (app t, CH(CH₃)₂), 17.1 (s, CH(CH₃)₂). Anal. Calcd. for C₃₄H₄₄B₂F₈SP₂Pd₂(%): C, 43.76; H, 4.75. Found: C, 43.66; H, 4.69.

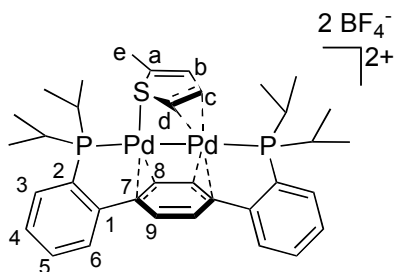
Synthesis of 2,5-dideuterothiophene

This procedure was adapted from a literature procedure.⁵ A ~6M solution of D₂SO₄ in D₂O (3 mL) was added to neat thiophene (1 mL) in a Schlenk tube with a magnetic stir bar. The tube was sealed with a Teflon screw-cap and heated to 100 °C with vigorous stirring. After 10 h, the organic phase from the reaction was separated from the aqueous phase, initially dried over MgSO₄, further dried over Na, degassed via freeze-pump-thaw, and isolated via vacuum transfer. GC-MS data confirmed dideuterated thiophene to be the major product with trace amounts of trideuterated product. By ¹H NMR (C₆D₆) the multiplet at 6.92 ppm in natural abundance thiophene is nearly absent relative to the multiplet at 6.82 ppm. This mixture of isotopomers was used without further purification.

Synthesis of thiophene-capped species d₂-7

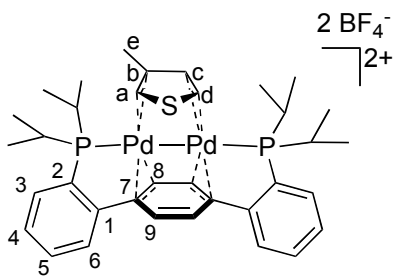
Synthesis was analogous to that for 7, but with 2,5-dideuterothiophene in place of natural abundance thiophene. ¹H NMR(CD₃NO₂, 300 MHz): The multiplet present in 7 at 8.80 ppm was absent in d₂-7.

2-Me-Thiophene-capped species 8



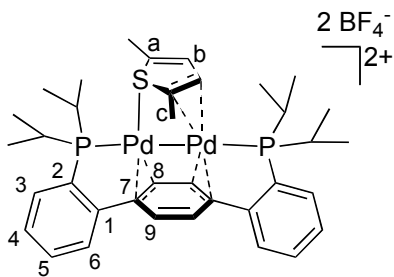
¹H NMR (400 MHz, CD₃NO₂) δ: 8.01 (m, 2H, Ar-H₆), 7.87 (m, 2H, Ar-H₅), 7.83 (m, 2H, Ar-H₄), 7.74 – 7.69 (app d, 2H, Ar-H₃), 7.65 (m, 1H, H_c), 7.02 (m, 1H, H_d) 6.11 (s, 4H, Ar-H₈ + Ar-H₉), 4.98 (m, 1H, H_b), 3.32 (br, 2H, CH(CH₃)₂), 3.22 (br, 2H, CH(CH₃)₂) 2.16 (s, 3H, H_e), 1.53 – 1.28 (m, 24H, CH(CH₃)₂). ³¹P NMR (121 MHz, CD₃NO₂) δ: 68.3 (s). ¹⁹F NMR (376 MHz, CD₃NO₂) δ: -152.4 (s). ¹³C NMR (CD₃NO₂, shifts determined from HSQC and HMBC 2D spectra): 149.9 (Ar-C_a), 145.9 (Ar-C₁), 134.9 (Ar-C₂), 133.6 (Ar-C₆), 133.5 (Ar-C₅), 132.3 (Ar-C₃), 132.0 (C_d), 130.0 (Ar-C₄), 117.5 (Ar-C₈ + Ar-C₉), 111.8 (Ar-C₇), 81.1 (C_c), 78.5 (C_b), 28.0 (CH(CH₃)₂), 27.6 (CH(CH₃)₂), 17.6 (CH(CH₃)₂), 17.1 (CH(CH₃)₂), 14.3 (C_e)

3-Me-Thiophene-capped species 9



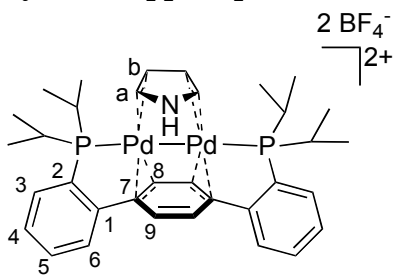
¹H NMR (300 MHz, CD₃NO₂) δ: 8.29 (app t, 1H, H_a), 8.11 (app td, J_{He} = 3.4 Hz, 1H, H_d), 8.04 – 7.92 (m, 2H, Ar-H₆), 7.86 (m, 2H, Ar-H₅), 7.82 (m, 2H, Ar-H₄), 7.64 (m, 2H, Ar-H₃), 6.91 (d, J = 3.4 Hz, 1H, H_c), 6.24 (br s, 4H, Ar-H₈ + Ar-H₉), 3.28 (m, 4H, CH(CH₃)₂), 2.24 (s, 3H, H_e), 1.66 – 1.17 (m, 24H, CH(CH₃)₂). ³¹P NMR (162 MHz, CD₃NO₂) δ: 65.9 (s). ¹⁹F NMR (376 MHz, CD₃NO₂) δ: -152.7 (s). ¹³C NMR (CD₃NO₂, shifts determined from HSQC and HMBC 2D spectra): 146.2 (Ar-C₁), 133.5 (Ar-C₆ + Ar-C₅), 133.2 (Ar-C₂), 132.0 (Ar-C₃), 130.3 (Ar-C₄), 127.5 (C_b), 119.5 (Ar-C₇), 115.4 (Ar-C₈ + Ar-C₉), 100.0 (C_e), 87.9 (C_a), 87.3 (C_d), 27.3 (CH(CH₃)₂), 17.1 (CH(CH₃)₂), 17.0 (CH(CH₃)₂), 16.5 (C_e).

2,5-Me₂-Thiophene-capped species 10



¹H NMR (400 MHz, CD₃NO₂) δ: 8.02 (app t, 2H, Ar-H₆), 7.85 (m, 4H, Ar-H₄ + Ar-H₅), 7.79–7.55 (br m, 2H, Ar-H₃), 7.09 (s, 2H, H_b), 6.15 (br s, 4H, Ar-H₈ + Ar-H₉), 3.28 (m, 4H, CH(CH₃)₂), 2.73 (s, 6H, H_c), 1.60 – 1.17 (m, 24H, CH(CH₃)₂). ³¹P NMR (121 MHz, CD₃NO₂) δ: 70.1 (d, J = 175 Hz), 65.6 (d, J = 175 Hz). ¹⁹F NMR (376 MHz, CD₃NO₂) δ: -152.7 (s). ¹³C NMR (CD₃NO₂, shifts determined from HSQC and HMBC 2D spectra): 145.9 (Ar-C₁), 133.7 (Ar-C₅), 133.2 (Ar-C₆), 132.2 (Ar-C₂), 131.5 (Ar-C₃), 129.9 (Ar-C₄), 126.1 (Ar-C₇), 124.3 (C_a), 108.4 (Ar-C₈ + Ar-C₉), 108.4 (C_b), 27.7 (CH(CH₃)₂), 17.5 (CH(CH₃)₂), 17.4 (CH(CH₃)₂), 15.4 (C_c).

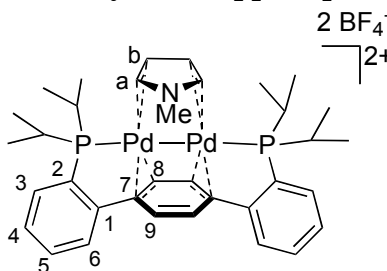
Pyrrole-capped species 11



¹H NMR (500 MHz, CD₃NO₂) δ: 9.76 (br s, 1H, N-H), 8.89 (m, 2H, H_a), 7.93 (m, 2H, Ar-H₆), 7.81 (m, 2H, Ar-H₅), 7.76 (m, 2H, Ar-H₄), 7.59 (app d, 2H, Ar-H₃), 6.24 (br s, 2H, Ar-H_{8/9}), 6.15 (br s, 4H, Ar-H_{8/9} + H_b), 3.21 (br m, 2H, CH(CH₃)₂), 3.04 (br m, 2H, CH(CH₃)₂), 1.55–1.37 (m, 12H, CH(CH₃)₂), 1.19 (m, 12H, CH(CH₃)₂). ³¹P{¹H} NMR (121 MHz, CD₃NO₂) δ: 60.2 (s). ¹⁹F{¹H} NMR (376 MHz, CD₃NO₂) δ: -152.7 (s). ¹³C NMR (CD₃NO₂, shifts determined from

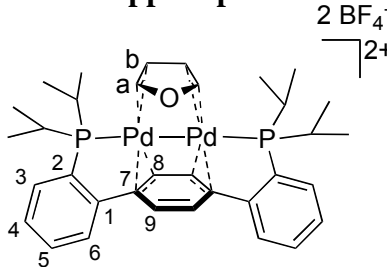
HSQC and HMBC 2D spectra): 146.3 (Ar-C₁), 135.2 (Ar-C₂), 133.4 (Ar-C₆), 132.9 (Ar-C₅), 132.0 (Ar-C₃), 129.7 (Ar-C₄), 105.2 (C_a), 79.2 (C_b), 117.0 (Ar-C_{8/9}), 111.7 (Ar-C₇) 103.5 (Ar-C_{8/9}), 27.2 (CH(CH₃)₂), 26.1 (CH(CH₃)₂), 18.3 (CH(CH₃)₂), 17.5 (CH(CH₃)₂), 16.8, (CH(CH₃)₂), 16.6 (CH(CH₃)₂).

N-Me-Pyrrole-capped species 12



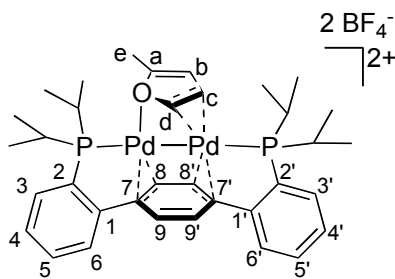
¹H NMR (400 MHz, CD₃NO₂) δ: 8.62 (s, 2H, H_a), 7.94 (m, 2H, Ar-H₆), 7.82 (m, 2H, Ar-H₅), 7.77 (m, 2H, Ar-H₄), 7.62 (app d, 2H, Ar-H₃), 6.28 (s, 2H, Ar-H_{8/9}), 6.17 (s, 2H, Ar-H_{8/9}), 6.09 (s, 2H, H_b), 3.22 (br m, 2H, CH(CH₃)₂), 3.02 (br m, 2H, CH(CH₃)₂), 1.55-1.37 (m, 12H, CH(CH₃)₂), 1.19 (m, 12H, CH(CH₃)₂). ³¹P NMR (121 MHz, CD₃NO₂) δ: 58.5 (s) ¹⁹F NMR (376 MHz, CD₃NO₂) δ: -152.7 (s). ¹³C NMR (CD₃NO₂, shifts determined from HSQC and HMBC 2D spectra): 145.5 (Ar-C₁), 134.3 (Ar-C₂), 133.4 (Ar-C₆), 132.9 (Ar-C₅), 132.0 (Ar-C₃), 129.6 (Ar-C₄), 115.6 (Ar-C_{8/9}), 111.5 (Ar-C₇), 103.6 (Ar-C_{8/9}), 109.4 (C_a), 78.8 (C_b), 35.5 (N-CH₃), 27.2 (CH(CH₃)₂), 26.2 (CH(CH₃)₂), 18.6 (CH(CH₃)₂), 17.5 (CH(CH₃)₂), 16.7 (CH(CH₃)₂), 16.6 (CH(CH₃)₂).

Furan-capped species 13



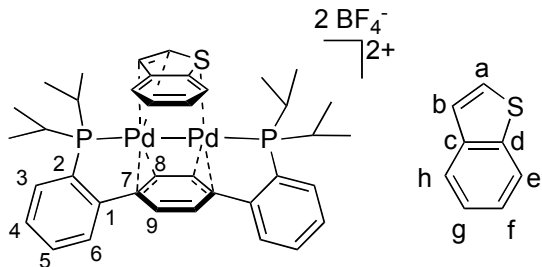
¹H NMR (400 MHz, CD₃NO₂) δ: 9.42 (m, H_a, 2H), 7.96 (m, Ar-H₆, 2H), 7.87 (m, Ar-H₅, 2H), 7.81 (m, Ar-H₄, 2H), 7.68 (app d, Ar-H₃, 2H), 6.41 (m, H_b, 2H), 6.32 (d, J = 1.4 Hz, Ar-H₉, 2H), 6.27 (d, J = 1.4 Hz, Ar-H₈, 2H), 3.27 (m, CH(CH₃)₂, 2H), 3.06 (m, CH(CH₃)₂, 2H), 1.54 (app dd, CH(CH₃)₂, 6H), 1.44 (app dd, CH(CH₃)₂, 6H), 1.19 (app dd, CH(CH₃)₂, 6H), 1.14 (app dd, CH(CH₃)₂, 6H). ¹⁹F{¹H} NMR (376 MHz, CD₃NO₂) δ: -152.5 (s). ³¹P{¹H} NMR (162 MHz, CD₃NO₂) δ: 61.5 (s). ¹³C{¹H} NMR (101 MHz, CD₃NO₂) δ: 145.4 (app t, Ar-C₁), 134.6 (app t, Ar-C₂), 133.9 (s, Ar-C₆), 133.4 (s, Ar-C₅), 132.3 (app t, Ar-C₃), 130.4 (app t, Ar-C₄), 120.8 (s, C_a), 119.1 (app t, Ar-C₉), 114.8 (app t, Ar-C₇), 103.3 (s, Ar-C₈), 83.0 (m, C_b), 27.7 (app td, CH(CH₃)₂), 26.4 (app t, CH(CH₃)₂), 18.8 (app t, CH(CH₃)₂), 17.6 (app t, CH(CH₃)₂), 16.8 (app t, CH(CH₃)₂), 16.6 (app t, CH(CH₃)₂). Anal. Calcd. for C₃₄H₄₄B₂F₈OP₂Pd₂(%): C, 44.53; H, 4.84. Found: C, 44.40; H, 4.64.

2-Me-Furan-capped species 14



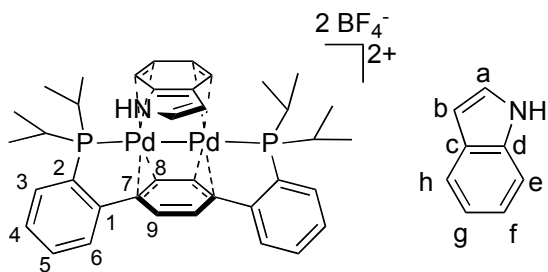
¹H NMR (400 MHz, CD₃NO₂) δ: 9.25 (app t, 1H, H_c), 8.02 – 7.92 (m, 2H, Ar-H₆ + Ar-H_{6'}), 7.91 – 7.74 (m, 4H, Ar-H₅ + Ar-H_{5'} + Ar-H₄ + Ar-H_{4'}), 7.73 – 7.60 (m, 2H, Ar-H₃ + Ar-H_{3'}), 7.28 (m, 1H, H_d), 6.38 – 6.25 (m, 2H, Ar-H_{8/9/8'/9'}), 6.21 (app dd, 1H, Ar-H_{8/9/8'/9'}), 6.08 (app dd, 1H, Ar-H_{8/9/8'/9'}), 5.61 (s, 1H, H_b), 3.33 (m, 1H, CH(CH₃)₂), 3.17 (m, 1H, CH(CH₃)₂), 3.04 (m, 2H, CH(CH₃)₂), 2.78 (d, J = 2.1 Hz, 3H, H_e), 1.70 – 1.03 (m, 24H, CH(CH₃)₂). ³¹P NMR (162 MHz, CD₃NO₂) δ: 60.9 (d, J = 162 Hz), 57.4 (d, J = 162 Hz). ¹⁹F NMR (376 MHz, CD₃NO₂) δ: -152.7 (s). ¹³C NMR (CD₃NO₂, shifts determined from HSQC and HMBC 2D spectra): 179.8 (C_a), 145.7 (Ar-C_{1/1'}), 145.5 (Ar-C_{1/1'}), 135.0 (Ar-C_{2/2'}), 134.0 (Ar-C_{2/2'}), 133.6 (Ar-C₆ + Ar-C_{6'}), 133.4 (Ar-C_{5/5'}), 133.2 (Ar-C_{5/5'}), 130.2 (Ar-C_{4/4'}), 130.1 (Ar-C_{4/4'}), 132.3 (Ar-C_{3/3'}), 131.8 (Ar-C_{3/3'}), 117.0 (Ar-C_{8/9/8'/9'}), 115.6 (Ar-C_{8/9/8'/9'}), 107.0 (Ar-C_{8/9/8'/9'}), 102.9 (C_c), 98.4 (Ar-C_{8/9/8'/9'}), 85.6 (C_b), 65.5 (C_d), 27.5 (CH(CH₃)₂), 26.2 (CH(CH₃)₂), 26.1 (2C, CH(CH₃)₂), 19.9 (C_e), 18.6 (CH(CH₃)₂), 18.3 (CH(CH₃)₂), 18.0 (CH(CH₃)₂), 17.7 (CH(CH₃)₂), 17.1 (CH(CH₃)₂), 17.0 (CH(CH₃)₂), 16.9 (CH(CH₃)₂), 16.2 (CH(CH₃)₂).

Benzothiophene-capped species 15



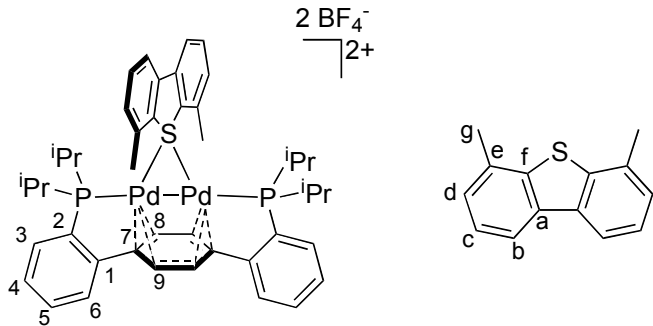
Recrystallization by vapor diffusion of Et₂O into a MeNO₂ solution yielded XRD-quality orange prisms (80.2 mg, 80%). ¹H NMR (400 MHz, CD₃NO₂) δ: 8.26 (app q, H_b, 1H), 8.09 – 7.96 (overlapping multiplets, H_f and one each of Ar-H₃₋₆ and Ar-H_{3'-6'}, 3H), 7.92 – 7.78 (overlapping multiplets, H_g and two each of Ar-H₃₋₆ and Ar-H_{3'-6'}, 5H), 7.73 – 7.68 (app d, one of Ar-H₃₋₆ or Ar-H_{3'-6'}, 1H), 7.61 (app d, one of Ar-H₃₋₆ or Ar-H_{3'-6'}, 1H), 7.57 (app td, H_h, 1H), 7.49 (app td, H_e, 1H), 6.13 (dd, J = 8.0, 2.0 Hz, Ar-H₉, 1H), 6.09 (dd, J = 8.0, 1.6 Hz, Ar-H_{9'}, 1H), 5.99 (dd, J = 7.2, 2.0 Hz, Ar-H₈, 1H), 5.75 (dd, J = 7.2, 1.6 Hz, Ar-H_{8'}, 1H), 5.18 (app t, H_a, 1H), 3.72 (m, CH(CH₃)₂, 1H), 3.31 (m, CH(CH₃)₂, 3H), 1.89 – 1.66 (m, CH(CH₃)₂, 9H), 1.66 – 1.56 (m, CH(CH₃)₂, 3H), 1.36 – 1.22 (m, CH(CH₃)₂, 3H), 1.13 – 0.92 (m, CH(CH₃)₂, 9H). ¹⁹F NMR (376 MHz, CD₃NO₂) δ: -152.5 (s). ³¹P{¹H} NMR (162 MHz, CD₃NO₂) δ: 67.3 (d, J = 168 Hz), 65.9 (d, J = 168 Hz). ¹³C NMR (101 MHz, CD₃NO₂) δ: 145.8 (overlapping multiplets, Ar-C₁ and Ar-C_{1'}), 139.6 (s, C_c), 138.8 (s, C_d), 134.7 (overlapping multiplets, Ar-C₂ and Ar-C_{2'}), 133.6 (s, Ar-C₆ or Ar-C_{6'}), 133.5 (s, Ar-C₆ or Ar-C_{6'}), 133.4 (s, Ar-C₅ and Ar-C_{5'}), 132.5 (app d, Ar-C₃ or Ar-C_{3'}), 132.1 (app d, Ar-C₃ or Ar-C_{3'}), 130.4 (app t, Ar-C₄ and Ar-C_{4'}), 130.0 (s, C_b), 129.5 (s, C_e), 127.5 (s, C_f), 125.5 (s, C_g), 119.0 (s, C₉), 117.4 (s, C_{9'}), 114.1 (t, C₇), 111.3 (t, C_{7'}), 99.5 (s, C₈), 97.4 (s, C_{8'}), 76.7 (s, C_b), 70.2 (s, C_a), 28.6 (m, CH(CH₃)₂), 27.7 (m, CH(CH₃)₂), 27.5 (m, CH(CH₃)₂), 27.2 (m, CH(CH₃)₂), 19.0 (br s, two of CH(CH₃)₂), 18.1 (app d, CH(CH₃)₂), 17.9 (br s, CH(CH₃)₂), 17.3 (br s, two of CH(CH₃)₂), 16.8 (app d, CH(CH₃)₂), 16.7 (app d, CH(CH₃)₂). Anal. Calcd. for C₃₈H₄₆B₂F₈P₂Pd₂S (%): C, 46.42; H, 4.72. Found: C, 46.30; H, 4.60.

Indole-capped species 16



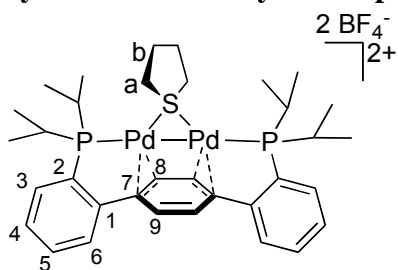
¹H NMR (400 MHz, CD₃NO₂) δ: 9.93 (br s, 1H, H_a), 9.09 (br s, 1H, N-H), 8.74 (m, 1H, H_h), 8.71 (m, 1H, H_e), 7.94 (br s, 2H, Ar-H₆), 7.84 (m, 2H, Ar-H₅), 7.81 (m, 2H, Ar-H₄), 7.52 (m, 2H, Ar-H₃), 7.14 (m, 1H, H_b), 6.48 (m, 2H, Ar-H_{8/9}), 5.97 (t, 1H, H_f), 5.87 (t, 1H, H_g), 5.57 (br s, 2H, Ar-H_{8/9}), 3.65 (m, 2H, CH(CH₃)₂), 3.23 (m, 2H, CH(CH₃)₂), 1.74 (m, 6H, CH(CH₃)₂), 1.09 (m, 6H, CH(CH₃)₂), 0.95 (m, 6H, CH(CH₃)₂). ³¹P NMR (121 MHz, CD₃NO₂) δ: 64.7 (br s). ¹⁹F NMR (376 MHz, CD₃NO₂) δ: -152.7 (s). ¹³C NMR (CD₃NO₂, shifts determined from HSQC and HMBC 2D spectra): 146.1 (Ar-C₁), 133.6 (Ar-C_{5/4}), 133.1 (Ar-C₆), 131.7 (Ar-C₃), 130.4 (C_a) 129.6 (Ar-C_{5/4}), 128.0 (C_b), 127.7 (Ar-C₂) 124.4 (C_d), 123.4 (Ar-C_{8/9}), 113.7 (Ar-C₇), 105.3 (Ar-C_{8/9}), 105.2 (C_c), 95.8 (Ar-C_{8/9}), 86.6 (C_{f/g}), 86.5 (C_{f/g}), 76.0 (C_h), 71.1 (C_e), 27.8 (CH(CH₃)₂), 26.2 (CH(CH₃)₂), 18.5 (CH(CH₃)₂), 17.7 (CH(CH₃)₂), 16.1 (CH(CH₃)₂), 16.0 (CH(CH₃)₂).

4,6-Dimethylbibenzothiophene-capped species 17



¹H NMR (400 MHz, CD₃NO₂) δ: 8.36 (app d, 2H, H_b), 7.95-7.78 (m, 10H, H_c + Ar-H_{3,6}), 7.50 (app d, 2H, H_d), 6.63 (s, 4H, Ar-H₈ + Ar-H₉), 2.66 (m, 4H, CH(CH₃)₂), 2.20 (s, 4H, H_g), 1.07 (app dd, 12H, CH(CH₃)₂), 0.90 (app dd, 12H, CH(CH₃)₂). ³¹P (121 MHz, CD₃NO₂) δ: 75.3 (s). ¹⁹F (376 MHz, CD₃NO₂) δ: -152.8 (s). ¹³C NMR (CD₃NO₂, shifts determined from HSQC and HMBC 2D spectra): 144.5 (Ar-C₁), 138.5 (C_a), 136.8 (Ar-C₂), 135.7 (C_e), 133.2 (C_c), (133.1, 132.3, 130.4), [overlapping peaks for (Ar-C₆), (Ar-C₅), (Ar-C₃), (Ar-C₄)], 132.0 (C_d), 126.3 (C_f), 122.9 (C_b), 113.3 (Ar-C₈ + Ar-C₉), 112.1 (Ar-C₇), 26.5 (CH(CH₃)₂), 21.4 (C_g), 18.4 (CH(CH₃)₂), 18.2(CH(CH₃)₂).

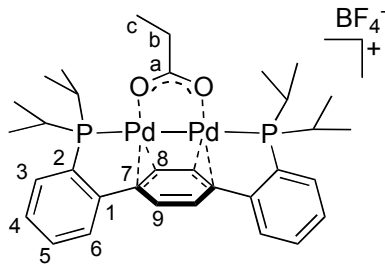
Synthesis of tetrahydrothiophene-capped species 18



Method A: **10** (75.8 mg, 0.08 mmol) was dissolved in CH₃NO₂ in a J. Young NMR tube. The solution was degassed with three cycles of freeze-pump-thaw, chilled with LN₂, and sealed under

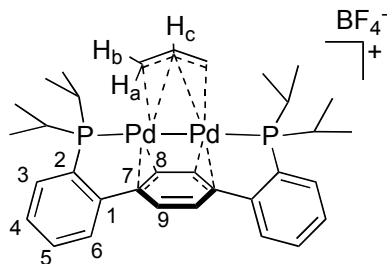
a ~1 atm stream of H₂ (regulated at r.t. with a Hg bubbler). The tube was warmed back up to r.t. and then continuously inverted. The reaction was monitored by ³¹P NMR and complete after 5h. The heterogeneous reaction mixture was filtered through Celite and volatiles were removed. The solids were triturated with THF, then filtered through Celite as a MeCN solution. Volatiles were removed again, yielding **18** an orange powder (75.0 mg, 99%). *Method B:* **18** was prepared from **3** (78.1 mg, 0.08 mmol) in the same manner as **7** (vide supra). The resulting orange solids (74.8 mg, 96%) were analytically pure. *Characterization:* ¹H NMR (300 MHz, CD₃CN) δ: 7.93 – 7.65 (m, Ar-H₃₋₆, 8H), 6.09 (s, Ar-H₈₊₉, 4H), 3.55 (app t, H_a, 4H), 2.81 (m, CH(CH₃)₂, 4H), 2.43 (m, H_b, 4H), 1.25 (app dd, CH(CH₃)₂, 12H), 1.10 (app dd, CH(CH₃)₂, 12H). ¹⁹F NMR (282 MHz, CD₃CN) δ: -151.6 (s). ³¹P{¹H} NMR (121 MHz, CD₃CN) δ: 69.8 (s). ¹³C{¹H} NMR (101 MHz, CD₃CN) δ: 146.2 (app t, Ar-C₁), 138.1 (app t, Ar-C₂), 134.6 (s, Ar-C₆), 133.9 (s, Ar-C₅), 133.6 (app t, Ar-C₃), 131.2 (s, Ar-C₄), 112.3 (s, Ar-C₈₊₉), 110.3 (app t, Ar-C₇), 46.2 (br s, C_a), 31.3 (s, C_b), 27.6 (m, CH(CH₃)₂), 20.4 (app q, CH(CH₃)₂), 19.4 (app d, CH(CH₃)₂). Anal. Calcd. for C₃₄H₄₈B₂F₈P₂Pd₂S (%): C, 43.57; H, 5.16. Found: C, 43.59; H, 5.09.

Synthesis of carboxylate-capped species **19**



A solution of **3** (23.4 mg, 0.025 mmol) in MeCN (3 mL) was added over NaO₂CEt (2.4 mg, 0.025 mmol). The ruby red solution did not appear to change color, but a reaction was evidenced by NMR spectroscopy. An orange precipitate was obtained by adding Et₂O to the crude MeCN mixture (18.5 mg, 89%) ¹H NMR (300 MHz, CD₃CN) δ: 7.74-7.46 (m, 8H, aryl-H₃₋₆), 5.89 (s, 4H, Ar-H₈₊₉), 2.65 (m, 4H, CH(CH₃)₂), 2.41 (q, J = 7.6 Hz, 2H, H_b), 1.29 (app dd, 12H, CH(CH₃)₂), 1.19-1.09 (m, 12H + 3H, CH(CH₃)₂ + H_c). ¹⁹F{¹H} NMR (282 MHz, CD₃CN) δ: -152.2 (s). ³¹P{¹H} NMR (121 MHz, CD₃CN) δ: 53.6 (s). ¹³C{¹H} NMR (101 MHz, CD₃CN) δ: 203.6 (app t, J = 4.8 Hz, C_a), 148.6 (app t, J = 13.8 Hz, Ar-C₁), 135.3 (t, J = 17.3 Hz, Ar-C₂), 133.9 (s, Ar-C₆), 133.2 (s, Ar-C₅), 132.2 (t, J = 8.7 Hz, Ar-C₃), 130.6 (s, Ar-C₄), 104.8 (s, Ar-C₈₊₉), 92.9 (t, J = 2.2 Hz, Ar-C₇), 32.9 (s, C_b), 26.8 (t, J = 9.1 Hz, CH(CH₃)₂), 19.4 (s, CH(CH₃)₂), 19.2 (t, J = 3.3 Hz, CH(CH₃)₂), 10.4 (s, C_c).

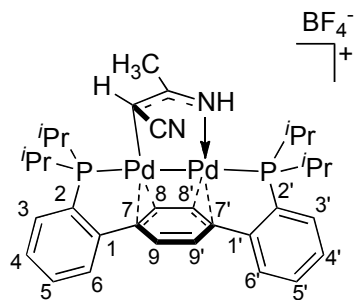
Synthesis of allyl-capped species **20**



To a red solution of **19** (10.6 mg, 0.0128 mmol) in MeCN (1 mL) was added tributylallyltin (4.0 uL, 0.0128 mmol). A yellow color evolved in less than a minute. After 10 minutes, the reaction mixture was filtered. The filtrate was concentrated under vacuum and washed with benzene. The remaining solid was redissolved in MeCN, filtered, and layered under Et₂O. XRD-quality yellow crystals were grown at -35 °C (8.1 mg, 79% yield). ¹H NMR (600 MHz, CD₃CN) δ: 7.88 (m, 2H, Ar-H₃), 7.70 (app t, 2H, Ar-H₄), 7.65 (app t, 2H, Ar-H₅), 7.58 (app d, 2H, Ar-H₆), 6.24 (s, 2H, Ar-H_{8/9}), 5.55 (s, 2H, Ar-H_{9/8}), 3.90 (m, 2H, allyl-H_{a/b}), 2.94 (m, 2H, CH(CH₃)₂), 2.76 (m, 2H,

$\text{CH}(\text{CH}_3)_2$, 2.40 (m, 1H, allyl- H_c), 1.26–1.15 (m, 12H + 2H, $\text{CH}(\text{CH}_3)_2$ + allyl- $H_{b/a}$), 1.07 (app dd, 6H, $\text{CH}(\text{CH}_3)_2$), 1.02 (app dd, 6H, $\text{CH}(\text{CH}_3)_2$). $^{19}\text{F}\{\text{H}\}$ NMR (282 MHz, CD_3CN) δ : -152.2 (s). $^{31}\text{P}\{\text{H}\}$ NMR (121 MHz, CD_3CN) δ : 50.5 (s). $^{13}\text{C}\{\text{H}\}$ NMR (101 MHz, CD_3CN) δ : 149.8 (app t, J = 13.5 Hz, Ar- C_1), 140.9 – 140.3 (app t, Ar- C_2), 134.2 (s, Ar- C_3), 133.5 (app t, J = 7.1 Hz, Ar- C_6), 132.7 (s, Ar- C_4), 130.0 (s, Ar- C_5), 120.4 (s, Ar- $C_{8/9}$), 117.0 (app t, J = 2.4 Hz, Ar- C_7), 97.3 (s, Ar- $C_{9/8}$), 70.5 (s, allyl-CH), 31.0 (s, allyl- CH_2), 27.4 (app t, J = 10.2 Hz, $\text{CH}(\text{CH}_3)_2$), 27.2 (t, J = 9.7 Hz, $\text{CH}(\text{CH}_3)_2$), 19.6 (t, J = 2.8 Hz, $\text{CH}(\text{CH}_3)_2$), 19.3 (t, J = 3.2 Hz, $\text{CH}(\text{CH}_3)_2$), 19.1 (s, $\text{CH}(\text{CH}_3)_2$), 18.9 (s, $\text{CH}(\text{CH}_3)_2$). Anal. Calcd. for $\text{C}_{33}\text{H}_{45}\text{BF}_4\text{P}_2\text{Pd}_2$ (%): C, 49.34; H, 5.65. Found: C, 49.27; H, 5.58.

Synthesis of diacetonitrile anion capped species **21**



Method A: To a solution of **3** (200 mg, 0.212 mmol) in CH_3CN (10 mL) was added $\text{KO}'\text{Bu}$ (23.8 mg, 0.212 mmol). The solution remained dark brown in color over 3 hours at room temperature. Volatiles were removed under vacuum, and the waxy solids were washed with hexanes, Et_2O , benzene, THF, and CH_2Cl_2 (separately, in that order). The solids were insoluble in hexanes and Et_2O , but some yellow color eluted with the benzene wash. THF washings initially eluted an intense dark brown color, but most of the crude material remained insoluble. The remaining crude was dissolved in CH_2Cl_2 and filtered through Celite. Crystallization of the eluent in $\text{CH}_2\text{Cl}_2/\text{Et}_2\text{O}$ yielded some XRD-quality crystals, but the mixture of solids was not pure **21**.

Method B: To a solution of **3** (63.7 mg, 0.07 mmol) in CH_3CN (10 mL) was added $[\text{Li}\{\text{N}(\text{H})\text{C}(\text{Me})=\text{C}(\text{H})\text{CN}\}]_n$ (18.1 mg, 0.07 mmol).⁶ The same purification procedures as in Method A yielded 41 mg of relatively clean **21**. *Characterization:* FAB-MS (-BF₄-dissociated cation; m/z: 757.1390; calcd.: 757.1132). ^1H NMR (600 MHz, CD_3CN) δ : 7.86 – 7.21 (m, Ar- H_{2-6} + Ar- $H_{2'-6'}$, 8H), 6.24 – 5.95 (broad, Ar- $H_{8/9}$, 2H), 5.81 (broad, NH, 1H) 5.80 – 5.38 (broad, Ar- $H_{9/8}$, 2H), 4.61 – 4.41 (broad, NCCH, 1H), 3.22 – 2.45 (broad, $\text{CH}(\text{CH}_3)_2$, 4H), 2.45 – 2.20 (broad, HNCCH₃, 3H), 1.76 – 0.50 (broad, $\text{CH}(\text{CH}_3)_2$, 24H). $^{31}\text{P}\{\text{H}\}$ NMR (121 MHz, CD_3CN) δ : 50.2, 49.2 (1:1, broad).

II. Nuclear Magnetic Resonance Spectra

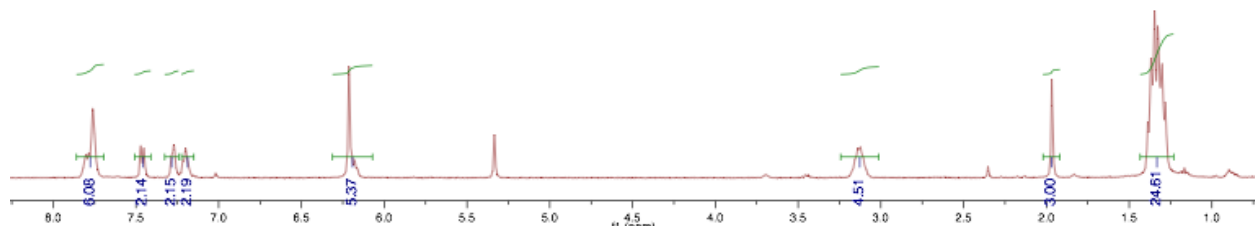


Figure S1. ^1H NMR (CD_2Cl_2 , 400 MHz) spectrum of **3**

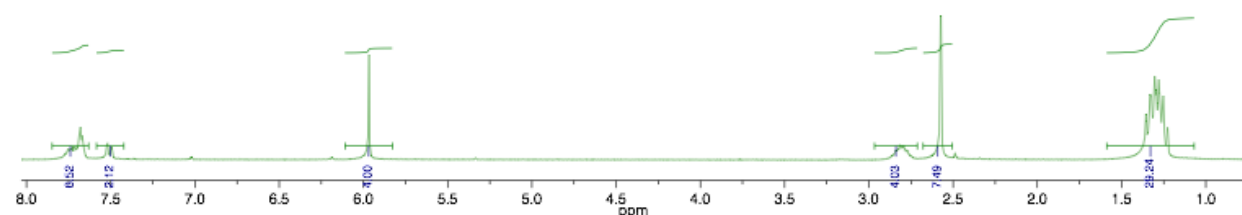


Figure S2. ^1H NMR (CD_2Cl_2 , 300 MHz) spectrum of toluene-free, acetonitrile-exchanged **3**

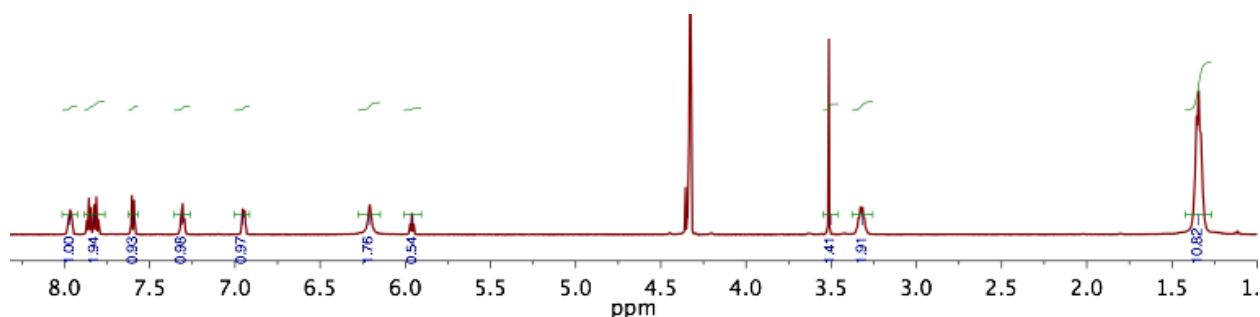


Figure S3. ^1H NMR (CD_3NO_2 , 400 MHz) spectrum of anisole complex **4**

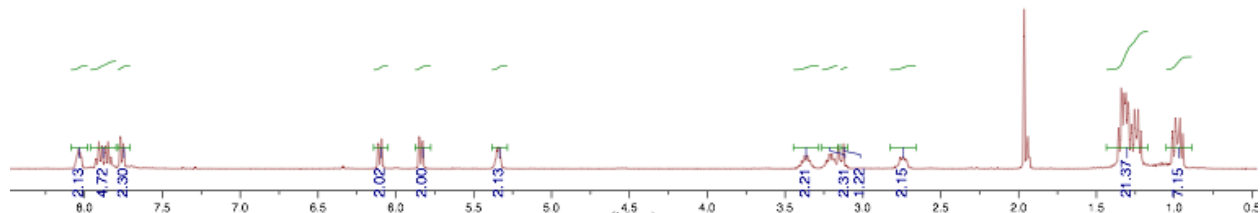


Figure S4. ^1H NMR (CD_3CN , 400 MHz) spectrum of butadiene complex **5**

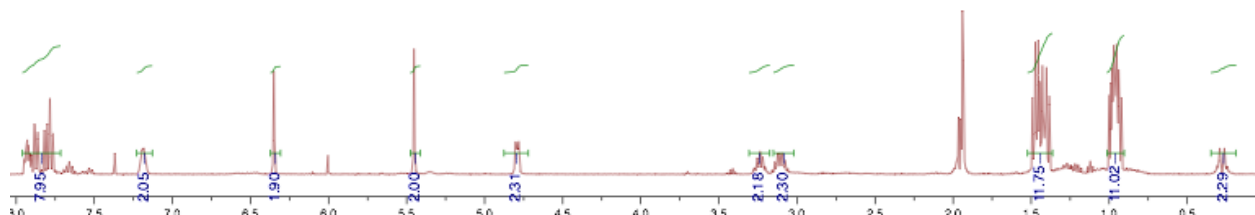


Figure S5. ^1H NMR (CD_3CN , 400 MHz) spectrum of 1,3-cyclohexadiene complex **6**

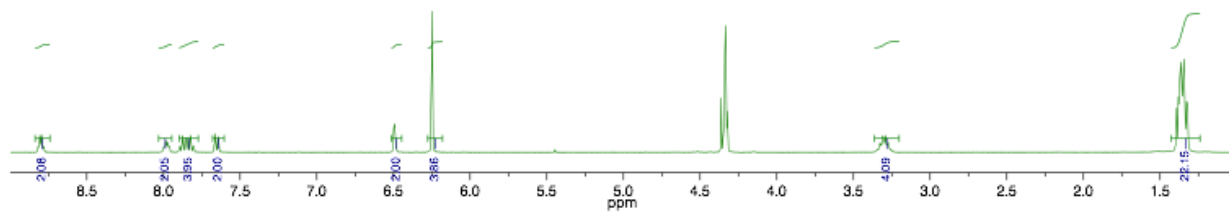


Figure S6. ^1H NMR (CD_3NO_2 , 400 MHz) spectrum of thiophene complex **7**

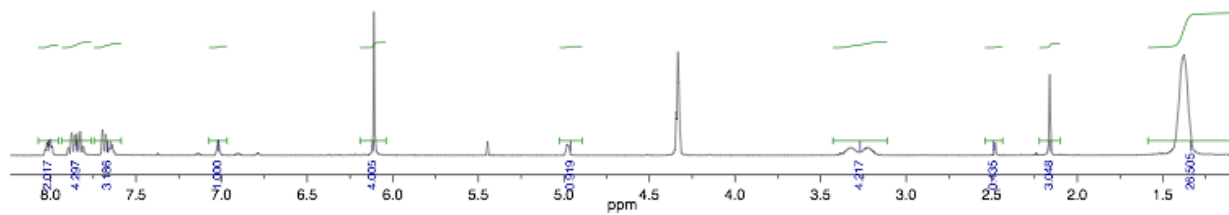


Figure S7. ^1H NMR (CD_3NO_2 , 400 MHz) spectrum of 2-methylthiophene complex **8**

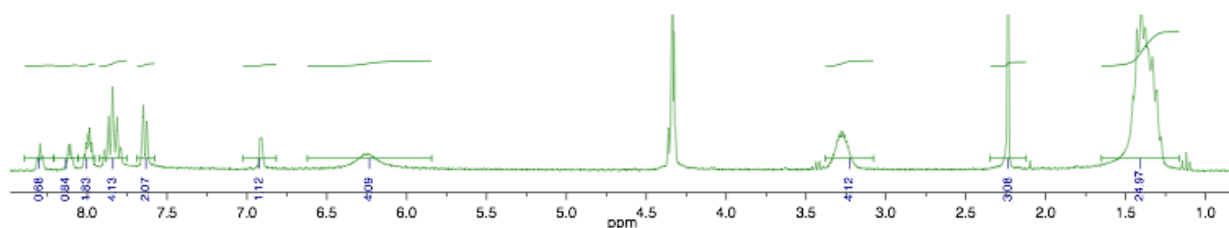


Figure S8. ^1H NMR (CD_3NO_2 , 400 MHz) spectrum of 3-methylthiophene complex **9**

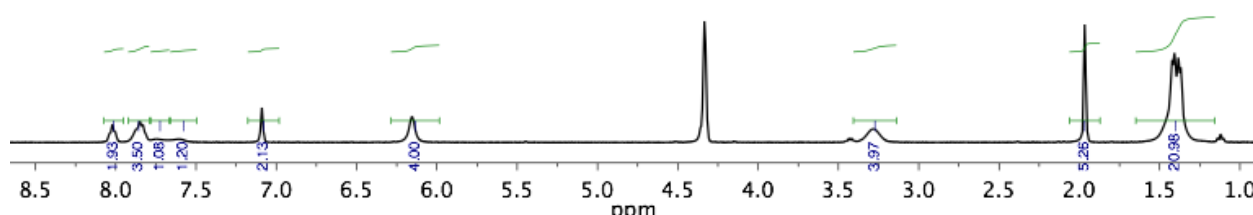


Figure S9. ^1H NMR (CD_3NO_2 , 400 MHz) spectrum of 2,5-dimethylthiophene complex **10**

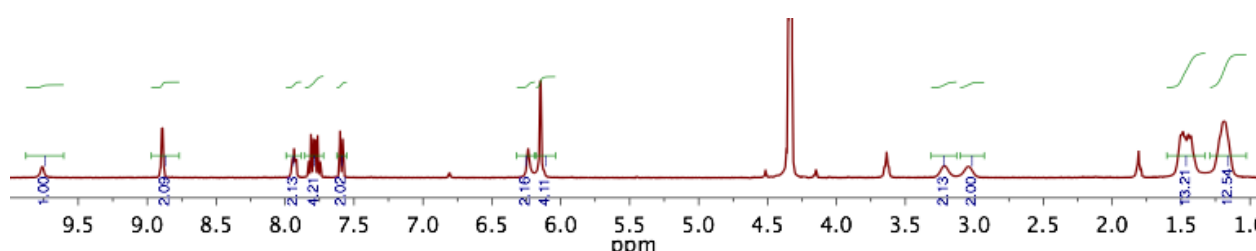


Figure S10. ^1H NMR (CD_3NO_2 , 400 MHz) spectrum of pyrrole complex **11**

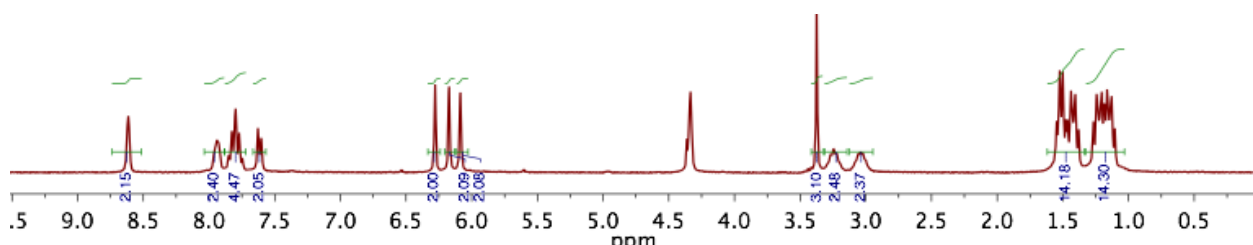


Figure S11. ^1H NMR (CD_3NO_2 , 400 MHz) spectrum of N-methylpyrrole complex **12**

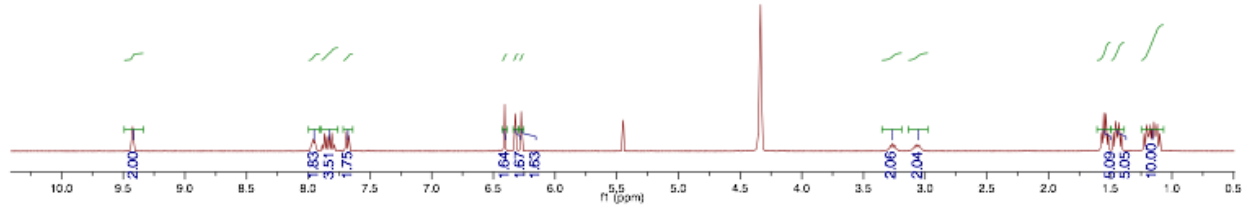


Figure S12. ^1H NMR (CD_3NO_2 , 400 MHz) spectrum of furan complex **13**

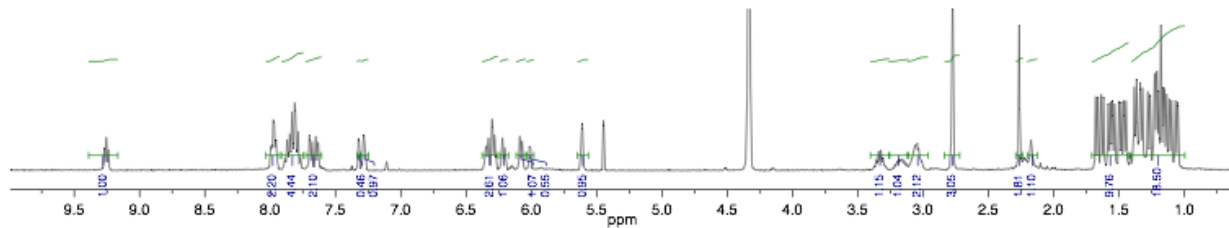


Figure S13. ^1H NMR (CD_3NO_2 , 400 MHz) spectrum of 2-methylfuran complex **14**

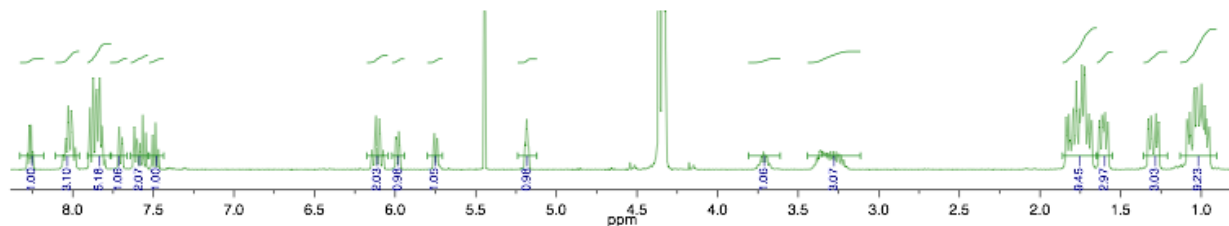


Figure S14. ^1H NMR (CD_3NO_2 , 400 MHz) spectrum of benzothiophene complex **15**

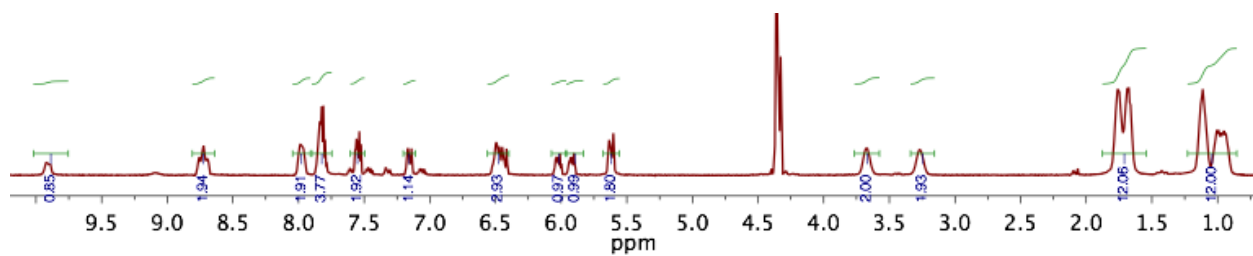


Figure S15. ^1H NMR (CD_3NO_2 , 400 MHz) spectrum of indole complex **16**

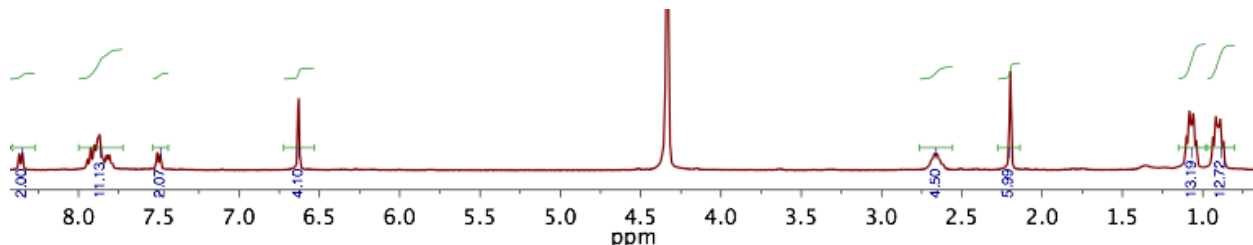


Figure S16. ^1H NMR (CD_3NO_2 , 400 MHz) spectrum of 4,6-dimethylbibenzothiophene complex **17**

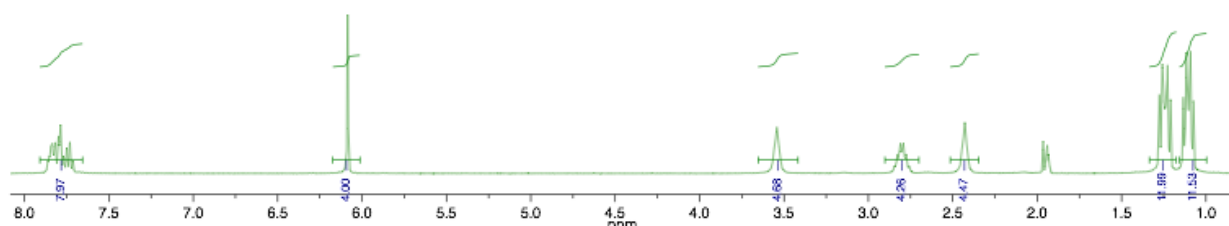


Figure S17. ^1H NMR (CD_3NO_2 , 400 MHz) spectrum of tetrahydrothiophene complex **18**

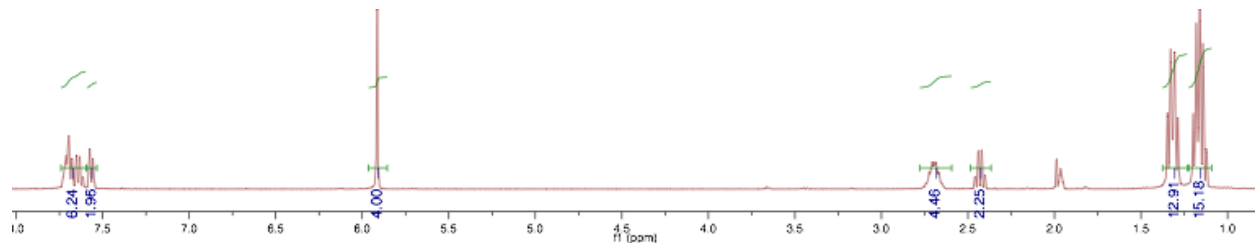


Figure S18. ¹H NMR (CD₃CN, 400 MHz) spectrum of propanoate complex **19**

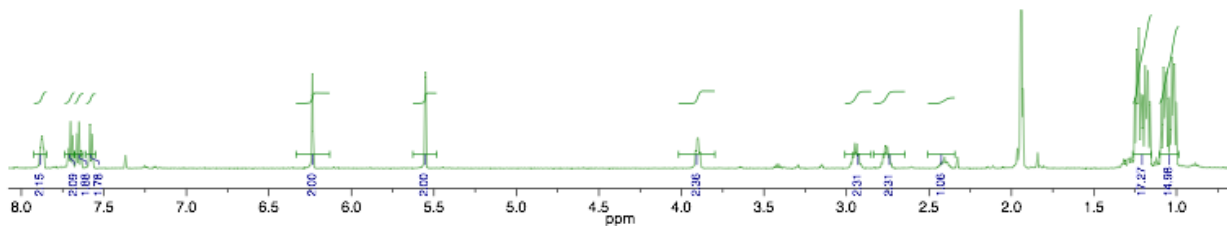


Figure S19. ¹H NMR (CD₃CN, 400 MHz) spectrum of allyl complex **20**

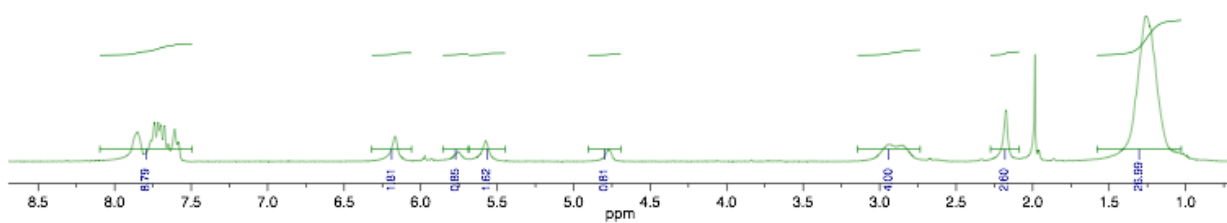


Figure S20. ¹H NMR (CD₃CN, 400 MHz) spectrum of diacetonitrilyl complex **21**

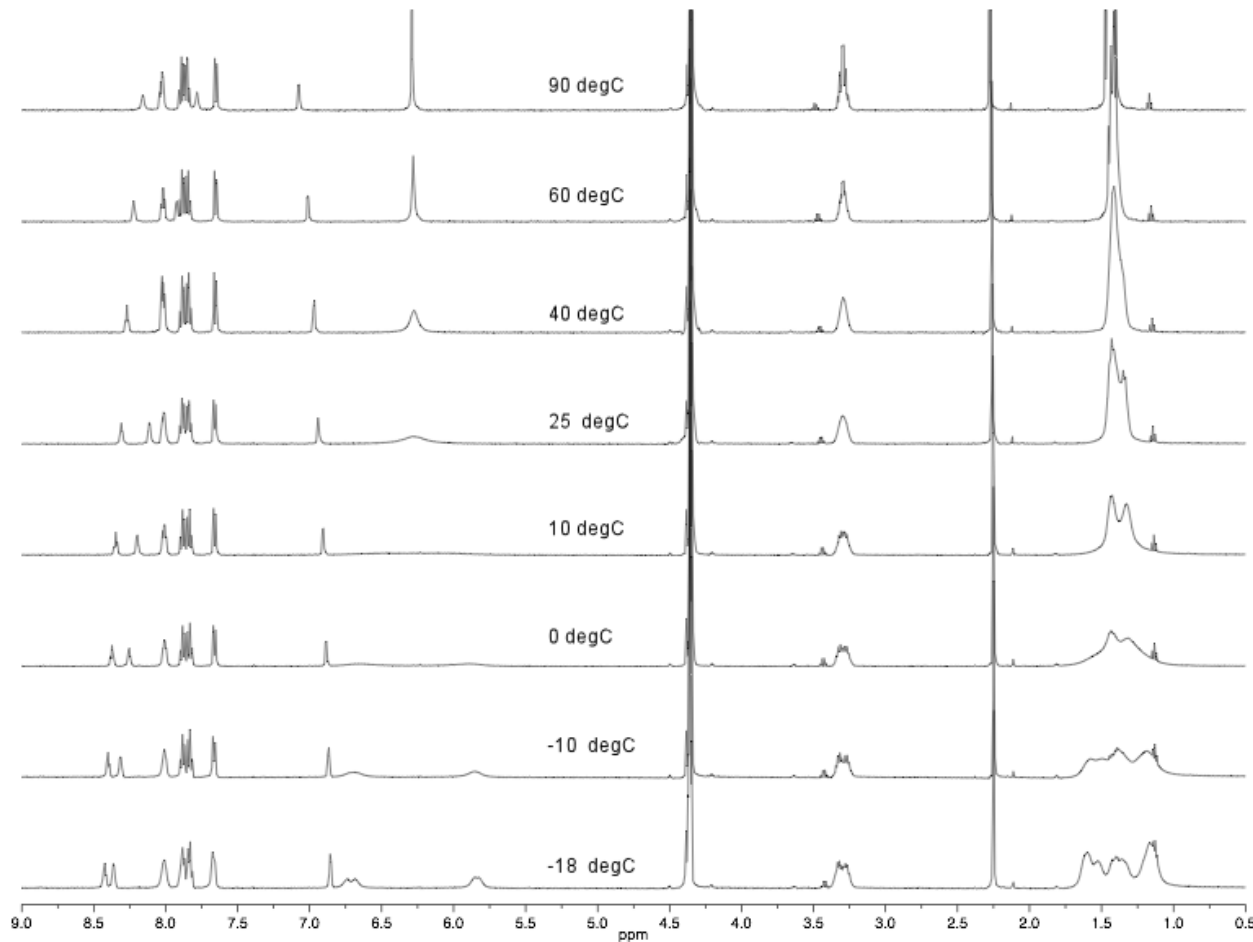


Figure S21. Variable temperature ¹H NMR (CD_3NO_2 , 500 MHz) spectra of 2-methylthiophene adduct **9**.

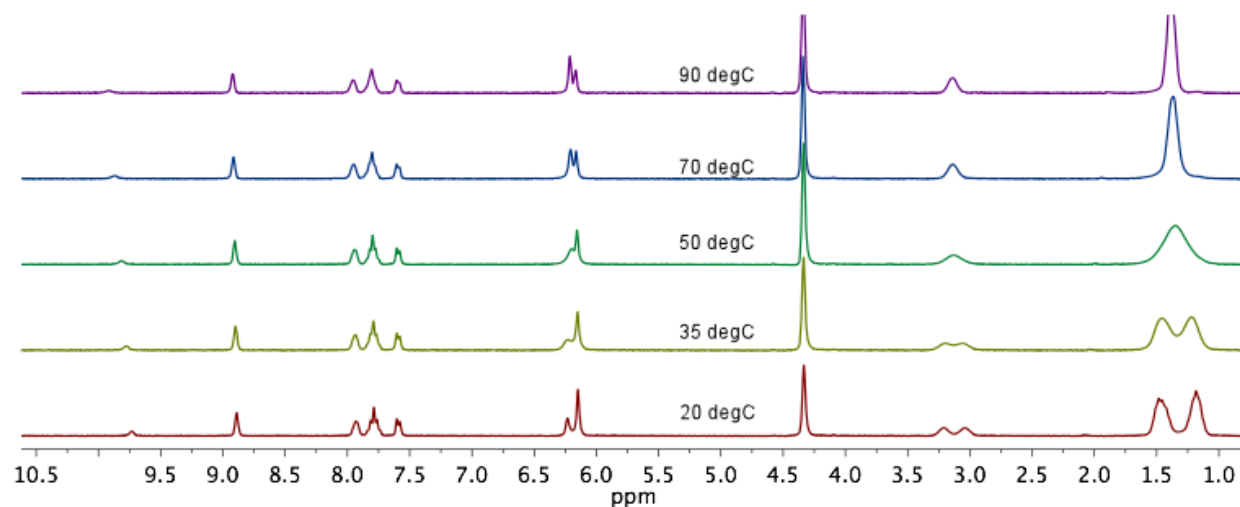


Figure S22. Variable temperature ¹H NMR (CD_3NO_2 , 300 MHz) spectra of pyrrole adduct **11**

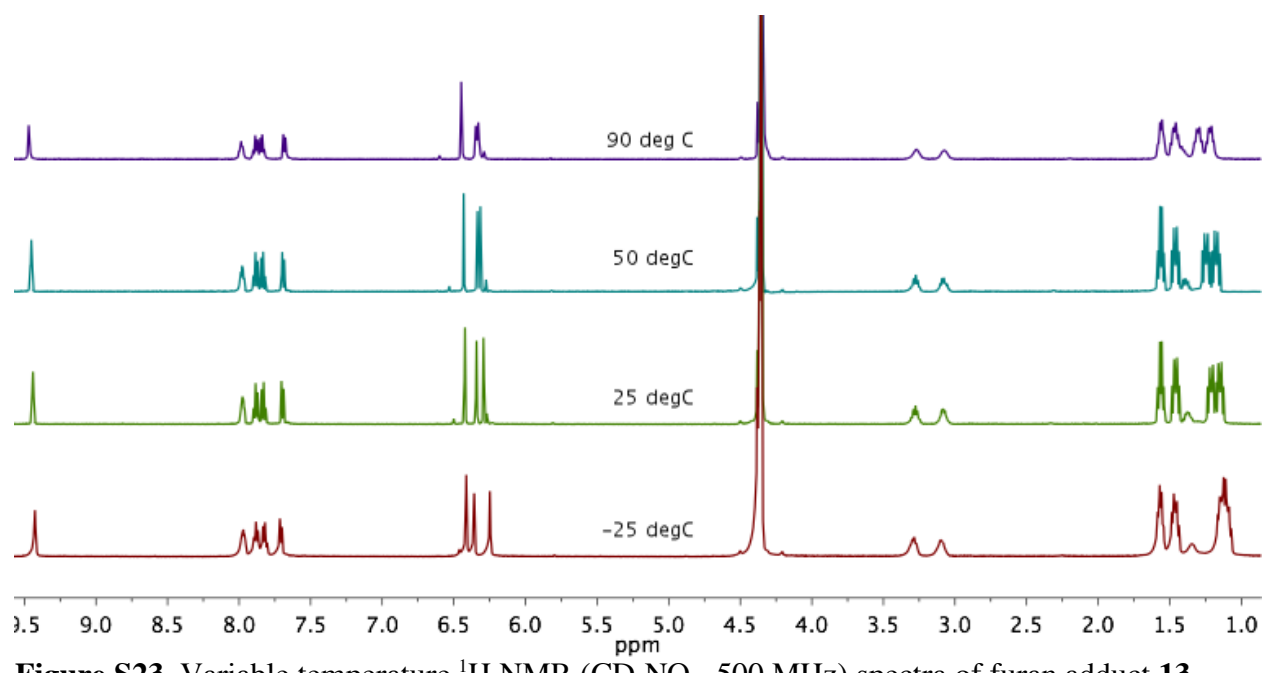


Figure S23. Variable temperature ¹H NMR (CD₃NO₂, 500 MHz) spectra of furan adduct **13**

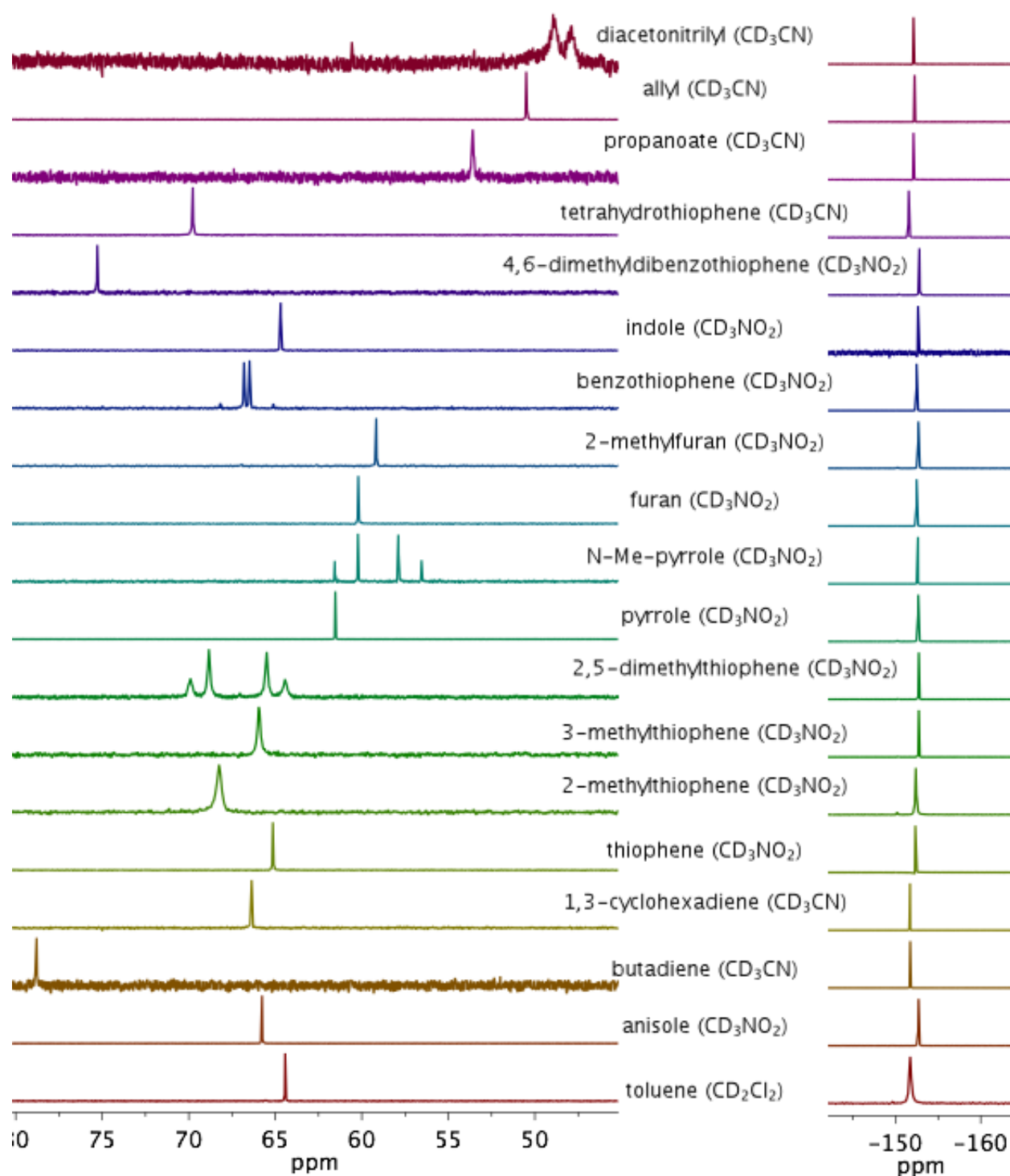


Figure S24. Stacked $^{31}\text{P}\{\text{H}\}$ (left) and $^{19}\text{F}\{\text{H}\}$ (right) NMR spectra of **3-21** (ordered bottom to top).

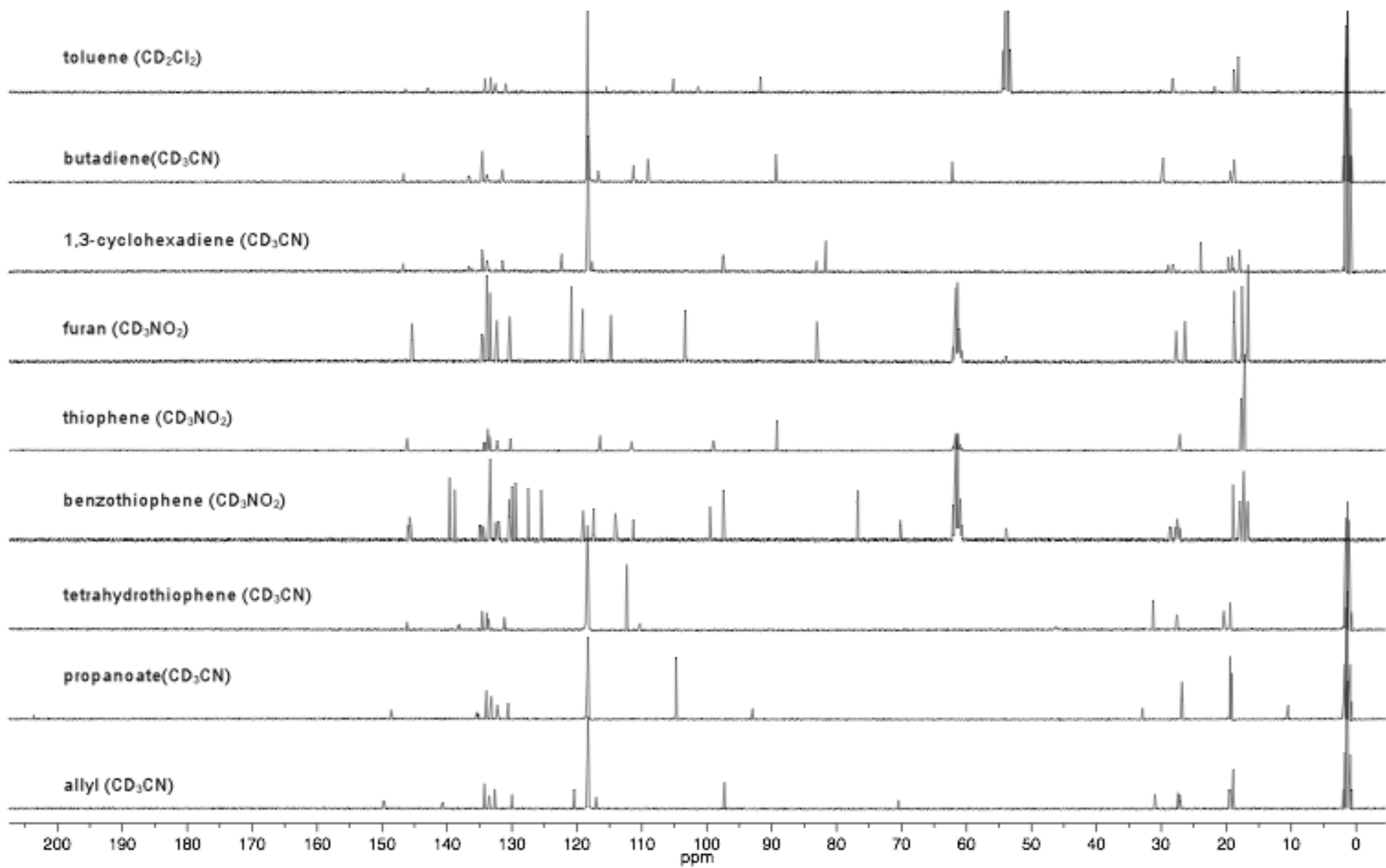


Figure S25. Stacked $^{13}\text{C}\{\text{H}\}$ NMR spectra of **3**, **5-7**, **13**, **15**, **18-20**.

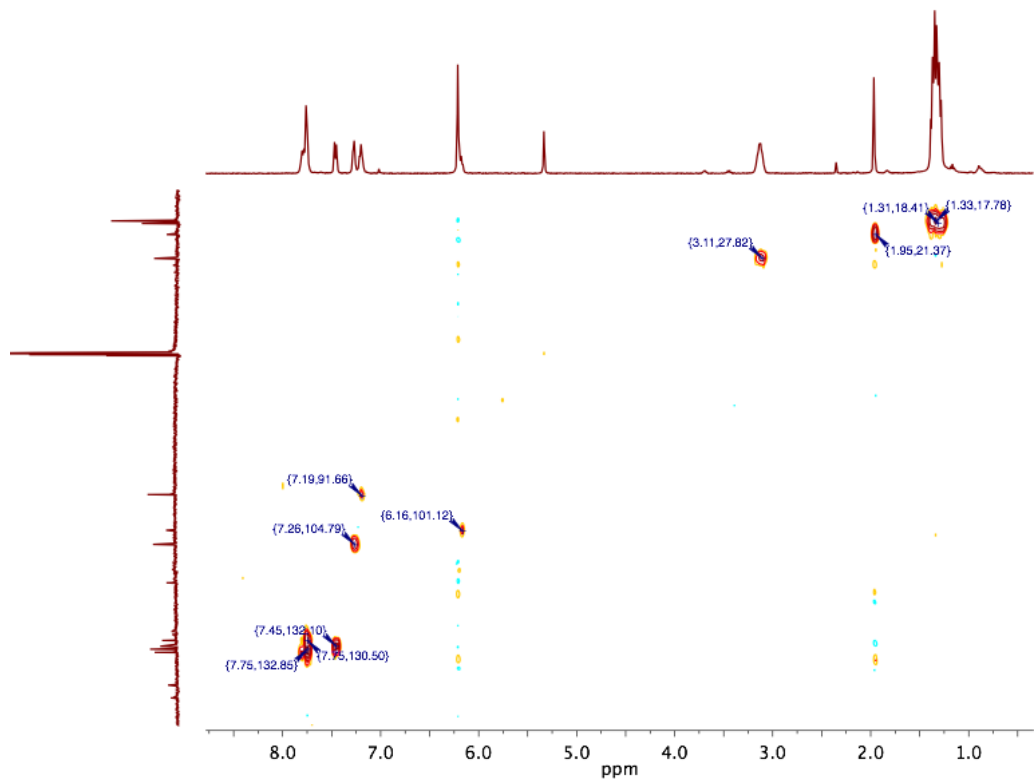


Figure S26. HSQC spectrum (CD₂Cl₂, 400 MHz) for toluene adduct **3**

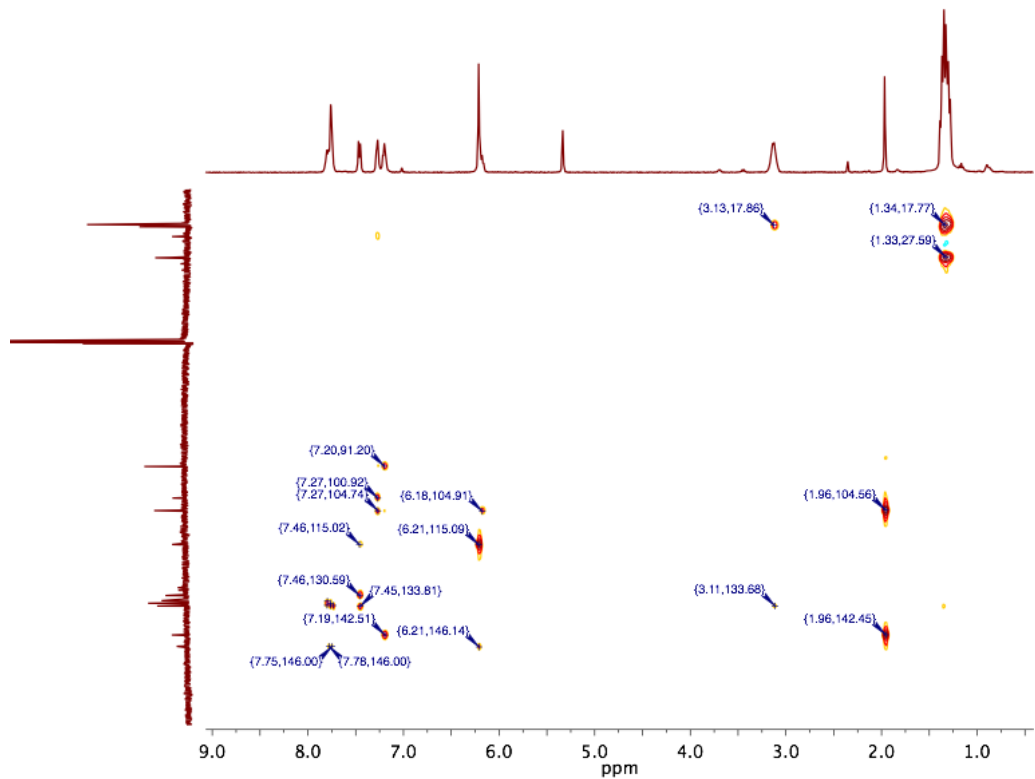


Figure S27. HMBC spectrum (CD₂Cl₂, 400 MHz) for toluene adduct **3**

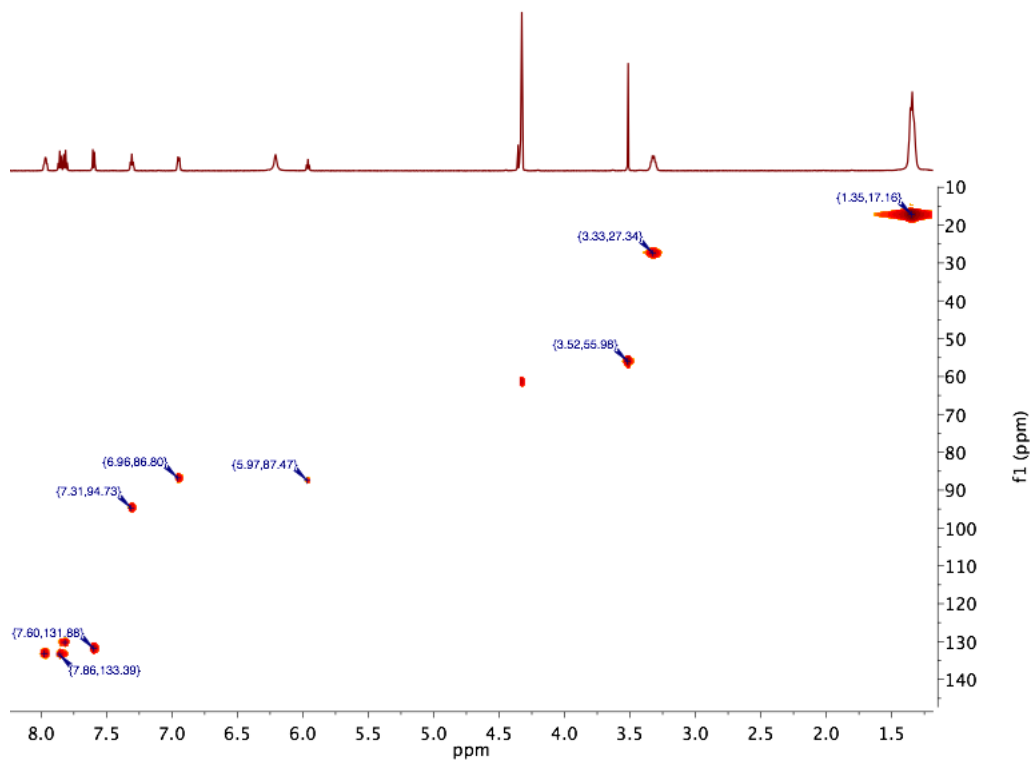


Figure S28. HSQC spectrum (CD_3NO_2 , 400 MHz) for anisole adduct **4**

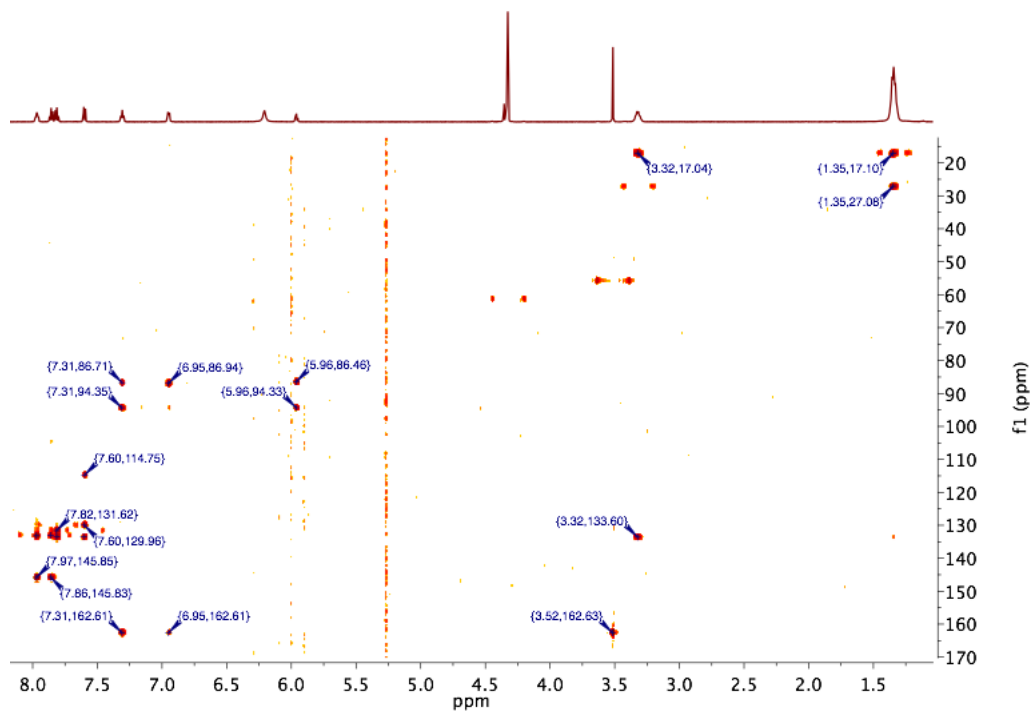


Figure S29. HMBC spectrum (CD_3NO_2 , 400 MHz) for anisole adduct **4**

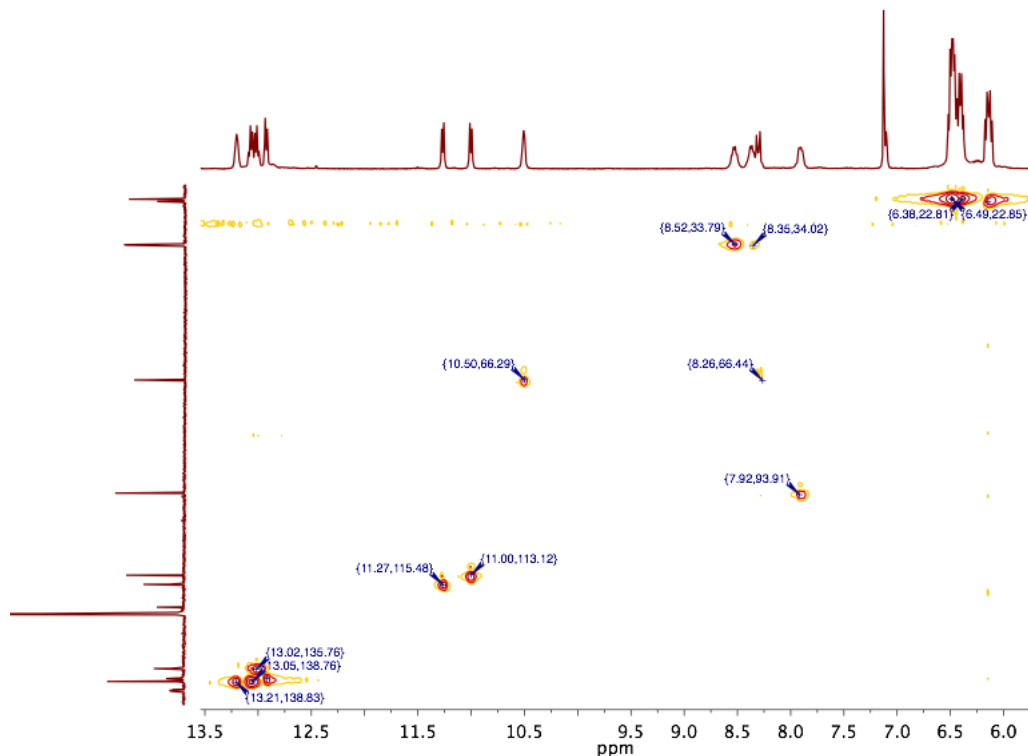


Figure S30. HSQC spectrum (CD₃CN, 400 MHz) for butadiene adduct **5**

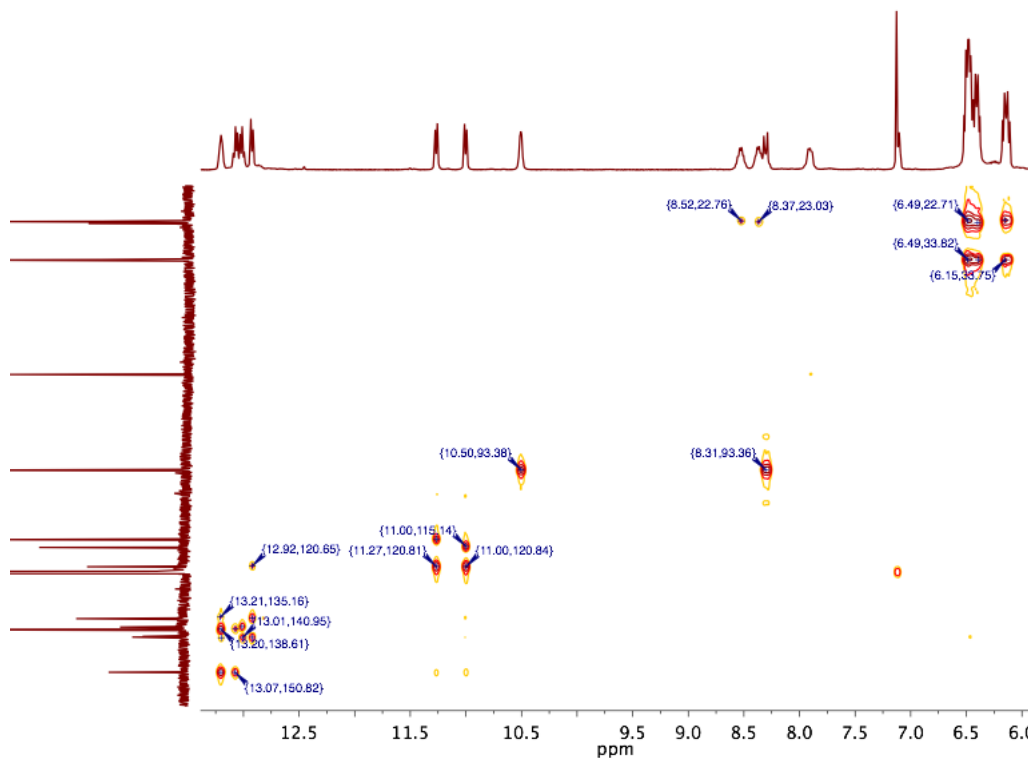


Figure S31. HMBC spectrum (CD₃CN, 400 MHz) for butadiene adduct **5**

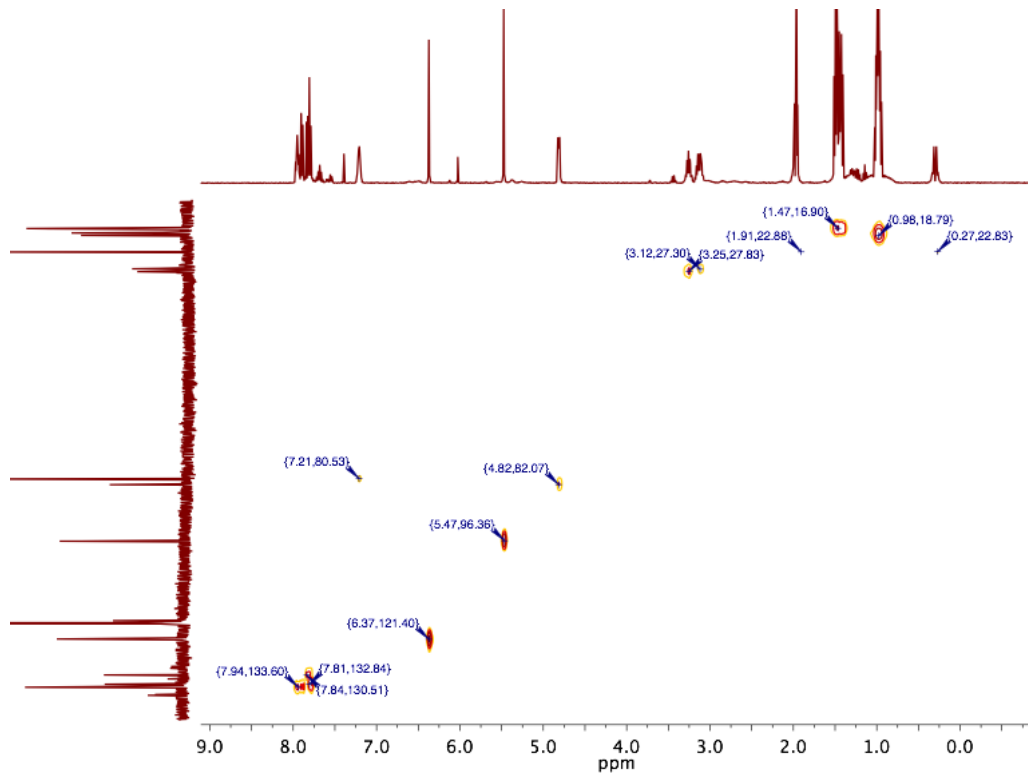


Figure S32. HSQC spectrum (CD_3CN , 400 MHz) for 1,3-cyclohexadiene adduct **6**

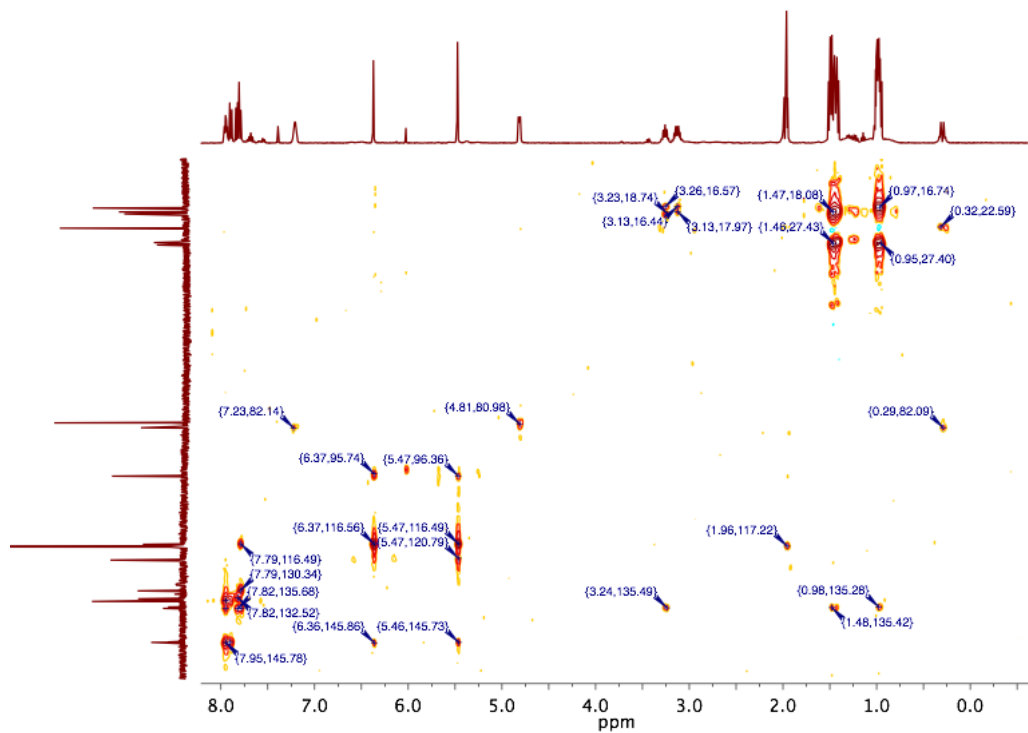


Figure S33. HMBC spectrum (CD_3CN , 400 MHz) for 1,3-cyclohexadiene adduct **6**

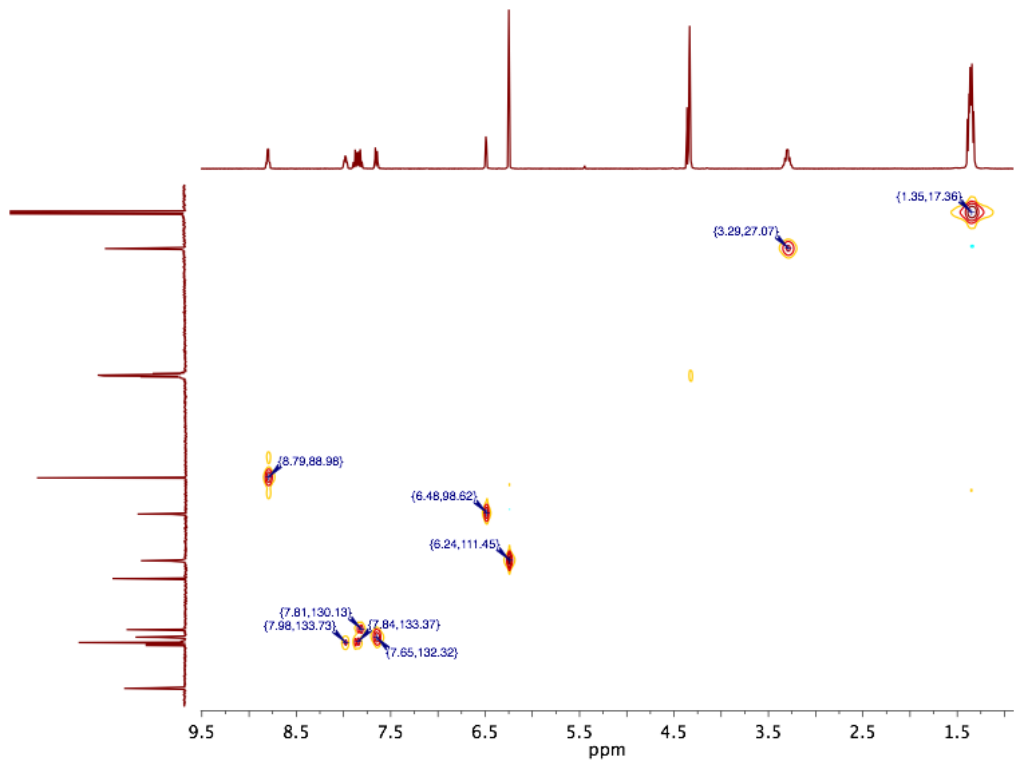


Figure S34. HSQC spectrum (CD_3NO_2 , 400 MHz) for thiophene adduct **7**

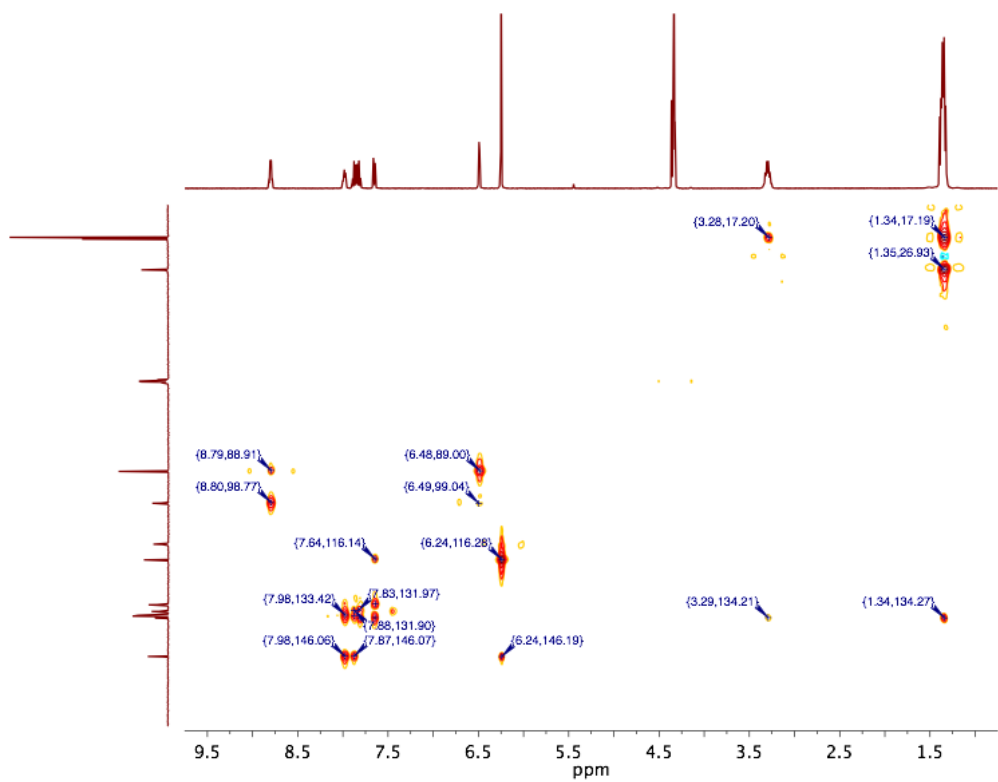


Figure S35. HMBC spectrum (CD_3NO_2 , 400 MHz) for thiophene adduct **7**

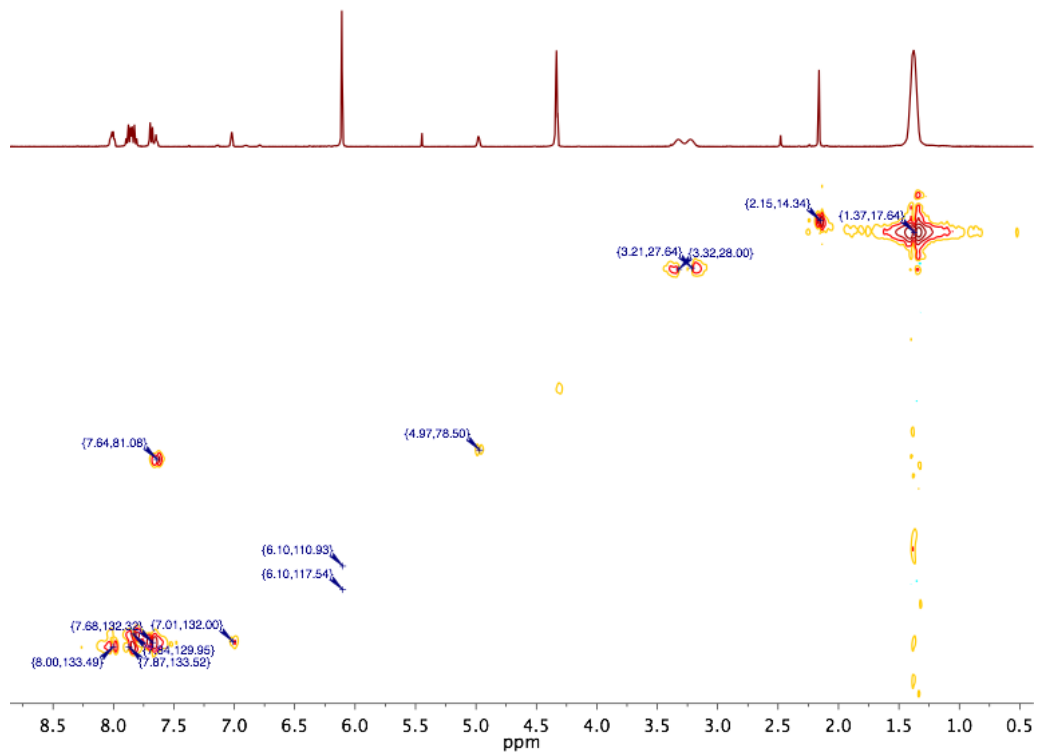


Figure S36. HSQC spectrum (CD_3NO_2 , 400 MHz) for 2-methylthiophene adduct **8**

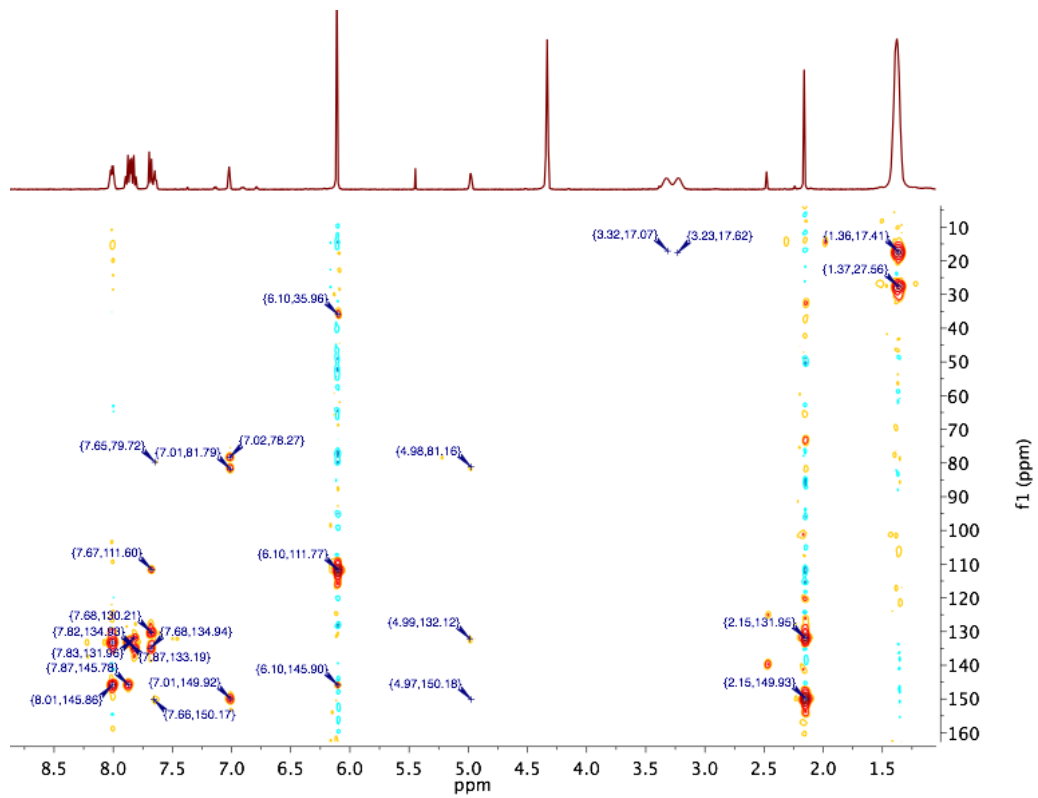


Figure S37. HMBC spectrum (CD_3NO_2 , 400 MHz) for 2-methylthiophene adduct **8**

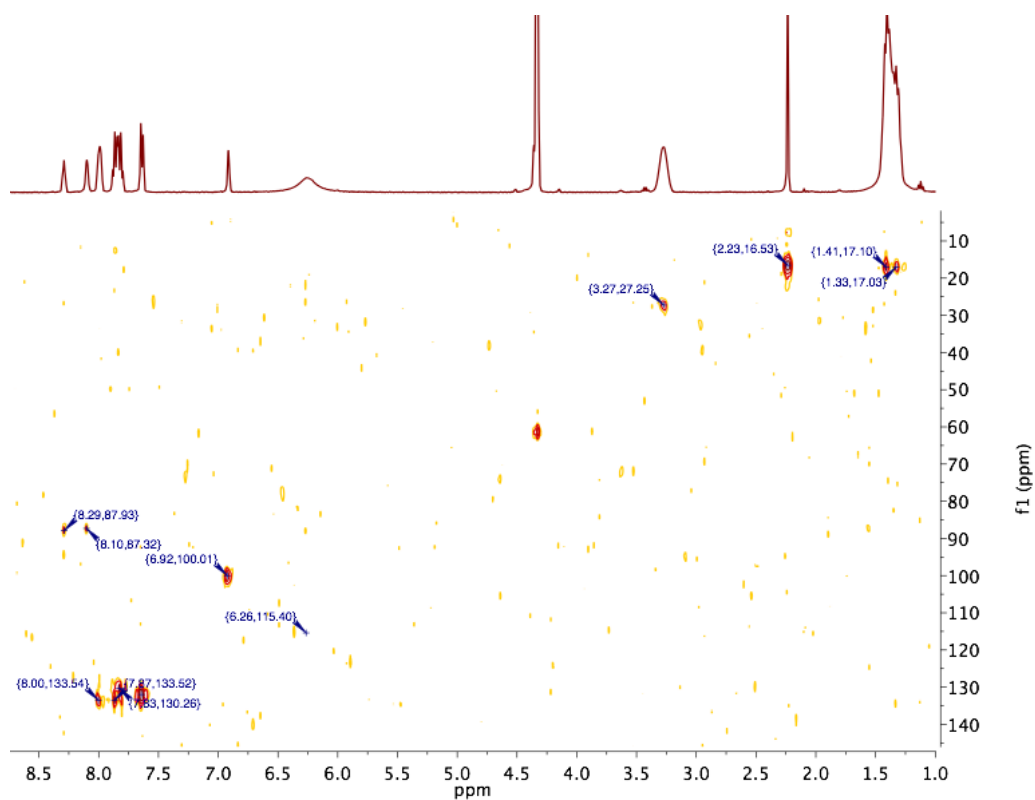


Figure S38. HSQC spectrum (CD_3NO_2 , 400 MHz) for 3-methylthiophene adduct **9**

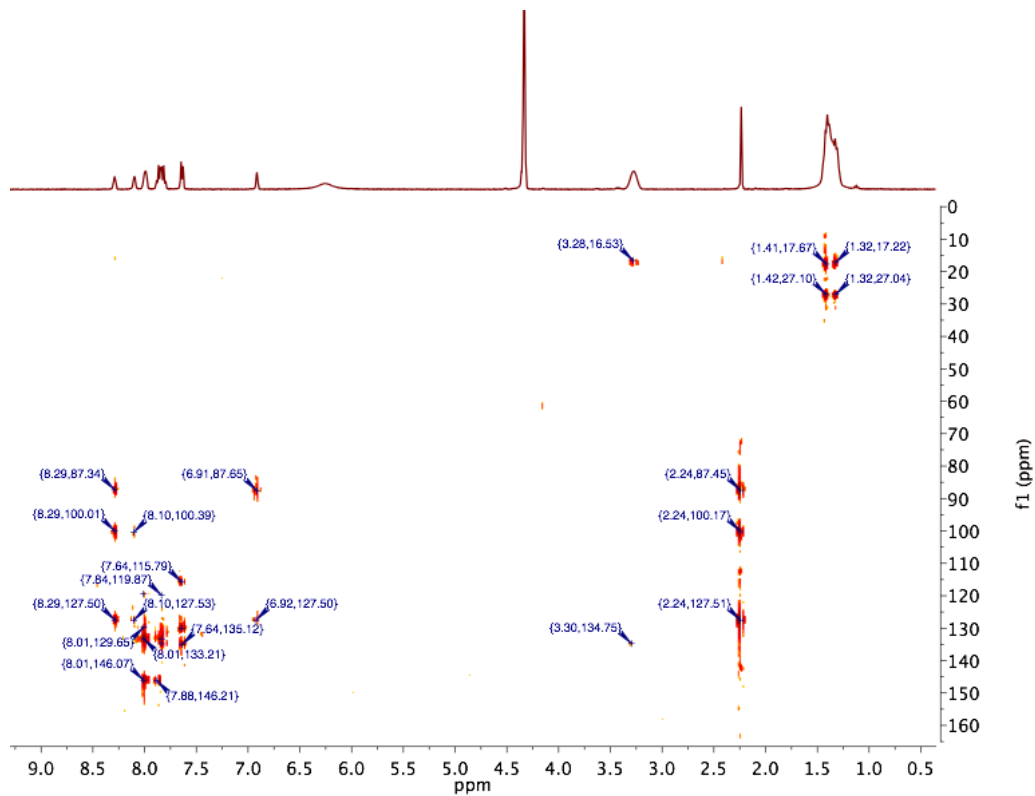


Figure S39. HMBC spectrum (CD_3NO_2 , 400 MHz) for 3-methylthiophene adduct **9**

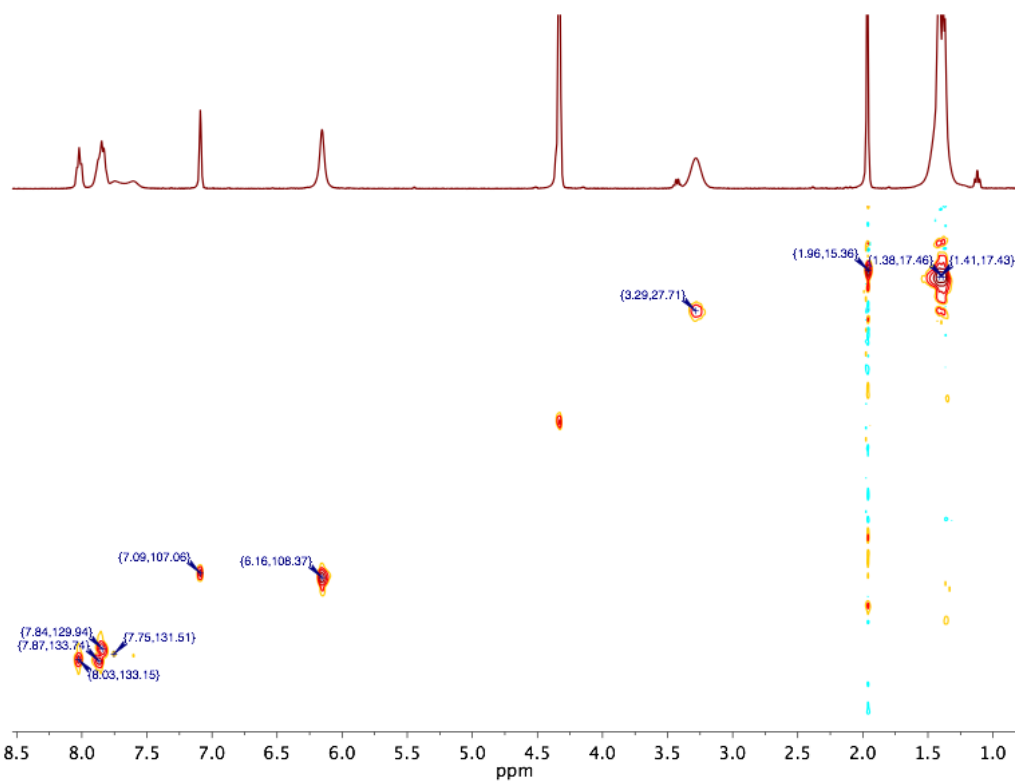


Figure S40. HSQC spectrum (CD_3NO_2 , 400 MHz) for 2,5-dimethylthiophene adduct **10**

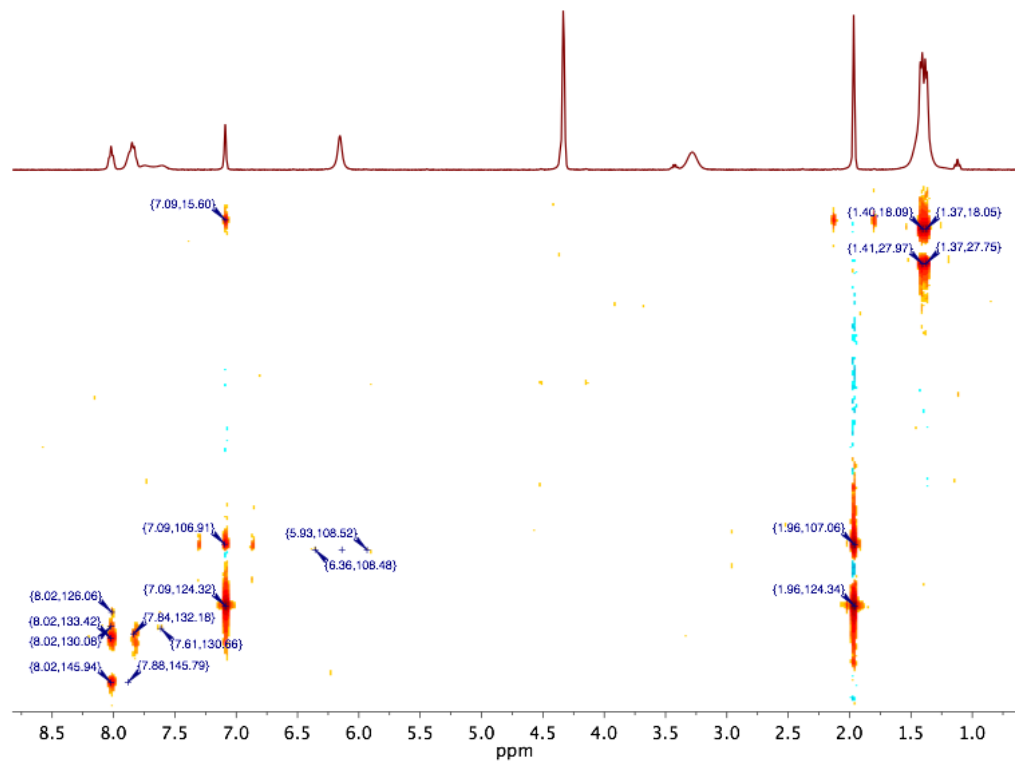


Figure S41. HMBC spectrum (CD_3NO_2 , 400 MHz) for 2,5-dimethylthiophene adduct **10**

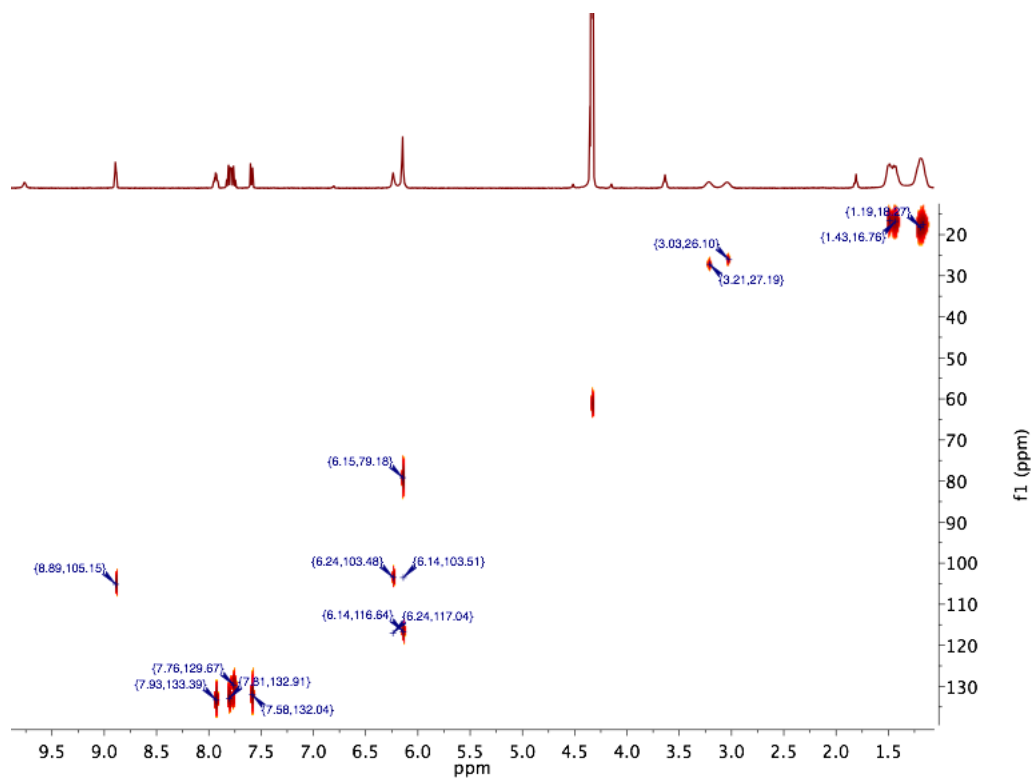


Figure S42. HSQC spectrum (CD_3NO_2 , 400 MHz) for pyrrole adduct **11**

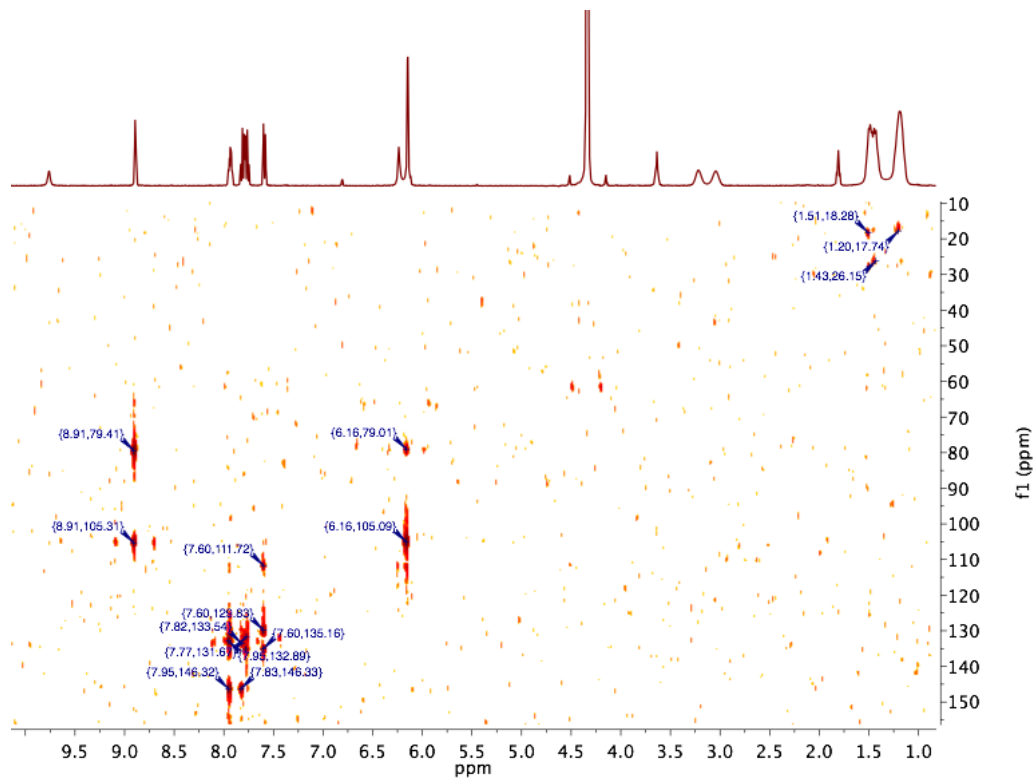


Figure S43. HMBC spectrum (CD_3NO_2 , 400 MHz) for pyrrole adduct **11**

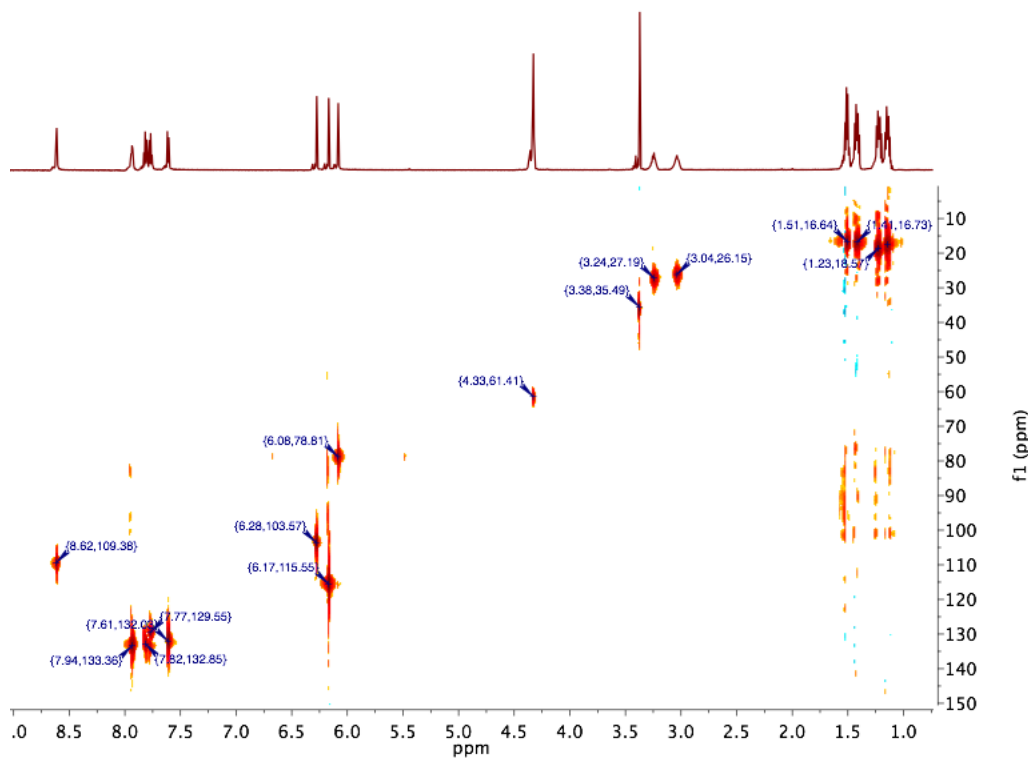


Figure S44. HSQC spectrum (CD₃NO₂, 400 MHz) for N-Me-pyrrole adduct **12**

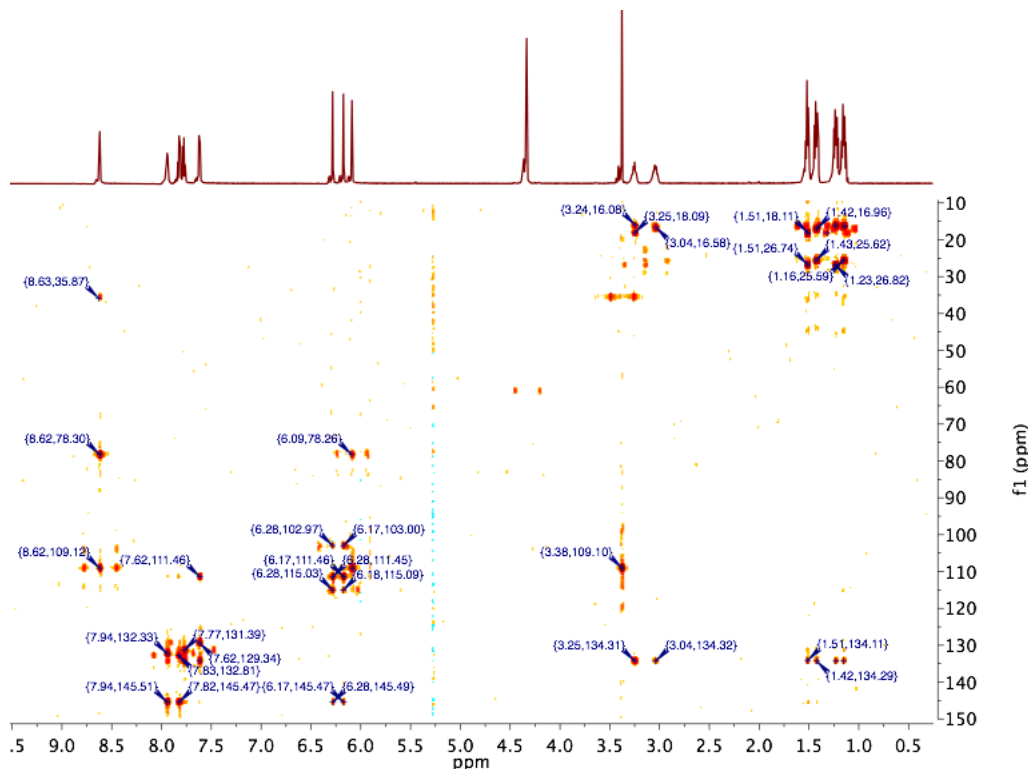


Figure S45. HMBC spectrum (CD₃NO₂, 400 MHz) for N-Me-pyrrole adduct **12**

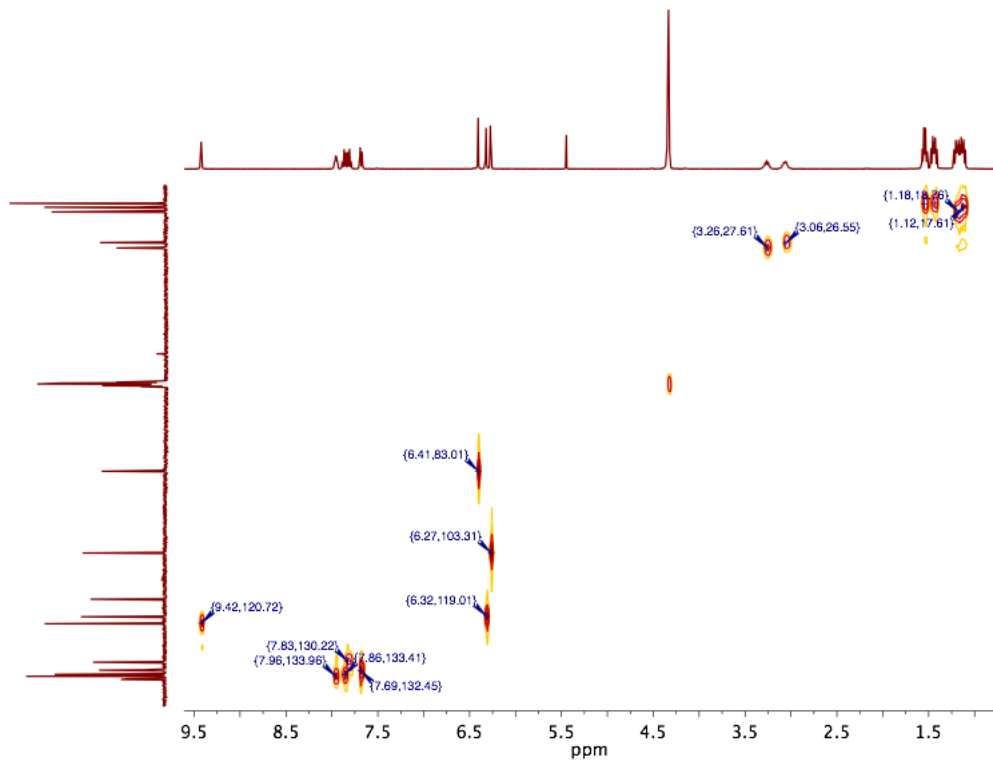


Figure S46. HSQC spectrum (CD_3NO_2 , 400 MHz) for furan adduct **13**

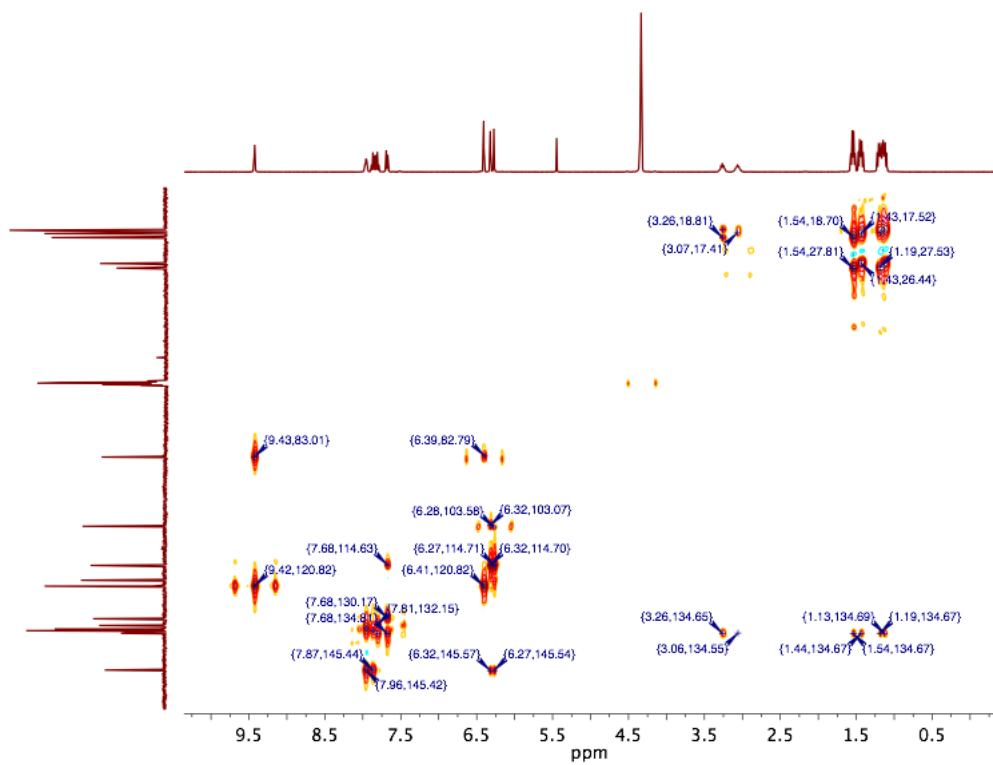


Figure S47. HMBC spectrum (CD_3NO_2 , 400 MHz) for furan adduct **13**

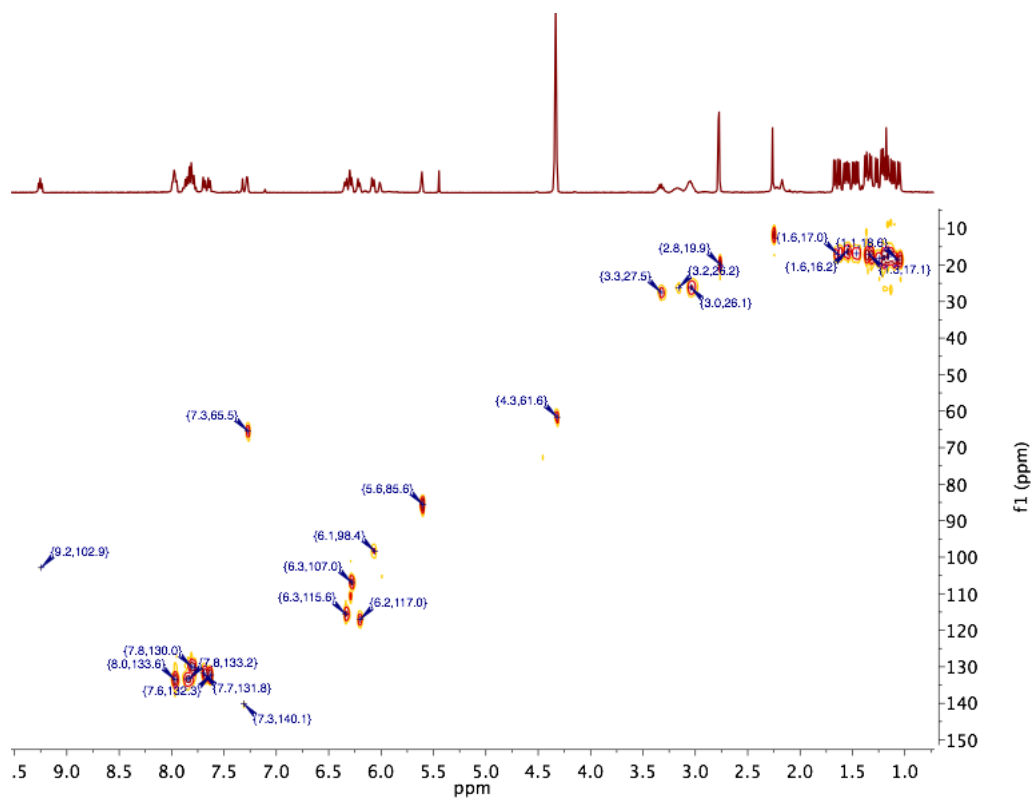


Figure S48. HSQC spectrum (CD_3NO_2 , 400 MHz) for 2-methylfuran adduct **14**

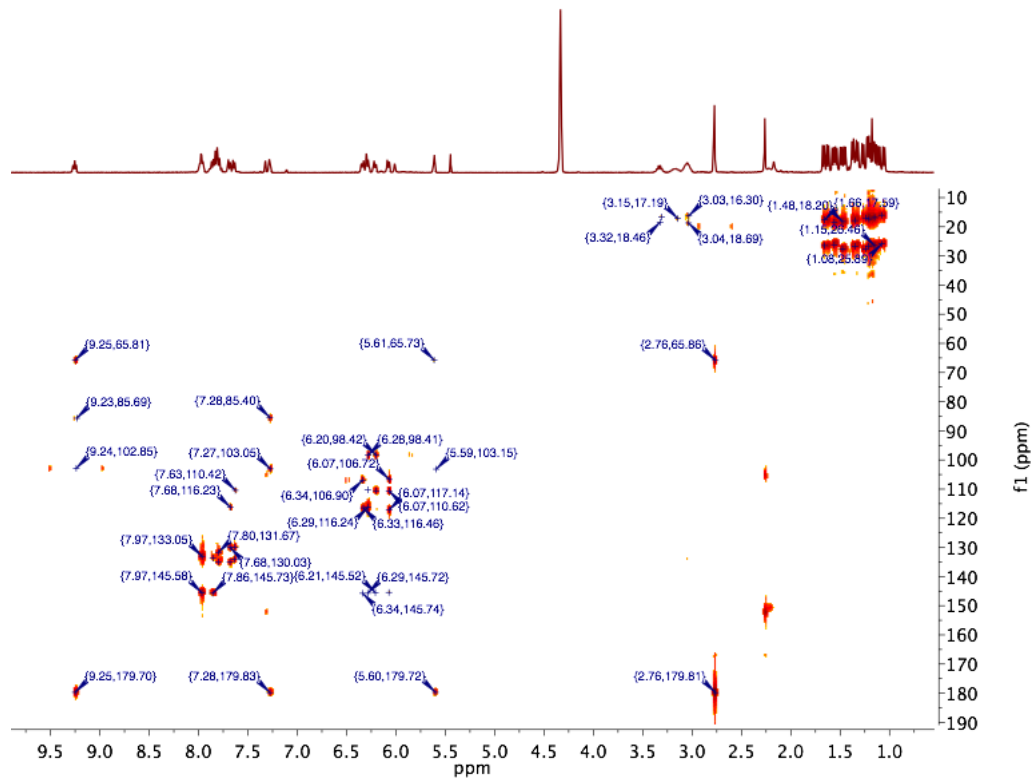


Figure S49. HMBC spectrum (CD_3NO_2 , 400 MHz) for 2-methylfuran adduct **14**

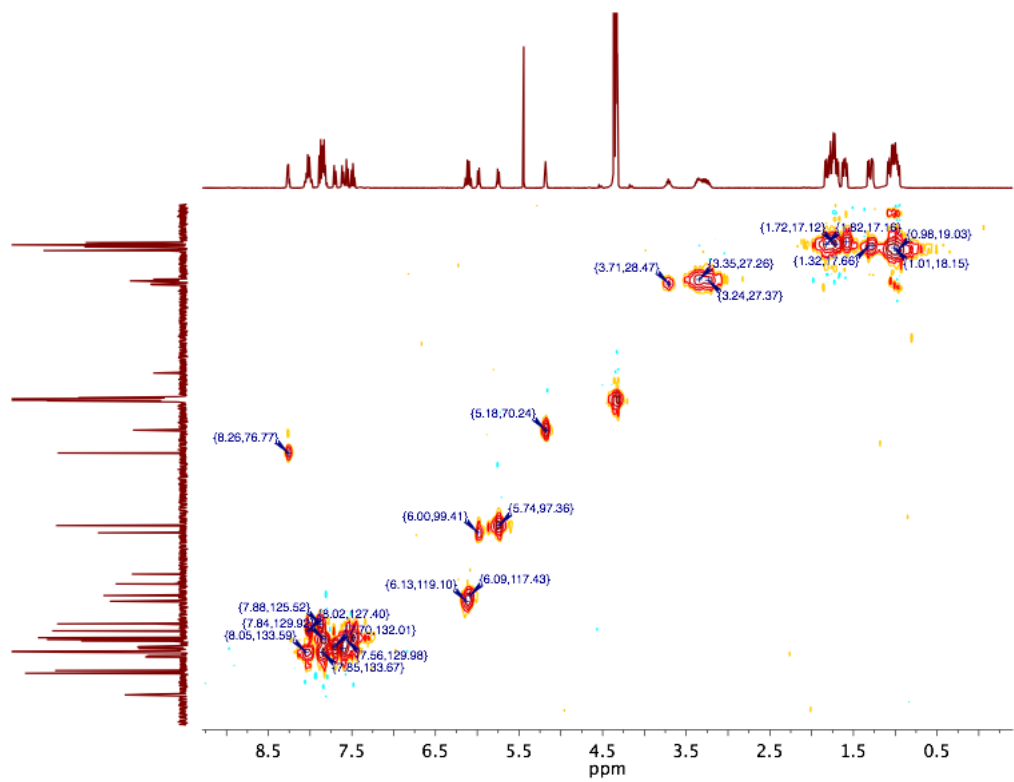


Figure S50. HSQC spectrum (CD_3NO_2 , 400 MHz) for benzothiophene adduct **15**

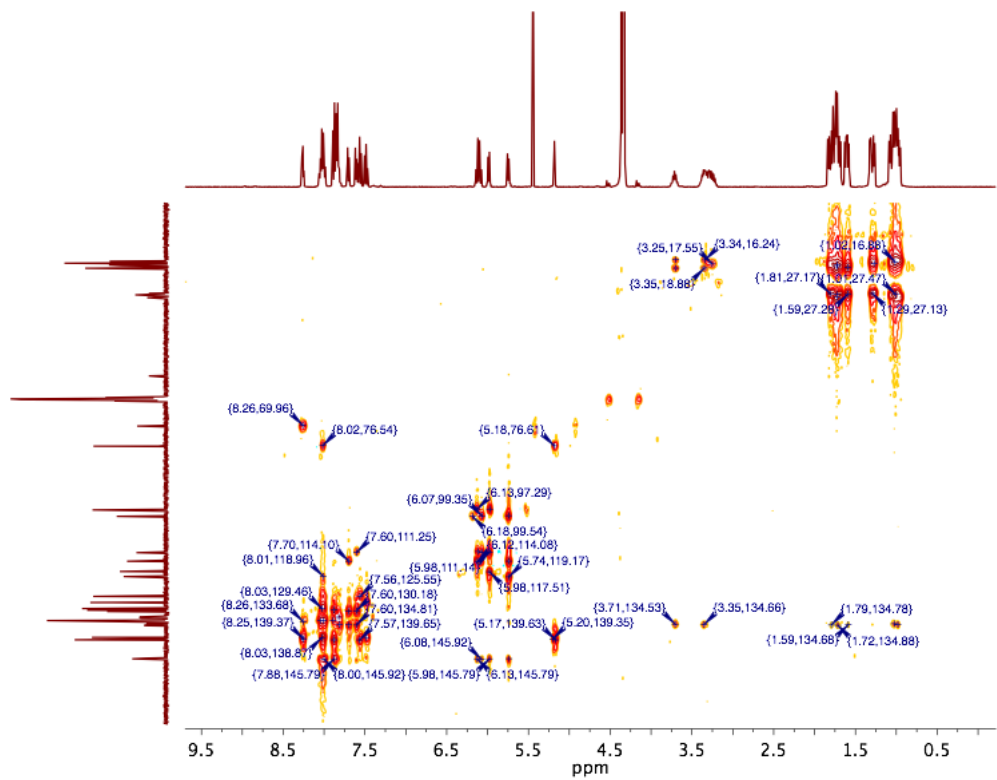


Figure S51. HMBC spectrum (CD_3NO_2 , 400 MHz) for benzothiophene **15**

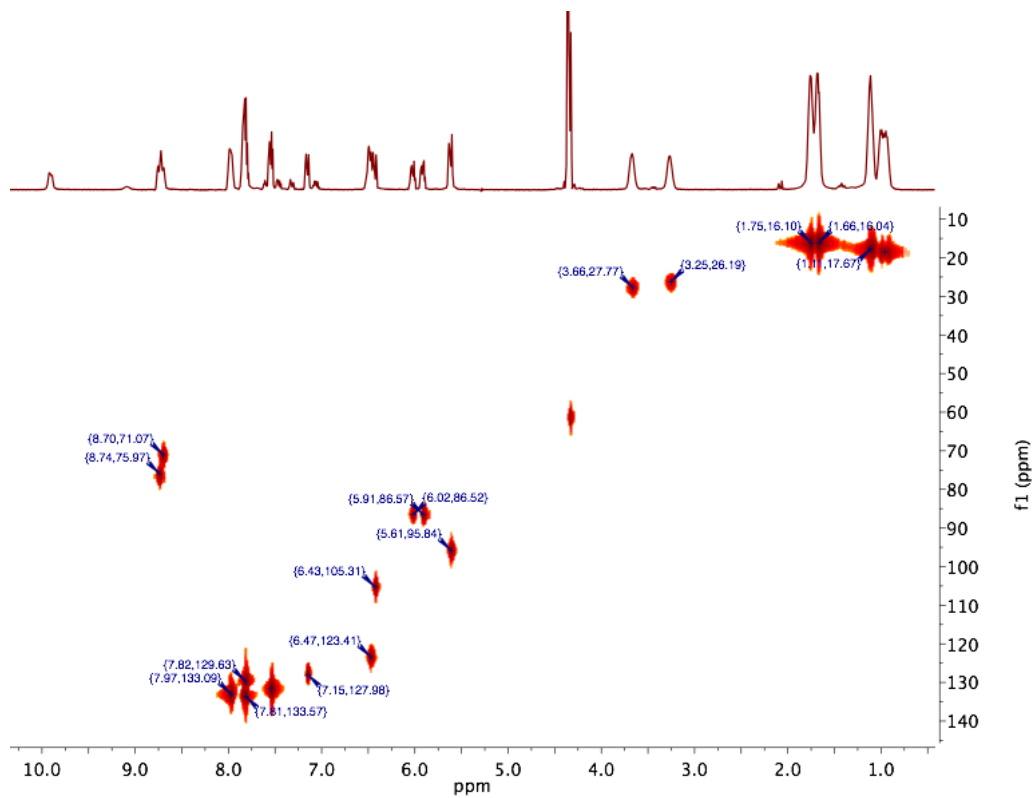


Figure S52. HSQC spectrum (CD_3NO_2 , 400 MHz) for indole adduct **16**

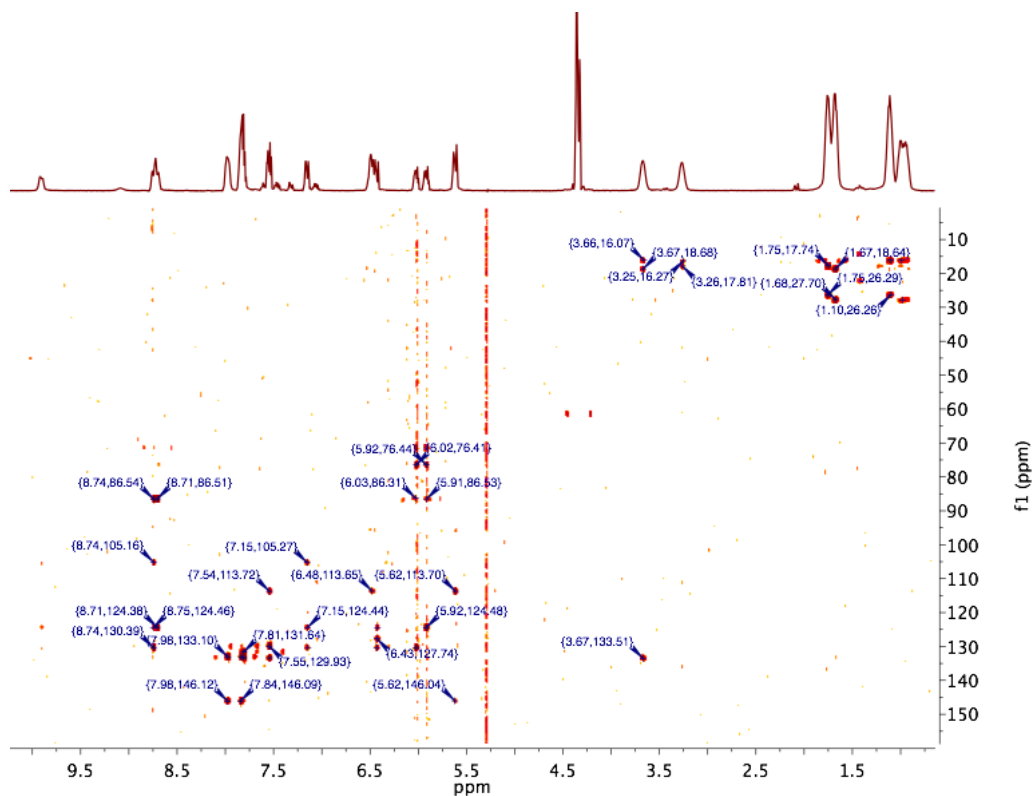


Figure S53. HMBC spectrum (CD_3NO_2 , 400 MHz) for indole adduct **16**

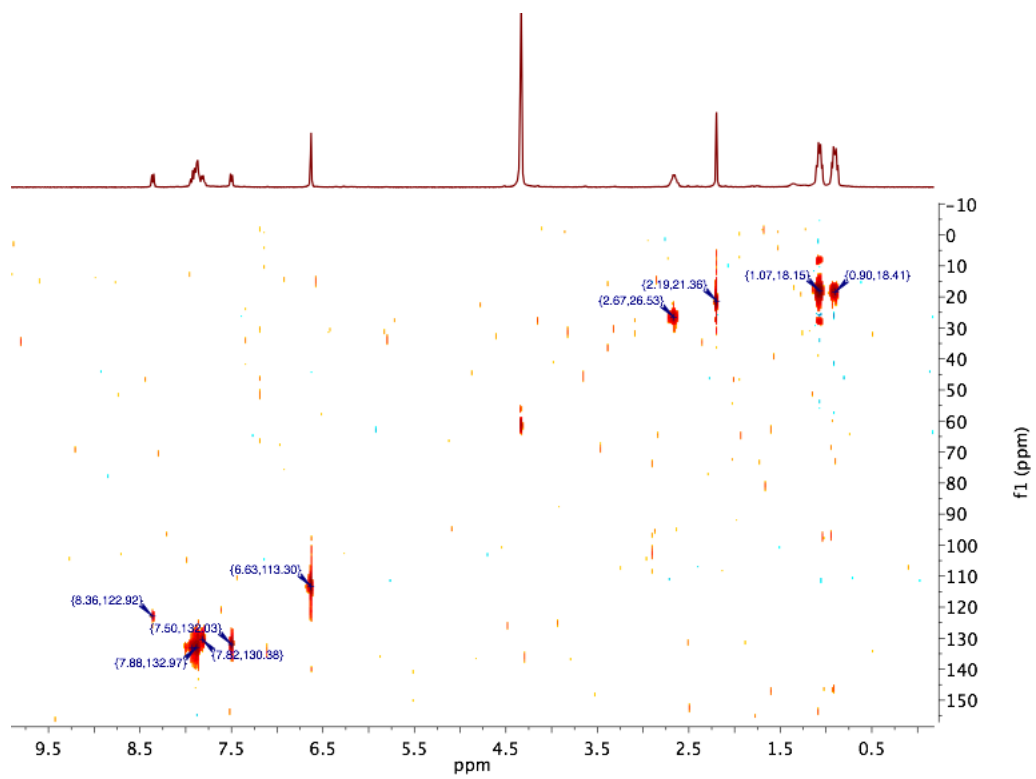


Figure S54. HSQC spectrum (CD_3NO_2 , 400 MHz) for 4,6-dimethyldibenzothiophene adduct **17**

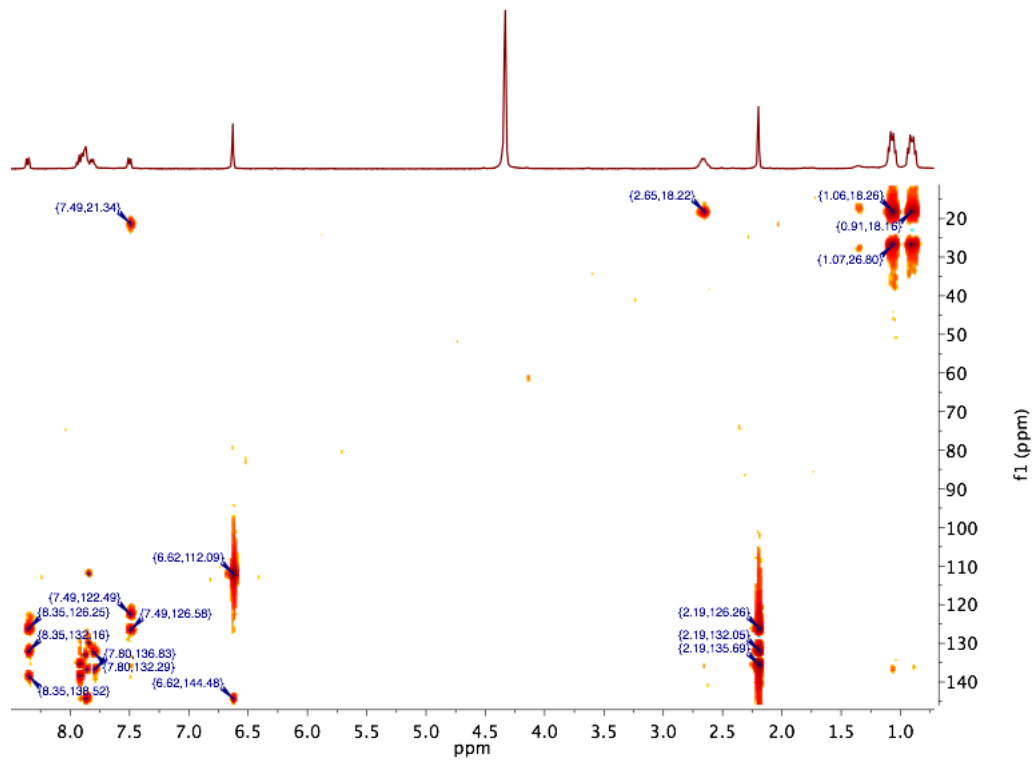


Figure S55. HMBC spectrum (CD_3NO_2 , 400 MHz) for 4,6-dimethyldibenzothiophene adduct **17**

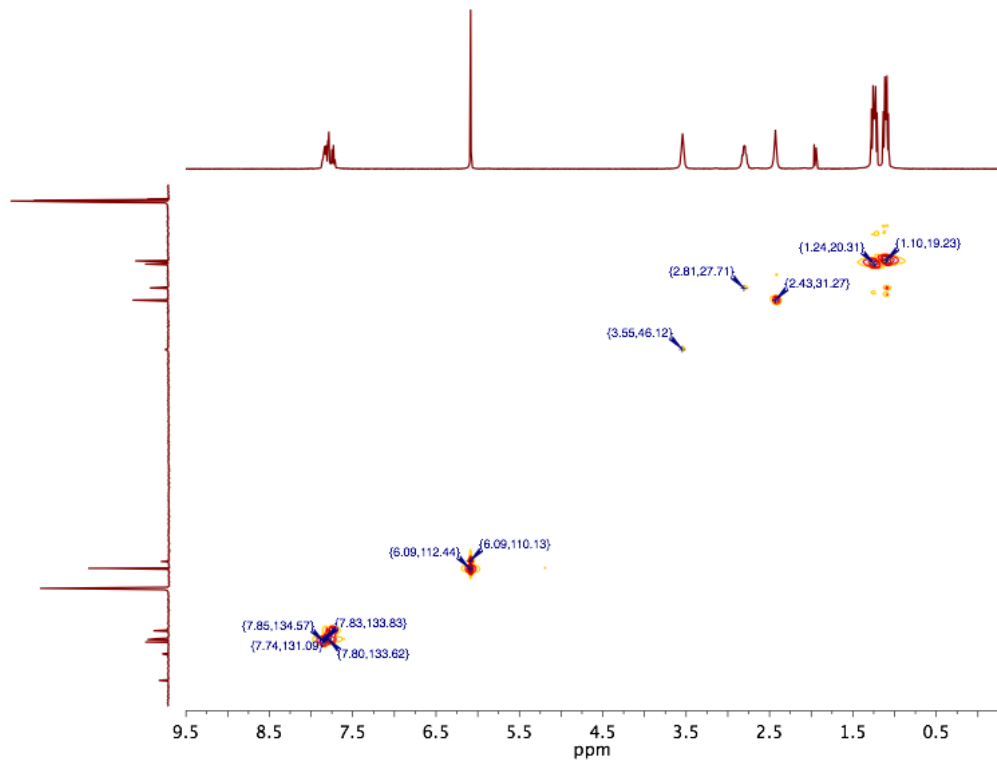


Figure S56. HSQC spectrum (CD₃CN, 400 MHz) for tetrahydrothiophene adduct **18**

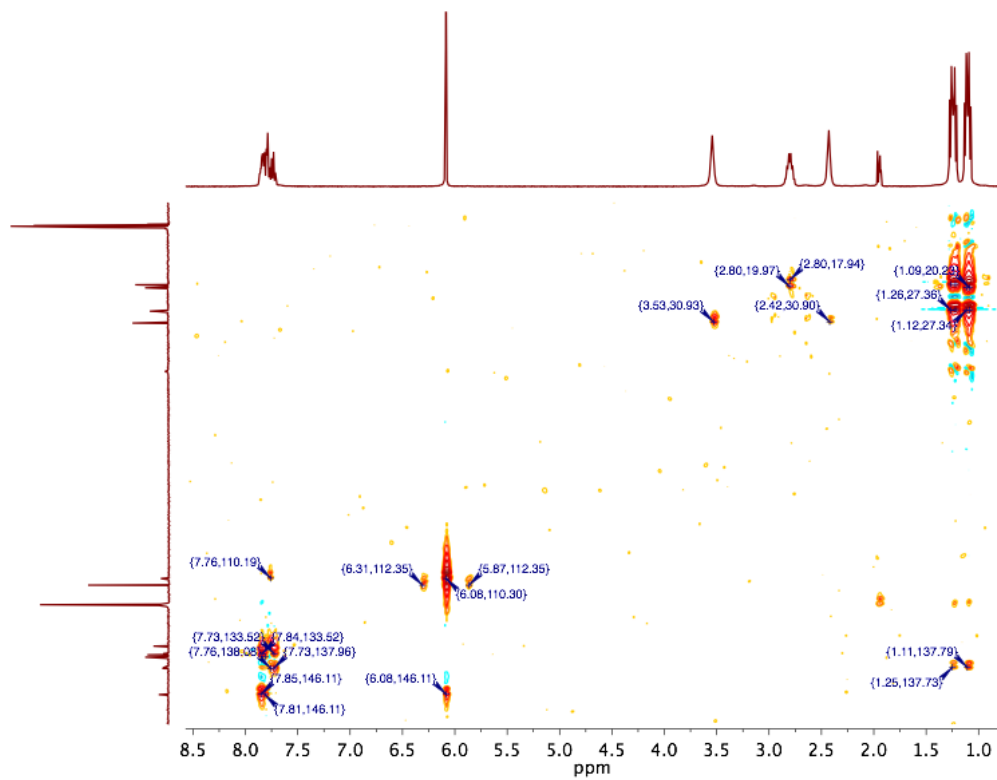


Figure S57. HMBC spectrum (CD₃CN, 400 MHz) for tetrahydrothiophene adduct **18**

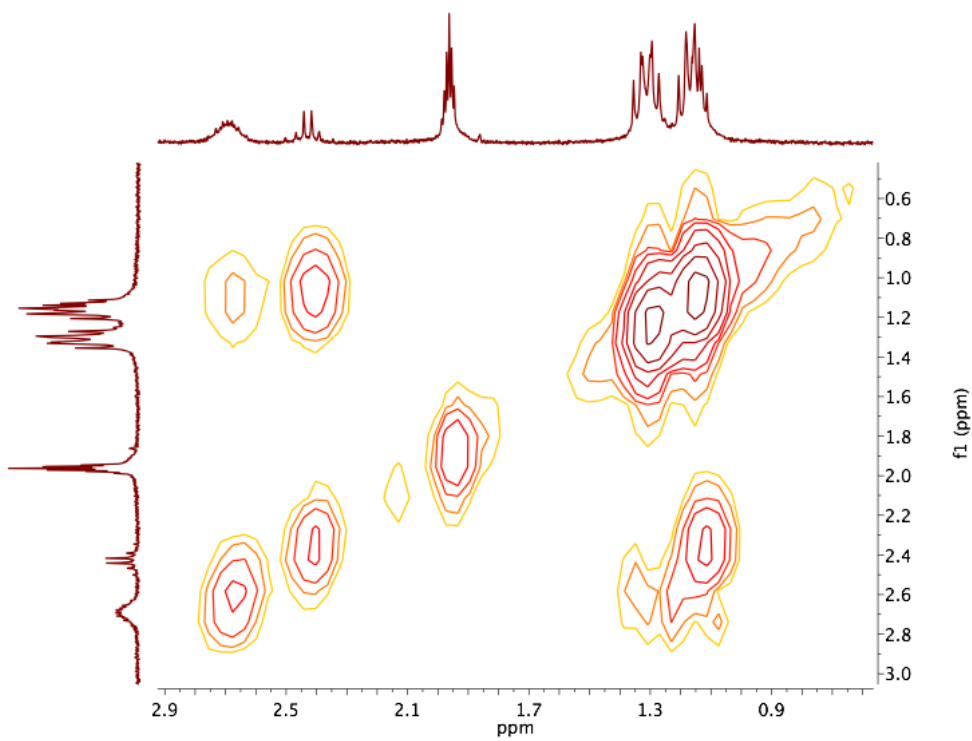


Figure S58. Aliphatic region of COSY spectrum (CD_3CN , 300 MHz) for propanoate complex **19**

III. Computational Details

All calculations were performed with DFT as implemented in Gaussian 09 Revision C.01.⁷ Geometry optimizations and electronic structure calculations were performed with the TPSSh hybrid functional^{8,9} that, incorporating 10% exact exchange (c.f. BLYP 0% and B3LYP 20%), has been shown to be effective for calculating transition metal-containing compounds.¹⁰⁻¹² The LANL2DZ basis set and effective core potential¹³ for Pd atoms and the 6-31++G(d,p) basis set¹⁴ for all other atoms was used. No solvent corrections were used. All optimizations of palladium complexes were performed ignoring molecular symmetry starting from a crystallographic set of coordinates and as singlet dications. The benzene adduct, although input as an $\eta^3:\eta^3$ structure from the experimentally obtained toluene adduct, always optimized to an $\eta^2:\eta^2$ minimum. Energetic minima were confirmed with a subsequent frequency calculation that did not return imaginary frequency vibrations < -10 cm⁻¹. All molecular orbital illustrations are depicted with a 0.05 isosurface value. The orbitals of “dipalladium diphosphine fragment” in the following figure were calculated based on the geometry from the benzene adduct with a single point energy calculation. L = a computational variant of the experimentally used diphosphine **1**, with methyls in place of isopropyls. Mulliken charges of heterocycles were calculated from geometry-optimized unbound heterocycles, and H atoms were summed into the nearest heavy atoms. While primitive, ground-state Mulliken charge calculations have been shown to be predictive, for instance, for relative pK_as of substituted benzoic acids, phenols, and anilines.¹⁵⁻¹⁷ Electrostatic potentials were mapped using GaussView, the GUI component of the Gaussian software package, onto the 0.004 electron density isosurface. Red indicates potential energy lower or equal to -0.02 Hartrees, and blue signifies potential energy higher or equal to +0.02 Hartrees.

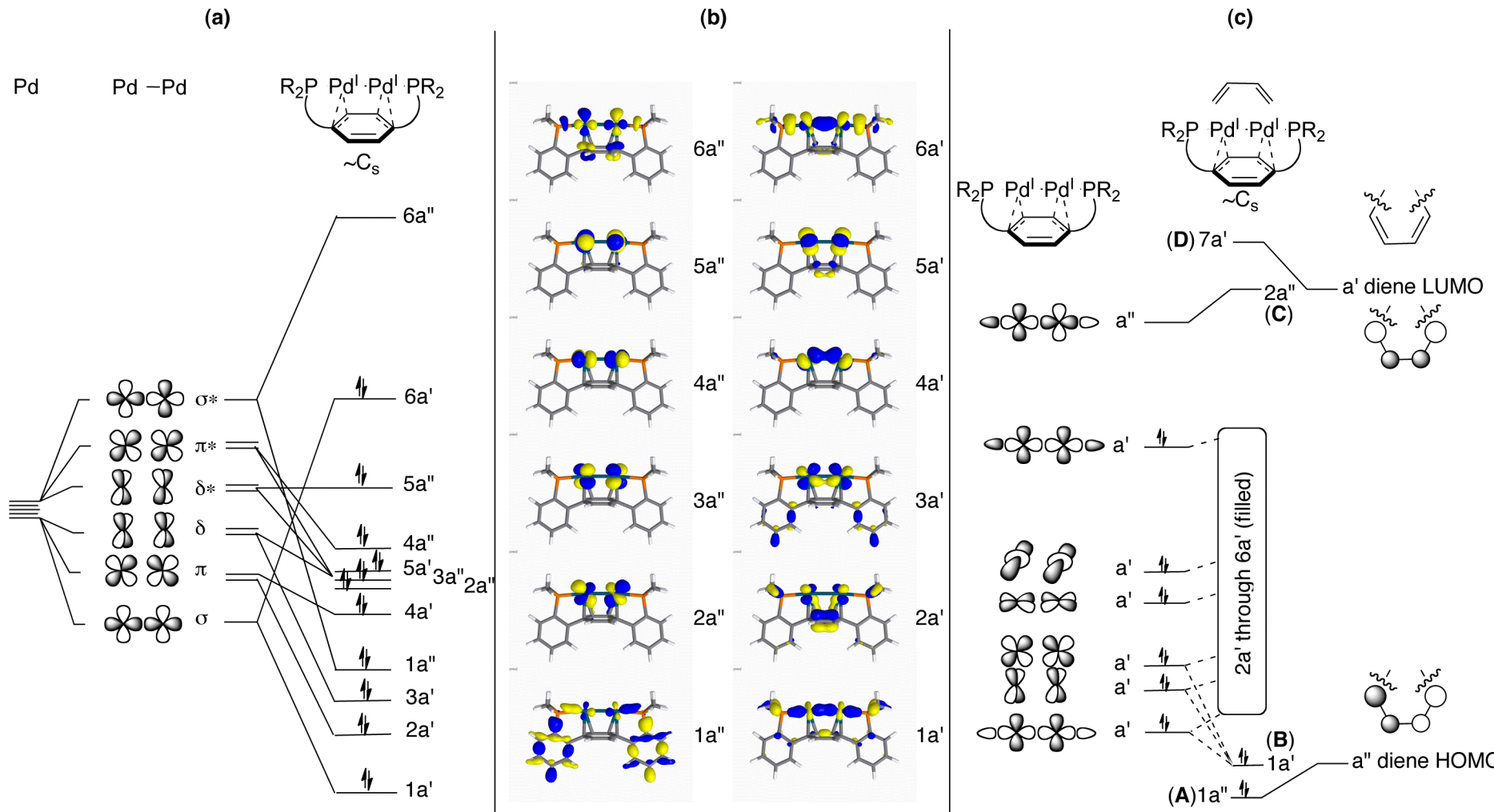


Figure S14. Qualitative MO bonding analysis. (a) Frontier orbitals of a C_s -symmetric dipalladium diphosphine fragment (b) DFT-calculated orbitals of a dipalladium diphosphine fragment (c) Interaction diagram of frontier orbitals with those of a diene, assuming C_s symmetry.

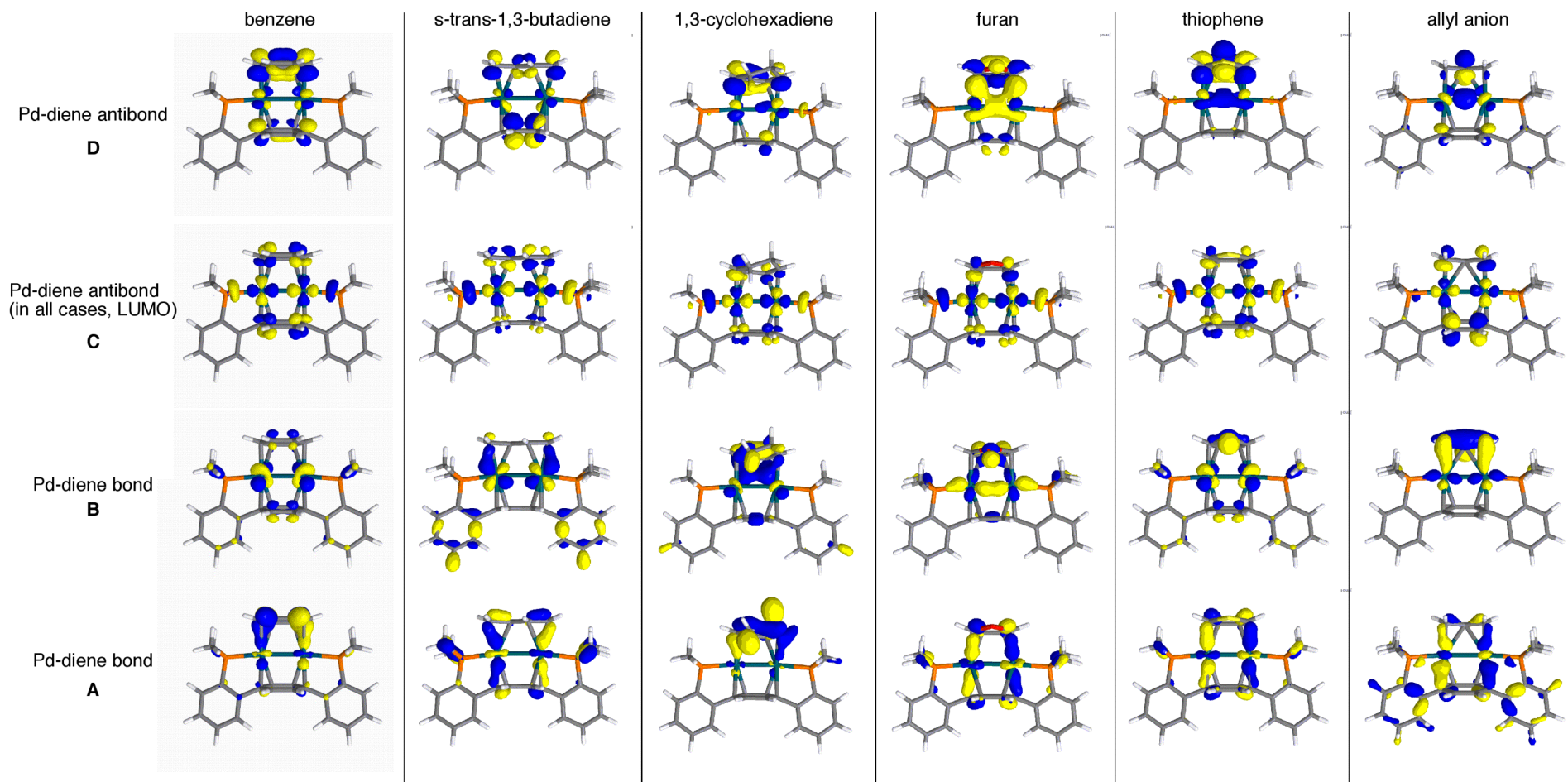


Figure S15. Examples of molecular orbitals displaying bonding interactions between $[\text{Pd}_2\text{L}]^{2+}$ and various capping ligands, corresponding to MOs **A-D** in Figure S14c.

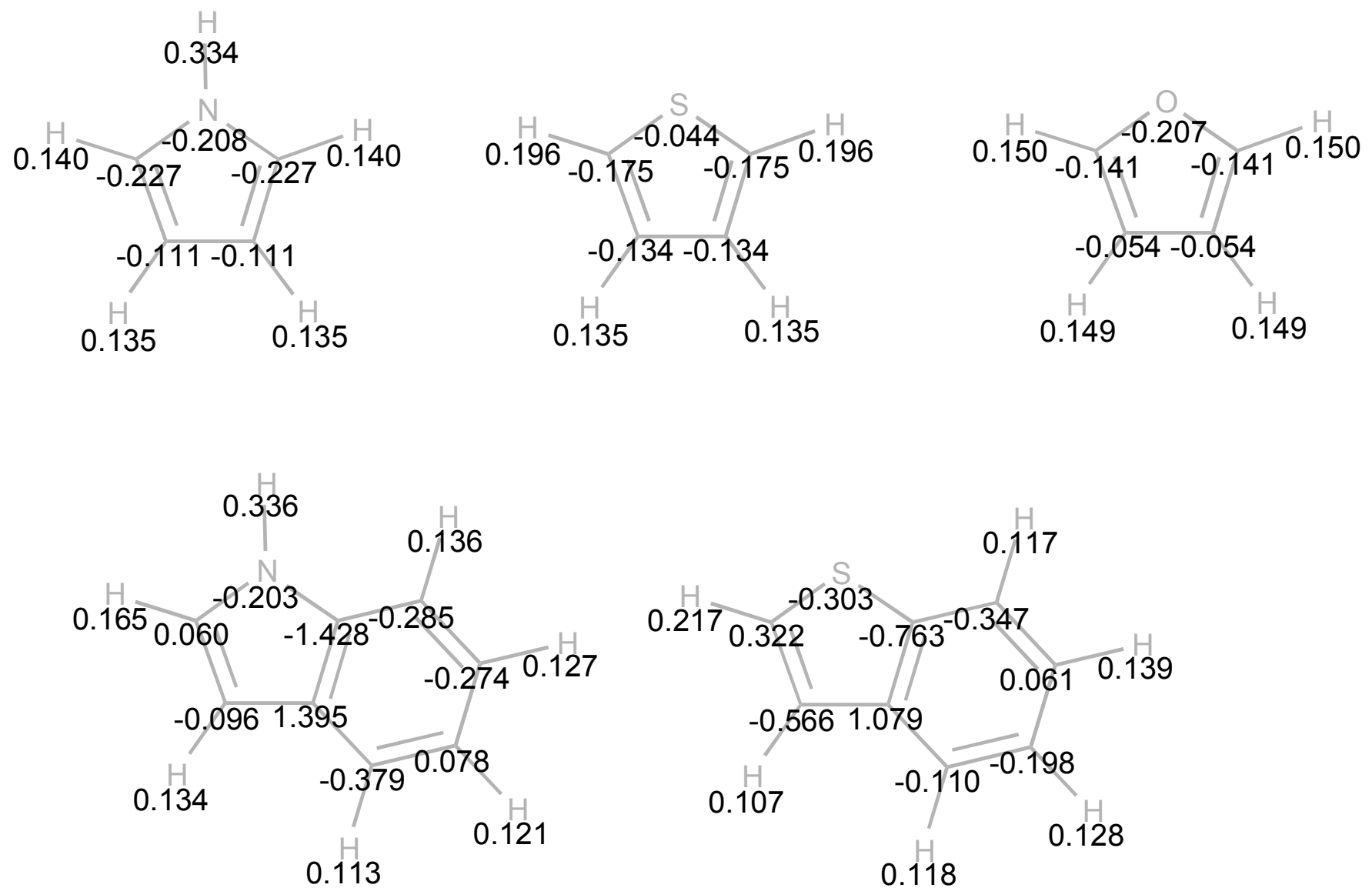


Figure S16. Mulliken charges for unbound unsaturated organics.

Cartesian coordinates for [Pd₂L(C₆H₆)]²⁺

Pd	-1.37541	-0.80823	-0.16239	C	4.52783	-1.27028	1.48124
Pd	1.37541	-0.80823	-0.16189	H	4.45914	-2.36152	1.50909
P	-3.71555	-0.61808	-0.03487	H	5.58488	-0.98618	1.48934
P	3.71555	-0.61804	-0.03415	H	4.04123	-0.85625	2.36717
C	-3.99181	1.17822	-0.04018	C	-4.52752	-1.27075	1.48050
C	-5.26610	1.76771	-0.09547	H	-5.58463	-0.98685	1.48880
C	-5.39280	3.15674	-0.04166	H	-4.45861	-2.36199	1.50813
C	-4.25049	3.95774	0.07160	H	-4.04086	-0.85678	2.36643
C	-2.98112	3.37563	0.12283	C	-4.67835	-1.33557	-1.42555
C	-2.84217	1.97946	0.05891	H	-4.55216	-2.42186	-1.44659
C	-1.45029	1.40312	0.09587	H	-5.74321	-1.11308	-1.30343
C	-0.70964	1.23001	-1.11776	H	-4.33258	-0.91599	-2.37297
C	0.70926	1.22992	-1.11793				
C	1.45026	1.40310	0.09546				
C	0.68812	1.49910	1.32508				
C	-0.68783	1.49908	1.32527				
C	2.84211	1.97952	0.05814				
C	2.98099	3.37574	0.12107				
C	4.25035	3.95785	0.06975				
C	5.39272	3.15681	-0.04263				
C	5.26609	1.76774	-0.09551				
C	3.99180	1.17826	-0.04015				
C	1.42214	-2.99882	0.23129				
C	0.70939	-2.93499	-0.99799				
C	-0.70773	-2.93498	-0.99885				
H	-6.15776	1.15203	-0.17380				
H	-6.37668	3.61223	-0.08354				
H	-4.34750	5.03772	0.11552				
H	-2.09965	4.00542	0.20225				
H	-1.23161	1.27855	-2.06934				
H	1.23099	1.27831	-2.06968				
H	1.22906	1.63952	2.25594				
H	-1.22851	1.63944	2.25629				
H	2.09948	4.00555	0.19986				
H	4.34731	5.03787	0.11293				
H	6.37660	3.61233	-0.08457				
H	6.15779	1.15203	-0.17324				
H	2.46315	-3.30258	0.22824				
H	1.23865	-3.02693	-1.94150				
C	-1.42199	-2.99897	0.22954				
H	-2.46293	-3.30294	0.22518				
C	-0.68974	-3.03582	1.46899				
C	0.68841	-3.03570	1.46985				
H	1.23226	-3.12169	2.40495				
H	-1.23582	-3.02677	-1.94299				
H	-1.23474	-3.12191	2.40340				
C	4.67802	-1.33593	-1.42485				
H	5.74296	-1.11373	-1.30288				
H	4.55151	-2.42219	-1.44584				
H	4.33227	-0.91629	-2.37225				

Cartesian coordinates for [Pd₂L(C₄H₆)]²⁺

Pd	1.43943	-0.96225	-0.11452	C	4.53045	-1.09278	-1.85517
Pd	-1.43943	-0.96227	0.11449	H	5.58252	-0.79062	-1.84696
P	3.75405	-0.68390	-0.24223	H	4.47668	-2.16938	-2.03840
P	-3.75406	-0.68385	0.24217	H	4.01447	-0.56646	-2.66102
C	3.98381	1.09528	0.05171	C	4.77244	-1.55668	1.01183
C	5.24572	1.70911	0.11184	H	4.72266	-2.63769	0.85682
C	5.34286	3.07008	0.40820	H	5.81616	-1.23886	0.92461
C	4.18384	3.81642	0.64946	H	4.41111	-1.31694	2.01438
C	2.92594	3.21125	0.58139	H	2.10301	-3.28607	1.03809
C	2.81637	1.84498	0.27512	H	-2.10333	-3.28617	-1.03809
C	1.44109	1.24953	0.14430				
C	0.58006	1.16317	1.28549				
C	-0.81269	1.16844	1.14925				
C	-1.44110	1.24950	-0.14437				
C	-0.58006	1.16336	-1.28557				
C	0.81270	1.16863	-1.14932				
C	-2.81636	1.84501	-0.27512				
C	-2.92589	3.21133	-0.58118				
C	-4.18378	3.81651	-0.64931				
C	-5.34284	3.07011	-0.40836				
C	-5.24572	1.70911	-0.11220				
C	-3.98381	1.09527	-0.05197				
C	1.88989	-3.09191	-0.01142				
C	0.55735	-3.04886	-0.45336				
C	-0.55758	-3.04888	0.45329				
H	6.15141	1.13375	-0.05827				
H	6.31761	3.54391	0.45935				
H	4.25881	4.87258	0.88727				
H	2.03085	3.80126	0.75620				
H	1.01862	1.20567	2.27805				
H	-1.42961	1.25675	2.03886				
H	-1.01860	1.20597	-2.27813				
H	1.42960	1.25703	-2.03893				
H	-2.03078	3.80136	-0.75579				
H	-4.25873	4.87271	-0.88694				
H	-6.31758	3.54395	-0.45960				
H	-6.15144	1.13371	0.05769				
H	2.66226	-3.37858	-0.71777				
H	0.34505	-3.13822	-1.51763				
C	-1.89012	-3.09195	0.01139				
H	-2.66247	-3.37850	0.71783				
H	-0.34524	-3.13824	1.51755				
C	-4.52995	-1.09231	1.85547				
H	-5.58197	-0.78995	1.84765				
H	-4.47628	-2.16887	2.03895				
H	-4.01355	-0.56587	2.66098				
C	-4.77268	-1.55696	-1.01143				
H	-4.72392	-2.63785	-0.85523				
H	-5.81616	-1.23813	-0.92503				
H	-4.41072	-1.31861	-2.01408				

Cartesian coordinates for [Pd₂L(C₆H₈)]²⁺

Pd	-1.36571	-0.76247	-0.24902	H	4.34247	-0.97657	-2.30612
Pd	1.36814	-0.78299	-0.17932	C	4.49435	-1.30318	1.55033
P	-3.70105	-0.55574	-0.04533	H	4.41531	-2.39362	1.57399
P	3.71112	-0.64287	0.02307	H	5.55382	-1.02915	1.57358
C	-3.96381	1.24293	0.02390	H	4.00039	-0.88817	2.43165
C	-5.23603	1.83939	0.02910	C	-4.49378	-1.26654	1.45364
C	-5.35454	3.22729	0.12002	H	-5.54704	-0.97150	1.49475
C	-4.20530	4.02112	0.20927	H	-4.43552	-2.35835	1.42808
C	-2.93791	3.43255	0.20190	H	-3.98707	-0.90023	2.34926
C	-2.80730	2.03761	0.10254	C	-4.69905	-1.19874	-1.44826
C	-1.41759	1.45524	0.09075	H	-4.60267	-2.28636	-1.51232
C	-0.69017	1.32955	-1.13579	H	-5.75579	-0.95332	-1.30337
C	0.72752	1.31062	-1.15119	H	-4.35426	-0.75294	-2.38394
C	1.48484	1.42829	0.05855	H	0.36520	-2.02053	2.05258
C	0.73837	1.44371	1.29469	H	-1.00441	-4.59148	1.13521
C	-0.64532	1.45340	1.30914				
C	2.88832	1.97677	0.03285				
C	3.05449	3.37107	0.05045				
C	4.33694	3.92598	0.03034				
C	5.46527	3.09874	-0.00609				
C	5.31106	1.71135	-0.01826				
C	4.02361	1.14889	0.00344				
C	1.32281	-2.92746	0.34257				
C	0.77841	-2.81131	-0.94697				
C	-0.65421	-2.71174	-1.14266				
H	-6.13312	1.22966	-0.03277				
H	-6.33724	3.68724	0.12445				
H	-4.29547	5.10020	0.28128				
H	-2.05108	4.05648	0.26608				
H	-1.22107	1.41779	-2.07964				
H	1.24122	1.37440	-2.10636				
H	1.28608	1.52810	2.22861				
H	-1.17127	1.53927	2.25532				
H	2.18405	4.02033	0.07569				
H	4.45513	5.00468	0.04032				
H	6.45966	3.53250	-0.02347				
H	6.19207	1.07607	-0.04341				
H	2.34347	-3.28483	0.43850				
H	1.40782	-2.94469	-1.82302				
C	-1.53747	-2.95542	-0.07379				
H	-2.55829	-3.22992	-0.32579				
C	-1.00133	-3.49540	1.23421				
C	0.42331	-3.00746	1.57031				
H	0.88091	-3.67390	2.30792				
H	-1.02777	-2.65548	-2.16188				
H	-1.67548	-3.26305	2.06304				
C	4.67599	-1.38904	-1.35124				
H	5.74246	-1.17794	-1.22360				
H	4.53565	-2.47387	-1.35927				

Cartesian coordinates for [Pd₂L(C₄H₄O)]²⁺

Pd	1.33779	-0.83710	-0.11452	H	4.47551	-2.50632	1.45483
Pd	-1.33786	-0.83713	-0.11500	H	5.60488	-1.13775	1.45735
P	3.69837	-0.70679	-0.00353	H	4.08750	-1.03457	2.38292
P	-3.69844	-0.70668	-0.00444	O	-0.00037	-3.05315	1.33846
C	3.99368	1.09036	0.02654				
C	5.27720	1.66145	0.05213				
C	5.42295	3.04977	0.07393				
C	4.28980	3.87094	0.06951				
C	3.01064	3.30866	0.04344				
C	2.85406	1.91345	0.02149				
C	1.45438	1.35585	0.00541				
C	0.69613	1.27710	1.23385				
C	-0.69555	1.27706	1.23412				
C	-1.45427	1.35582	0.00598				
C	-0.70407	1.30317	-1.21517				
C	0.70371	1.30316	-1.21543				
C	-2.85393	1.91347	0.02251				
C	-3.01040	3.30867	0.04579				
C	-4.28953	3.87103	0.07190				
C	-5.42275	3.04995	0.07501				
C	-5.27709	1.66164	0.05197				
C	-3.99361	1.09048	0.02640				
C	1.11194	-2.96903	0.52589				
C	0.72071	-2.92959	-0.82492				
C	-0.72040	-2.92960	-0.82528				
H	6.16293	1.03218	0.05456				
H	6.41491	3.48897	0.09359				
H	4.40141	4.95025	0.08573				
H	2.13606	3.95284	0.04051				
H	1.23032	1.31388	2.17846				
H	-1.22937	1.31373	2.17895				
H	-1.23225	1.38850	-2.16044				
H	1.23155	1.38839	-2.16091				
H	-2.13578	3.95279	0.04377				
H	-4.40106	4.95033	0.08913				
H	-6.41468	3.48921	0.09467				
H	-6.16288	1.03243	0.05351				
H	2.03017	-3.28438	0.99919				
H	1.35657	-3.08394	-1.68692				
C	-1.11229	-2.96906	0.52533				
H	-2.03074	-3.28444	0.99818				
H	-1.35582	-3.08400	-1.68760				
C	-4.54586	-1.41479	1.46625				
H	-5.60475	-1.13770	1.45668				
H	-4.47572	-2.50655	1.45346				
H	-4.08715	-1.03519	2.38195				
C	-4.63116	-1.38286	-1.43807				
H	-4.51577	-2.46982	-1.47951				
H	-5.69597	-1.14967	-1.33724				
H	-4.25805	-0.94536	-2.36687				
C	4.63090	-1.38343	-1.43708				
H	5.69570	-1.15007	-1.33651				
H	4.51562	-2.47041	-1.47809				
H	4.25758	-0.94631	-2.36597				
C	4.54591	-1.41457	1.46723				

Cartesian coordinates for [Pd₂L(C₄H₄S)]²⁺

Pd	-1.37476	-0.78933	-0.16082	H	-4.55233	-2.40245	-1.44366
Pd	1.37606	-0.79112	-0.15982	H	-5.74255	-1.09272	-1.30230
P	-3.71480	-0.59751	-0.03397	H	-4.33160	-0.89785	-2.37182
P	3.71630	-0.60230	-0.03187	S	-0.02450	-3.01339	1.38978
C	-3.98989	1.19897	-0.04150				
C	-5.26379	1.78921	-0.09774				
C	-5.38959	3.17839	-0.04564				
C	-4.24678	3.97878	0.06686				
C	-2.97781	3.39591	0.11903				
C	-2.83975	1.99958	0.05683				
C	-1.44826	1.42237	0.09474				
C	-0.70749	1.24731	-1.11854				
C	0.71141	1.24631	-1.11845				
C	1.45230	1.42047	0.09487				
C	0.68999	1.51846	1.32422				
C	-0.68595	1.51933	1.32417				
C	2.84453	1.99594	0.05710				
C	2.98430	3.39214	0.11837				
C	4.25405	3.97337	0.06658				
C	5.39592	3.17145	-0.04462				
C	5.26839	1.78240	-0.09584				
C	3.99371	1.19381	-0.04001				
C	1.42129	-2.98126	0.23602				
C	0.70881	-2.91846	-0.99347				
C	-0.70832	-2.91753	-0.99459				
H	-6.15583	1.17402	-0.17549				
H	-6.37317	3.63447	-0.08825				
H	-4.34310	5.05889	0.10946				
H	-2.09594	4.02522	0.19785				
H	-1.22926	1.29505	-2.07028				
H	1.23335	1.29320	-2.07016				
H	1.23085	1.65965	2.25502				
H	-1.22672	1.66117	2.25491				
H	2.10319	4.02262	0.19624				
H	4.35171	5.05337	0.10847				
H	6.38011	3.62627	-0.08693				
H	6.15971	1.16602	-0.17267				
H	2.46210	-3.28570	0.23353				
H	1.23818	-3.01189	-1.93677				
C	-1.42284	-2.97957	0.23375				
H	-2.46397	-3.28287	0.22957				
H	-1.23629	-3.01012	-1.93871				
C	4.67856	-1.32250	-1.42154				
H	5.74362	-1.10084	-1.29963				
H	4.55134	-2.40869	-1.44123				
H	4.33325	-0.90378	-2.36950				
C	4.52787	-1.25323	1.48445				
H	4.45847	-2.34439	1.51361				
H	5.58511	-0.96981	1.49240				
H	4.04138	-0.83781	2.36979				
C	-4.52748	-1.24782	1.48204				
H	-5.58440	-0.96321	1.48981				
H	-4.45927	-2.33906	1.51101				
H	-4.04071	-0.83309	2.36756				
C	-4.67781	-1.31606	-1.42395				

Cartesian coordinates for [Pd₂L(C₃H₅)]⁺

Pd	1.35920	-0.99280	-0.12344	H	-1.22659	1.70457	2.16502
Pd	-1.35927	-0.99284	-0.12359	H	6.15476	0.84078	0.01984
P	3.64881	-0.84111	0.20992	H	2.20301	3.84339	-0.16052
P	-3.64892	-0.84106	0.20947	H	-2.20271	3.84344	-0.15946
C	-1.44900	1.28934	0.04031	H	6.47122	3.28407	-0.17948
C	-2.86777	1.79535	-0.02077	H	4.48986	4.79084	-0.26471
C	1.44910	1.28940	0.04011	H	-4.48948	4.79112	-0.26331
C	2.86790	1.79530	-0.02116	H	1.22697	1.70464	2.16484
C	3.99108	0.94805	0.03603	H	-1.27975	-3.40205	0.99566
C	0.71376	1.00546	-1.14666	H	-2.09886	-3.48502	-0.64228
C	-3.99102	0.94819	0.03614	H	0.00004	-3.04627	-1.79185
C	-5.46821	2.87151	-0.13210	H	2.09875	-3.48500	-0.64195
C	-0.71379	1.00545	-1.14657	H	1.27941	-3.40201	0.99586
C	-5.28549	1.49220	-0.02196	C	4.37414	-1.31668	1.83810
C	-0.69043	1.49472	1.24420	H	4.26195	-2.39488	1.98420
C	5.28559	1.49194	-0.02225	H	5.43720	-1.05897	1.88128
C	3.06525	3.18362	-0.12130	H	3.84586	-0.79726	2.64088
C	-3.06500	3.18373	-0.12044	C	4.76084	-1.68273	-0.99479
C	5.46843	2.87120	-0.13285	H	5.81130	-1.44389	-0.80121
C	4.35457	3.71703	-0.17976	H	4.62840	-2.76547	-0.91155
C	-4.35428	3.71727	-0.17873	H	4.50162	-1.37451	-2.01030
C	-1.26949	-3.10135	-0.05289	C	-4.76081	-1.68218	-0.99572
C	1.26931	-3.10127	-0.05269	H	-4.62855	-2.76497	-0.91273
C	-0.00005	-3.02904	-0.70314	H	-5.81128	-1.44322	-0.80233
C	0.69068	1.49476	1.24410	H	-4.50130	-1.37374	-2.01109
H	1.23044	0.97472	-2.10185	C	-4.37449	-1.31721	1.83737
H	-6.47097	3.28449	-0.17857	H	-5.43752	-1.05940	1.88058
H	-1.23061	0.97477	-2.10169	H	-4.26244	-2.39549	1.98299
H	-6.15471	0.84110	0.01992	H	-3.84621	-0.79822	2.64042

III. Crystallographic Data

CCDC deposition numbers 702664 and 944713-944724 contain the supplementary crystallographic data for this paper. These data can be obtained free of charge from The Cambridge Crystallographic Data Centre via www.ccdc.cam.ac.uk/data_request/cif.

Refinement Details. In each case, crystals were mounted on a glass fiber or nylon loop using Paratone oil, then placed on the diffractometer under a nitrogen stream. Low temperature (100 K) X-ray data were obtained on a Bruker APEXII CCD based diffractometer (Mo sealed X-ray tube, $K_{\alpha} = 0.71073 \text{ \AA}$) or at Beamline 12-2 at the Stanford Synchrotron Radiation Lightsource (SSRL; DECTRIS PILATUS 6M detector, $K_{\alpha} = 0.72930 \text{ \AA}$). Loop-mounted samples sent to SSRL were submerged in LN₂ during transport (~1 day). All diffractometer manipulations, including data collection, integration and scaling were carried out using the Bruker APEXII software.¹⁸ Absorption corrections were applied using SADABS.¹⁹ Space groups were determined on the basis of systematic absences and intensity statistics and the structures were solved by direct methods using XS²⁰ (incorporated into SHELXTL) and refined by full-matrix least squares on F². All non-hydrogen atoms were refined using anisotropic displacement parameters. Hydrogen atoms were placed in idealized positions and refined using a riding model. The structure was refined (weighted least squares refinement on F²) to convergence. Graphical representation of structures with 50% probability thermal ellipsoids was generated using Diamond visualization software.²¹

Table S1. Crystal and refinement data for **3-9, 14-17, 20, 21**

	3	4	5	6	7	8	9	14	15	16	17	20	21
CCDC no.	702664	944713	944714	944715	944716	944717	944718	944719	944720	944721	944722	944723	944724
Empirical formula	C ₃₇ H ₄₈ B ₂ F ₈ P ₂ Pd ₂	C ₃₇ H ₄₈ B ₂ F ₈ OP ₂ Pd ₂	C ₃₄ H ₄₂ B ₂ F ₈ P ₂ Pd ₂	C ₃₆ H ₄₈ B ₂ F ₈ P ₂ Pd ₂	C ₃₄ H ₄₄ B ₂ F ₈ P ₂ Pd ₂ S	C ₃₅ H ₄₆ B ₂ F ₈ P ₂ Pd ₂ S	C ₃₅ H ₄₆ B ₂ F ₈ P ₂ Pd ₂	C ₃₉ H ₄₉ B ₂ F ₈ NO ₂ P ₂ Pd ₂ S	C ₃₈ H ₄₇ B ₂ F ₈ NP ₂ Pd ₂	C ₄₄ H ₅₂ B ₂ F ₈ P ₂ Pd ₂ S	C ₃₃ H ₄₅ BF ₄ P ₂ Pd ₂	C ₃₄ H ₄₅ BF ₄ N ₂ P ₂ Pd ₂	
Formula wt	941.11	957.11	899.04	929.10	933.11	947.14	947.14	931.08	1044.21	966.13	1061.27	803.24	843.27
a, Å	13.1190(6)	18.020(4)	15.2809(8)	11.8911(5)	19.2900(11)	17.950(4)	18.338(4)	11.880(2)	9.9974(4)	31.050(6)	19.395(1)	8.6364(3)	14.6826(6)
b, Å	15.2041(7)	15.340(3)	12.8833(6)	13.5564(6)	16.1824(9)	15.271(3)	15.222(3)	19.070(4)	14.9331(6)	15.190(3)	11.1339(6)	15.3772(6)	13.1786(5)
c, Å	18.3188(9)	13.560(3)	18.3268(9)	23.4012(11)	23.3891(13)	13.363(3)	13.065(3)	16.440(3)	28.042(1)	20.770(4)	20.589(1)	25.239(1)	17.8342(7)
α, °	90.00	90.00	90.00	90.00	90.00	90.00	90.00	90.00	90.00	90.00	90.00	90.00	90.00
β, °	90.00	90.00	90.062(3)	100.514(2)	90.00	90.00	90.00	98.53(3)	94.887(2)	121.85(3)	103.026(2)	91.591(2)	94.303(2)
γ, °	90.00	90.00	90.00	90.00	90.00	90.00	90.00	90.00	90.00	90.00	90.00	90.00	90.00
Volume, Å ³	3653.9(3)	3748.3(13)	3608.0(3)	3708.9(3)	7301.1(7)	3663(1)	3647(1)	3683.3(13)	4171.2(3)	8321(3)	4331.5(4)	3350.6(2)	3441.1(2)
Z	4	4	4	4	8	4	4	4	4	8	4	4	4
Cryst syst	Orthorhombic	Orthorhombic	Monoclinic	Monoclinic	Orthorhombic	Orthorhombic	Orthorhombic	Monoclinic	Monoclinic	Monoclinic	Monoclinic	Monoclinic	Monoclinic
Space group	P2 ₁ 2 ₁ 2 ₁	Pnma	P2 ₁ /c	P2 ₁ /c	Pbca	Pnma	Pnma	P2 ₁ /c	P2 ₁ /n	C 2/c	C 2/c	P2 ₁ /c	P2 ₁ /c
d _{calcd} (g/cm ³)	1.711	1.696	1.655	1.664	1.698	1.717	1.725	1.679	1.663	1.542	1.627	1.592	1.628
θ range, °	1.71 to 33.00	1.93 to 33.57	1.58 to 27.53	1.74 to 27.10	3.48 to 99.28	1.95 to 31.37	1.96 to 31.37	1.69 to 33.63	3.992 to 55.14	1.59 to 32.43	2.03 to 27.52	1.55 to 40.23	1.92 to 30.62
μ, mm ⁻¹	1.141	1.115	1.151	1.123	1.196	1.193	1.199	1.133	1.061	1.005	1.019	1.213	1.187
Absorption correction	Semi-empirical from equivalents	Empirical	Semi-empirical from equivalents	Semi-empirical from equivalents	Empirical	Empirical	Empirical	Empirical	Empirical	Empirical	Empirical	Semi-empirical from equivalents	Semi-empirical from equivalents
GoF ^a	1.558	1.106	1.026	1.097	1.060	1.069	0.781	1.113	1.111	1.159	1.667	1.072	1.056
R1 ^b , wR2 ^c	0.0250, 0.0421	0.0242, 0.0651	0.0711, 0.1838	0.1656, 0.3240	0.0269, 0.0624	0.0333, 0.0880	0.0376, 0.1086	0.0406, 0.1093	0.0214, 0.0479	0.0377, 0.0479	0.0322, 0.1010	0.0398, 0.0614	0.0509, 0.1012
Type of diffractometer	Bruker	SSRL	Bruker	Bruker	Bruker	SSRL	SSRL	SSRL	Bruker	SSRL	Bruker	Bruker	Bruker

^a GoF = S = { Σ[w(F_o²-F_c²)²] / (n-p) }^{1/2}

^b R1 = Σ||F_o|-|F_c|| / Σ|F_o|

^c wR2 = { Σ[w(F_o²-F_c²)²] / Σ[w(F_o²)²] }^{1/2}

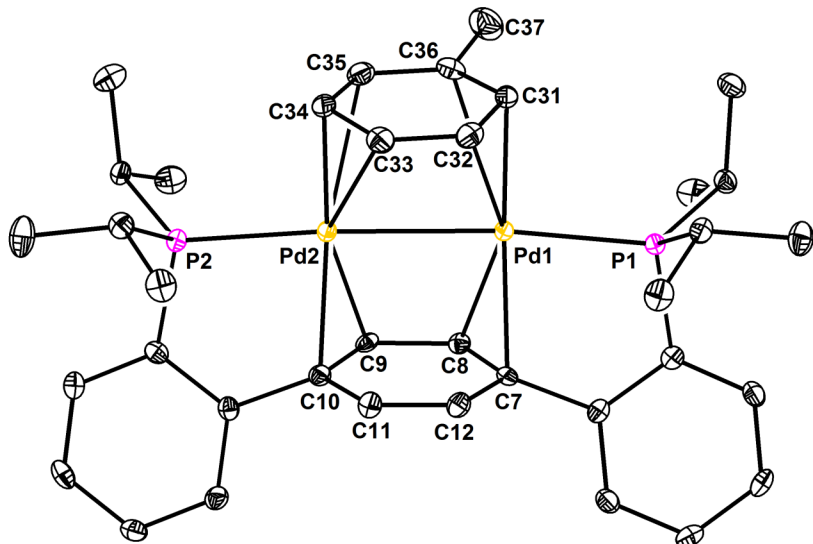


Figure S62. Structural drawing of **3** with 50% probability ellipsoids. Outer-sphere tetrafluoroborate ions and hydrogen atoms are not shown for clarity.

Special refinement details for **3.** The largest disagreements in structure factors indicate twinning and the Flack parameter suggests a racemic twin ratio of 0.546:0.454. The refined coordinates suggest the higher symmetry space group *Pnma*. However, although there is 98% agreement between the coordinates and the higher symmetry, the diffraction intensities do not support that assignment. Therefore the correct space group assignment is as assigned, *P2₁2₁2₁*. Hydrogen atoms were refined from the difference map without constraints.

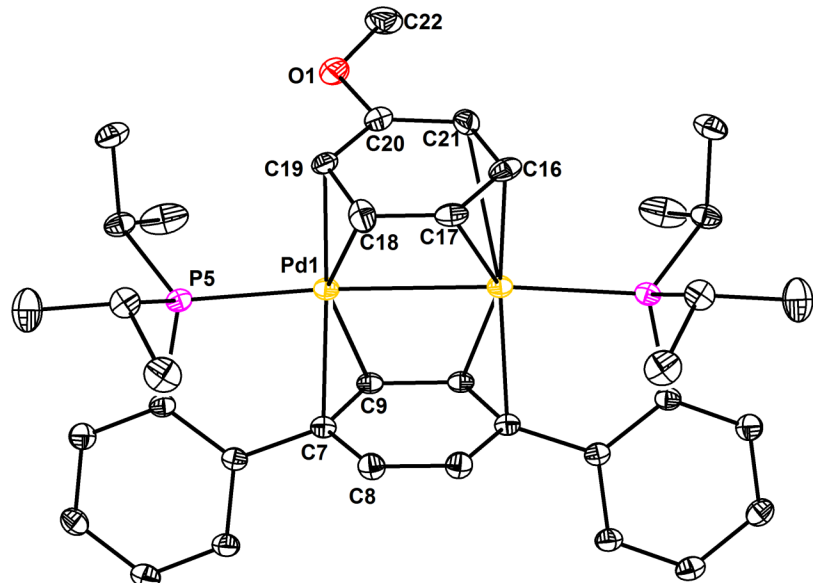


Figure S63. Structural drawing of **4** with 50% probability ellipsoids. Outer-sphere tetrafluoroborate ions and hydrogen atoms are not shown for clarity.

Special refinement details for **5.** A solution in *Pnma* was elusive at first, so structure refinement was performed in *P-1* space group. Reduction of the solution to *Pnma* using PLATON's Addsym function gave an instructions file with the proper unit cell. Reprocessing the raw hkl file with

Pnma space group, using the PLATON output, and refining led to the final solution. Anisole was disordered over two sites and modeled with the PART -1 instruction.

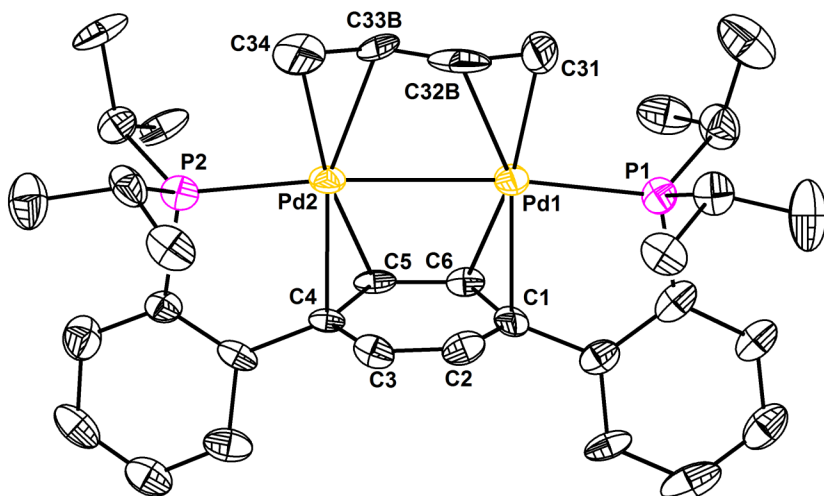


Figure S64. Structural drawing of **5** with 50% probability ellipsoids. Outer-sphere tetrafluoroborate ions and hydrogen atoms are not shown for clarity.

Special refinement details for 5. The dataset was twinned and disorder in the butadiene fragment precludes accurate determination of the butadiene structure. The solution was obtained in monoclinic $P2_1/c$; attempted solutions in orthorhombic *Pnma* gave worse R values and esds.

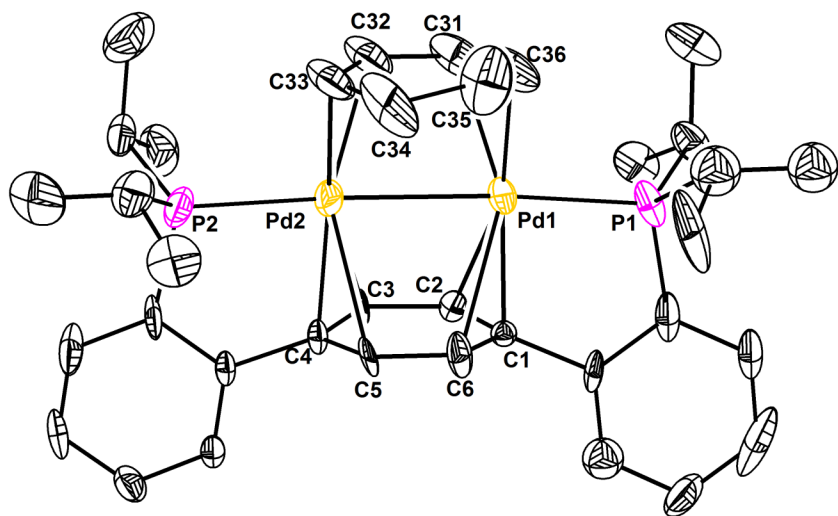


Figure S65. Structural drawing of **6** with 50% probability ellipsoids. Outer-sphere tetrafluoroborate ions and hydrogen atoms are not shown for clarity.

Special refinement details for 6. A yellow parallelepiped block of suitable size (0.40 x 0.23 x 0.16 mm) was selected from a representative sample of crystals of the same habit using an optical microscope and mounted onto a glass fiber. Low temperature (100 K) X-ray data were

obtained on a Bruker APEXII CCD based diffractometer (Mo sealed X-ray tube, $K_{\alpha} = 0.71073 \text{ \AA}$). All diffractometer manipulations, including data collection, integration and scaling were carried out using the Bruker APEXII software. While the crystals diffracted very well, the data could not be solved to give a satisfactory model. This is likely due to the crystal beginning to undergo a phase transition resulting in loss of symmetry and possible twinning that could not be accounted for. The systematic absence violations listed by XPREP for a 2_1 axis are [$N = 58$, $N(I > 3\sigma) = 9$, $\langle I \rangle = 0.1$, $\langle I/\sigma \rangle = 1.5$] and for a c-glide plane [$N = 3325$, $N(I > 3\sigma) = 1501$, $\langle I \rangle = 0.6$, $\langle I/\sigma \rangle = 4.5$] (for comparison, lattice exceptions for all reflections, $N = 156641$, $N(I > 3\sigma) = 113930$, $\langle I \rangle = 5.2$, $\langle I/\sigma \rangle = 9.6$). Despite the weakening or destruction of the c-glide, the structure refinement behaves better in $P2_1/c$ than in $P2_1$. While the $P2_1/c$ model does not produce accurate bond lengths and bond angles, this represents the best solution and no additional symmetry elements or changes were recommended by PLATON. The presented model does show with certainty the presence of the targeted cyclohexadiene adduct, which was also confirmed by multiple spectroscopic techniques (*vide supra*). Not all non-hydrogen atoms could be satisfactorily refined by using anisotropic displacement parameters. Hydrogen atoms were placed in idealized positions and refined using a riding model. The final least-squares refinement converged to $R_1 = 0.1656$ ($I > 2\sigma(I)$, 7869 data; $R(\text{int}) = 0.0360$) and $wR_2 = 0.3258$ (F^2 , 8182 data, 415 parameters, 0 restraint).

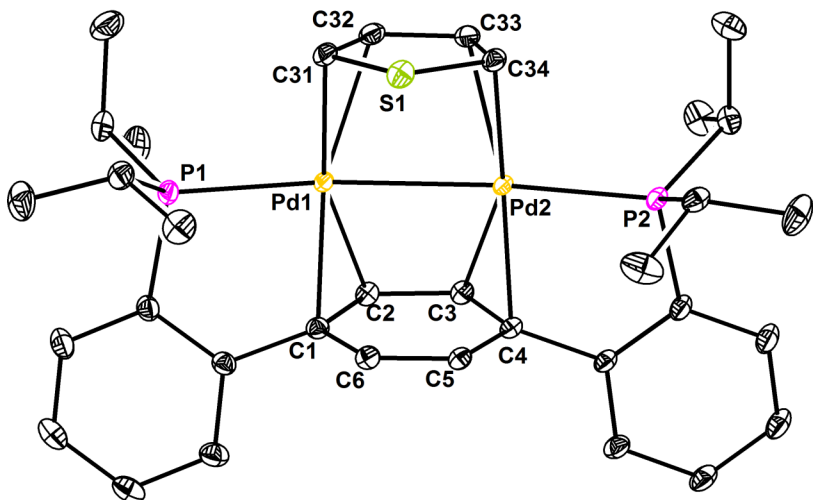


Figure S66. Structural drawing of **7** with 50% probability ellipsoids. Outer-sphere tetrafluoroborate ions and hydrogen atoms are not shown for clarity.

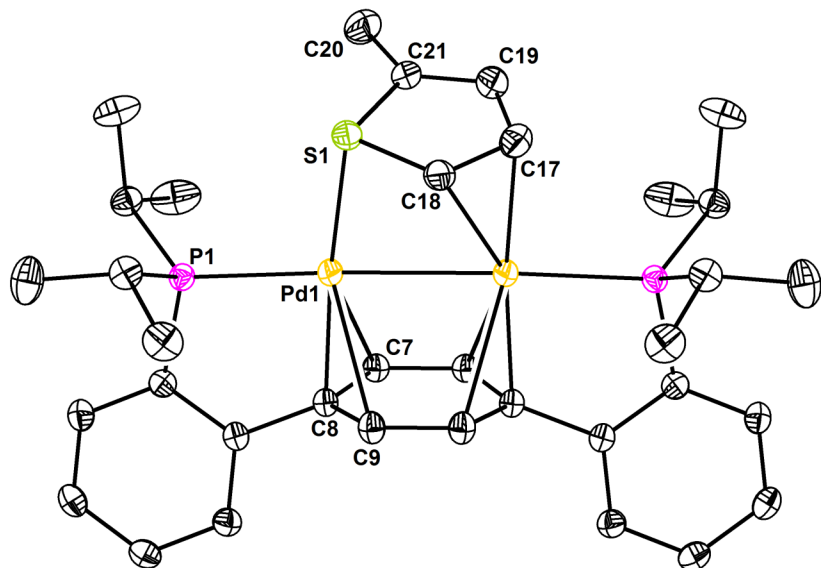


Figure S67. Structural drawing of **8** with 50% probability ellipsoids. Outer-sphere tetrafluoroborate ions and hydrogen atoms are not shown for clarity.

Special refinement details for **8.** The capping 2-methylthiophene was disordered and modeled as an exact 50:50 mixture of mirror conformations across the molecular mirror plane using the “PART -1” card in SHELX. Attempts to allow the relative population or geometries of the two conformations to float did not improve refinement statistics or significantly alter geometries.

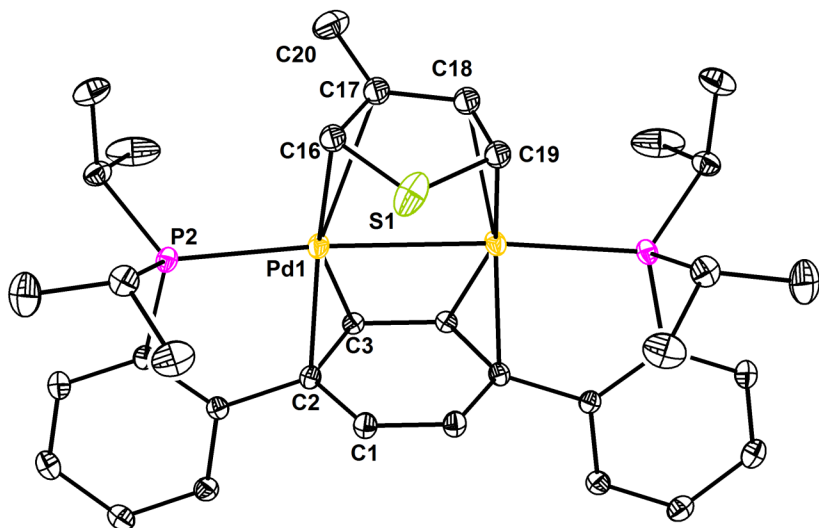


Figure S68. Structural drawing of **9** with 50% probability ellipsoids. Outer-sphere tetrafluoroborate ions and hydrogen atoms are not shown for clarity.

Special refinement details for **9.** The capping 3-methylthiophene was disordered and modeled as an exact 50:50 mixture of mirror conformations across the molecular mirror plane using the “PART -1” card in SHELX. Attempts to allow the relative population or geometries of the two conformations to float did not improve refinement statistics or significantly alter geometries.

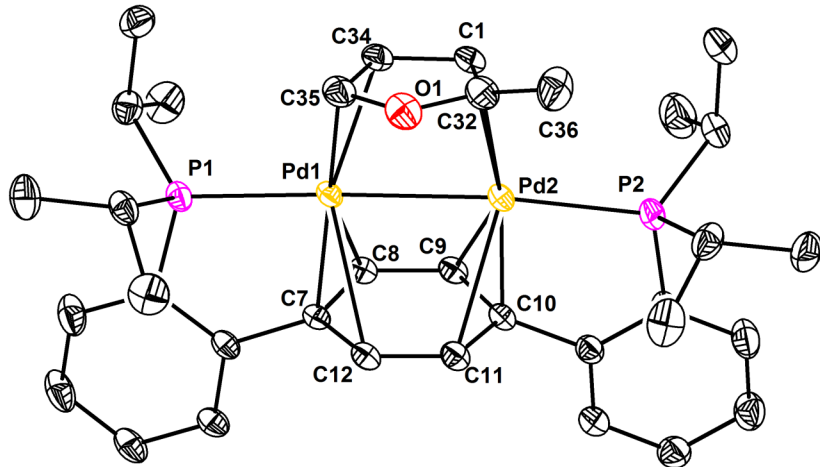


Figure S69. Structural drawing of **14** with 50% probability ellipsoids. Outer-sphere tetrafluoroborate ions and hydrogen atoms are not shown for clarity.

Special refinement details for **14.** The capping 2-methylfuran was modeled in only one conformation. A minor Q peak possibly corresponding to the methyl group of a mirror image 2-methylfuran was observed during refinement, but other binding conformations could not be modeled. Attempting to switch the positions of O1 and C1 resulted in unreasonable structures with worse refinement indicators.

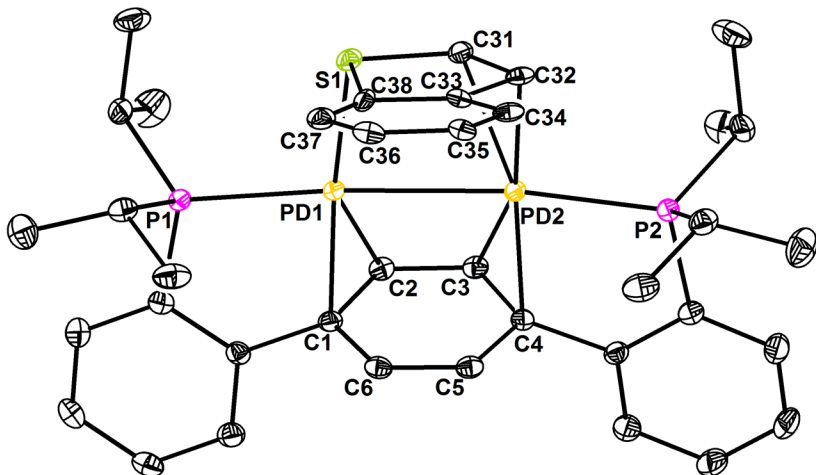


Figure S70. Structural drawing of **15** with 50% probability ellipsoids. Outer-sphere tetrafluoroborate ions, outer-sphere nitromethane, and hydrogen atoms are not shown for clarity.

Special refinement details for **15.** An outer-sphere nitromethane molecule and tetrafluoroborate anions were disordered and modeled in two conformations. The capping benzothiophene was disordered and initially modeled in two “SADI”-related conformations. Upon relaxation of these constraint, a 60:40 mixture of internally dissimilar benzothiophenes resulted.

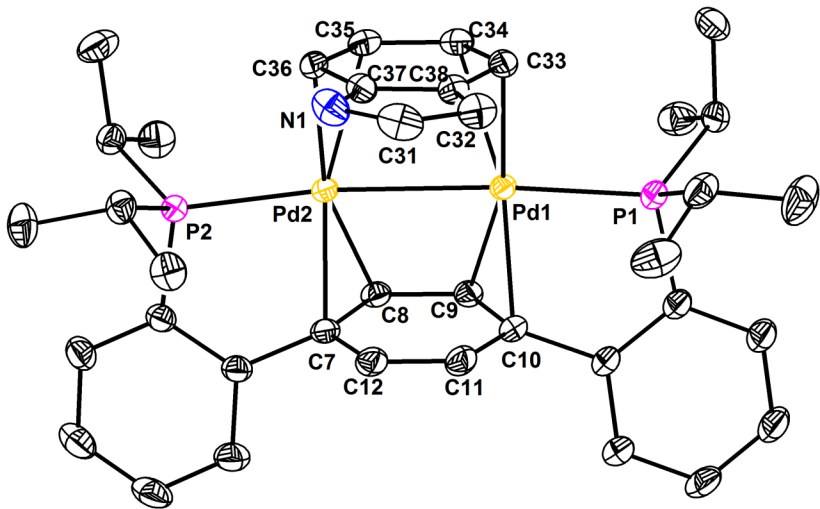


Figure S71. Structural drawing of **16** with 50% probability ellipsoids. Outer-sphere tetrafluoroborate ions and hydrogen atoms are not shown for clarity.

Special refinement details for 6. Outer-sphere electron density could not be accurately modeled and was analyzed using PLATON's squeeze algorithm. Four voids of 181.5 \AA^3 ($\sim 68 \text{ e}^-$) are left in the unit cell, which would correspond with either one indole (62 e^-) or two molecules of nitromethane (70 e^-) per dipalladium unit. Free indole and nitromethane were present in the crystallization conditions and observed in NMR spectra of freshly crystallized material.

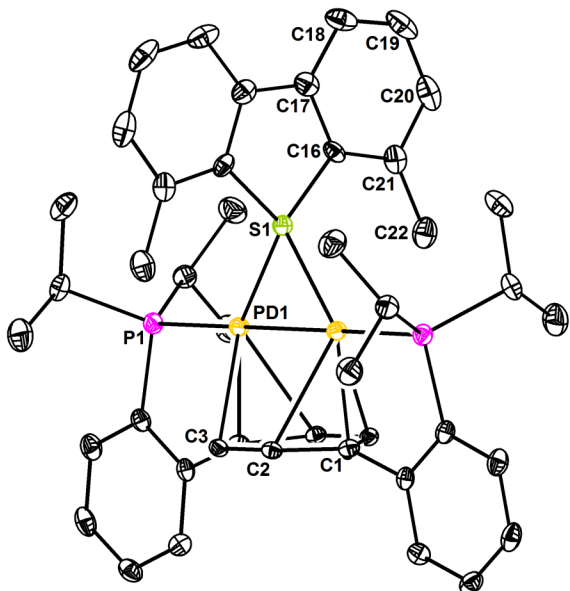


Figure S72. Structural drawing of **17** with 50% probability ellipsoids. Outer-sphere tetrafluoroborate ions and hydrogen atoms are not shown for clarity.

Special refinement details for 17. Atom S1 lies along a C_2 axis of symmetry and thus was modeled in the asymmetric unit with 0.5 relative population.

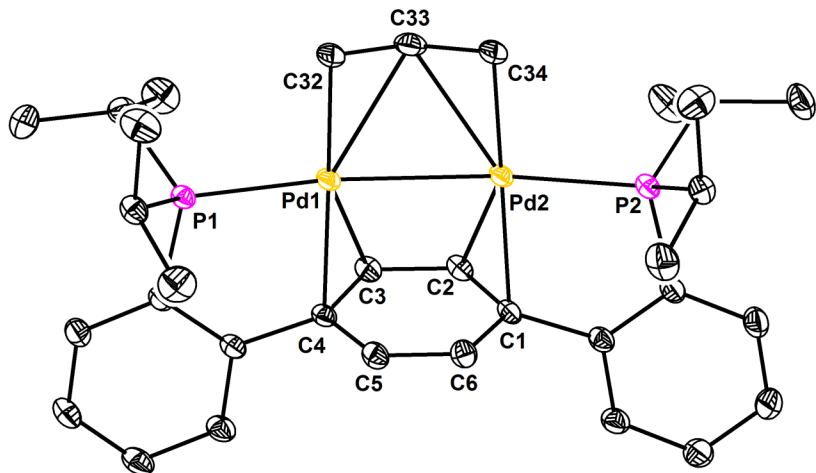


Figure S73. Structural drawing of **20** with 50% probability ellipsoids. Outer-sphere tetrafluoroborate ions and hydrogen atoms are not shown for clarity.

Special refinement details for **20.** An outer-sphere tetrafluoroborate ion was disordered and modeled in two conformations.

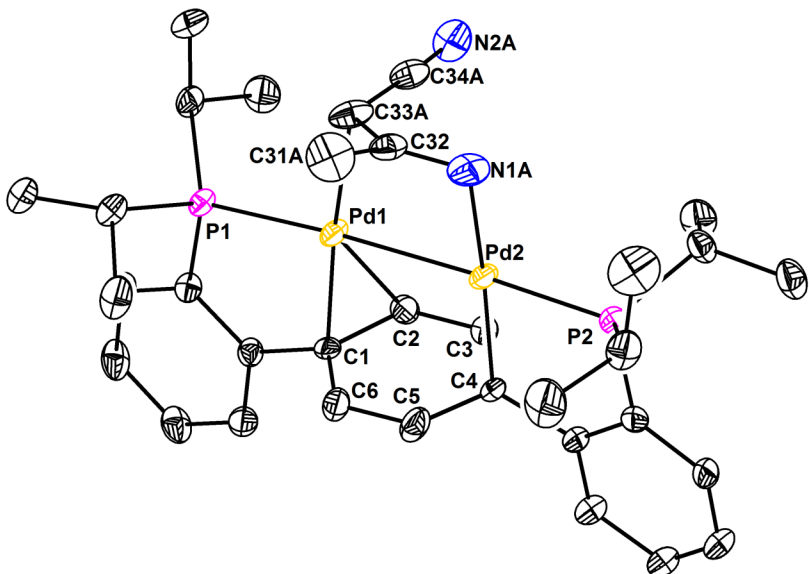


Figure S74. Structural drawing of **21** with 50% probability ellipsoids. Outer-sphere tetrafluoroborate ions and hydrogen atoms are not shown for clarity.

Special refinement details for **20.** Outer-sphere tetrafluoroborate ions were disordered and modeled in two conformations. The capping diacetonitrilyl was disordered and initially modeled in two internally “SADI”-related conformations with fixed populations. Upon relaxation of these constraint, a 60:40 mixture of internally dissimilar diacetonitrilyls resulted.

References

- (1) Murahashi, T.; Nagai, T.; Okuno, T.; Matsutani, T.; Kurosawa, H. *Chem. Commun.* **2000**, 1689.
- (2) Velian, A.; Lin, S.; Miller, A. J. M.; Day, M. W.; Agapie, T. *J. Am. Chem. Soc.* **2010**, 132, 6296.
- (3) Pangborn, A. B.; Giardello, M. A.; Grubbs, R. H.; Rosen, R. K.; Timmers, F. J. *Organometallics* **1996**, 15, 1518.
- (4) Fulmer, G. R.; Miller, A. J. M.; Sherden, N. H.; Gottlieb, H. E.; Nudelman, A.; Stoltz, B. M.; Bercaw, J. E.; Goldberg, K. I. *Organometallics* **2010**, 29, 2176.
- (5) Dawson, R.; Gillis, R. *Aust. J. Chem.* **1972**, 25, 1221.
- (6) Avent, A. G.; Frankland, A. D.; Hitchcock, P. B.; Lappert, M. F. *Chem. Commun.* **1996**, 0, 2433.
- (7) Gaussian 09, Revision C.01, Frisch, M. J.; Trucks, G. W.; Schlegel, H. B.; Scuseria, G. E.; Robb, M. A.; Cheeseman, J. R.; Scalmani, G.; Barone, V.; Mennucci, B.; Petersson, G. A.; Nakatsuji, H.; Caricato, M.; Li, X.; Hratchian, H. P.; Izmaylov, A. F.; Bloino, J.; Zheng, G.; Sonnenberg, J. L.; Hada, M.; Ehara, M.; Toyota, K.; Fukuda, R.; Hasegawa, J.; Ishida, M.; Nakajima, T.; Honda, Y.; Kitao, O.; Nakai, H.; Vreven, T.; Montgomery, Jr., J. A.; Peralta, J. E.; Ogliaro, F.; Bearpark, M.; Heyd, J. J.; Brothers, E.; Kudin, K. N.; Staroverov, V. N.; Kobayashi, R.; Normand, J.; Raghavachari, K.; Rendell, A.; Burant, J. C.; Iyengar, S. S.; Tomasi, J.; Cossi, M.; Rega, N.; Millam, J. M.; Klene, M.; Knox, J. E.; Cross, J. B.; Bakken, V.; Adamo, C.; Jaramillo, J.; Gomperts, R.; Stratmann, R. E.; Yazyev, O.; Austin, A. J.; Cammi, R.; Pomelli, C.; Ochterski, J. W.; Martin, R. L.; Morokuma, K.; Zakrzewski, V. G.; Voth, G. A.; Salvador, P.; Dannenberg, J. J.; Dapprich, S.; Daniels, A. D.; Farkas, Ö.; Foresman, J. B.; Ortiz, J. V.; Cioslowski, J.; Fox, D. J. Gaussian, Inc., Wallingford CT, 2009.
- (8) Tao, J.; Perdew, J. P.; Staroverov, V. N.; Scuseria, G. E. *Phys. Rev. Lett.* **2003**, 91, 146401.
- (9) Staroverov, V. N.; Scuseria, G. E.; Tao, J.; Perdew, J. P. *The Journal of Chemical Physics* **2003**, 119, 12129.
- (10) Jensen, K. P. *Inorg. Chem.* **2008**, 47, 10357.
- (11) Bühl, M.; Kabrede, H. *Journal of Chemical Theory and Computation* **2006**, 2, 1282.
- (12) Waller, M. P.; Braun, H.; Hojdis, N.; Bühl, M. *Journal of Chemical Theory and Computation* **2007**, 3, 2234.
- (13) Hay, P. J.; Wadt, W. R. *The Journal of Chemical Physics* **1985**, 82, 270.
- (14) Ditchfield, R.; Hehre, W. J.; Pople, J. A. *The Journal of Chemical Physics* **1971**, 54, 724.
- (15) Saeys, M.; Reyniers, M.-F. o.; Neurock, M.; Marin, G. B. *The Journal of Physical Chemistry B* **2003**, 107, 3844.
- (16) Hafner, J. *Monatsh. Chem.* **2008**, 139, 373.
- (17) Biffis, A.; Zecca, M.; Basato, M. *J. Mol. Catal. A: Chem.* **2001**, 173, 249.
- (18) APEX2, Version 2 User Manual, M86-E01078, Bruker Analytical X-ray Systems, Madison, WI, June 2006.
- (19) Sheldrick, G.M. “SADABS (version 2008/1): Program for Absorption Correction for Data from Area Detector Frames”, University of Göttingen, 2008.
- (20) Sheldrick, G.M. (2008). *Acta Cryst. A*64, 112-122.
- (21) Brandenburg, K. (1999). DIAMOND. Crystal Impact GbR, Bonn, Germany.